DIAGENESIS AND POROSITY DISTRIBUTION IN DELTAIC SANDSTONE, STRAWN SERIES (PENNSYLVANIAN), NORTH-CENTRAL TEXAS

APPROVED:

Earle F. McBride

Robert L. Folk

DIAGENESIS AND POROSITY DISTRIBUTION IN DELTAIC SANDSTONE, STRAWN SERIES (PENNSYLVANIAN) NORTH-CENTRAL TEXAS

by

SHIRLEY JEAN PETERSON, B.A.

THESIS

Presented to the Faculty of the Graduate School of
The University of Texas at Austin
in Partial Fulfillment
of the Requirements
for the Degree of

MASTER OF ARTS

THE UNIVERSITY OF TEXAS AT AUSTIN

May 1977

ACKNOWLEDGEMENTS

A grant from the Oil and Gas Division of the Denver office of the U.S. Geological Survey provided financial support for the thesis. Dr. Thomas Ahlbrandt served as my contact with the U.S.G.S.

The cores and electric logs used in this study were provided by Exxon Production Research Company. Dr. J.P. Shannon coordinated my use of the cores and obtained other information necessary to the project.

The cores were stored and examined at the Well Sample Library of the Bureau of Economic Geology of the University of Texas at Austin. Douglas Ratcliff and his assistants set up the cores whenever I needed to work on them.

Dr. R.L. Folk and Dr. L.S. Land served on my committee, and they offered many helpful observations and suggestions, as well as editing the manuscript. Cynthia Haynes served as the student editor.

Finally, special thanks go to my supervisor, Dr. E.F. McBride, who gave so generously of his time, talent, and enthusiasm to my project.

This thesis was submitted to the Committee in March 1977.

DIAGENESIS AND POROSITY DISTRIBUTION IN DELTAIC SANDSTONE, STRAWN SERIES (PENNSYLVANIAN) NORTH-CENTRAL TEXAS

by

Shirley J. Peterson

ABSTRACT

Extensive diagenetic changes have occurred in deltaic sandstones of the "Gray" interval, Strawn Series (Pennsylvanian) from Taylor County, Texas. The present burial depth of the "Gray" interval is 4500 feet (1370 m.), and maximum burial was about 7500 feet (2300 m.). Sandstone beds were deposited in delta slope, bar crest, and distributary channel environments in a high-constructive elongate delta. Petrographically, the rocks are fine to very fine, submature to mature, shale-bearing sublitharenite. Except for clay clasts, the framework grains, more than 95% quartz, are very mature mineralogically.

Good primary porosity occurred in sediments deposited in high energy environments such as bar crest and channel. These sediments had large mean grain size ($\bar{X}$ = 2.8 ϕ or .15 mm.), contained an average of only 1.4% detrital clay matrix, and were located farther away vertically from shale beds. It is estimated that depositional porosity of about 35% was reduced to 22% by compaction.

Cementation began with authigenic chlorite rims, followed by quartz overgrowths. Calcite cement filled the remaining pore space and replaced unstable grains such as feldspar. Later, dissolution of calcite produced secondary porosity. Further compaction was prevented by quartz cement, so the secondary porosity was preserved. Kaolinite, barite, and ferroan dolomite precipitated as late cements that reduced secondary porosity.

Samples from high energy environments contain the most cement, but they also retain the highest porosity. Original textures and depositional environments in a formation may be used to predict where porosity will survive diagenesis.

TABLE OF CONTENTS

LIST OF TABLES

LIST OF FIGURES

INTRODUCTION

The purpose of this study was to examine the diagenesis of a deltaic sandstone body, and to relate that diagenesis to the present distribution of porosity. The rocks that were studied are from the "Gray" interval of the Pennsylvanian Strawn Series, from in or near the West Tuscola field in Taylor County, Texas (Fig. 1). There is oil and gas production from "Gray" sandstones in several fields in Taylor County, but the West Tuscola field contains the largest reserves (Shannon and Dahl, 1971).

A knowledge of the factors controlling porosity distribution in sandstones would aid in the exploration for hydrocarbons. Porosity has been related to several different factors by previous workers. Depth variation is often considered one of the most important controls on porosity (e.g. Fox et al., 1975), but all the samples in this study were from essentially the same depth, so it would not have been an important factor here. Other variables such as depositional environment (e.g. Levandowski et al., 1973), proximity to shale beds (e.g. Fothergill, 1955), grain size (e.g. Adams, 1964), grain composition (e.g. Galloway, 1974), pore water chemistry (e.g. Carrigy and Mellon, 1964), hydrocarbon migration (e.g. Levandowski et al., 1973), and authigenic clay coats (e.g. Heald and Larese, 1974) have all

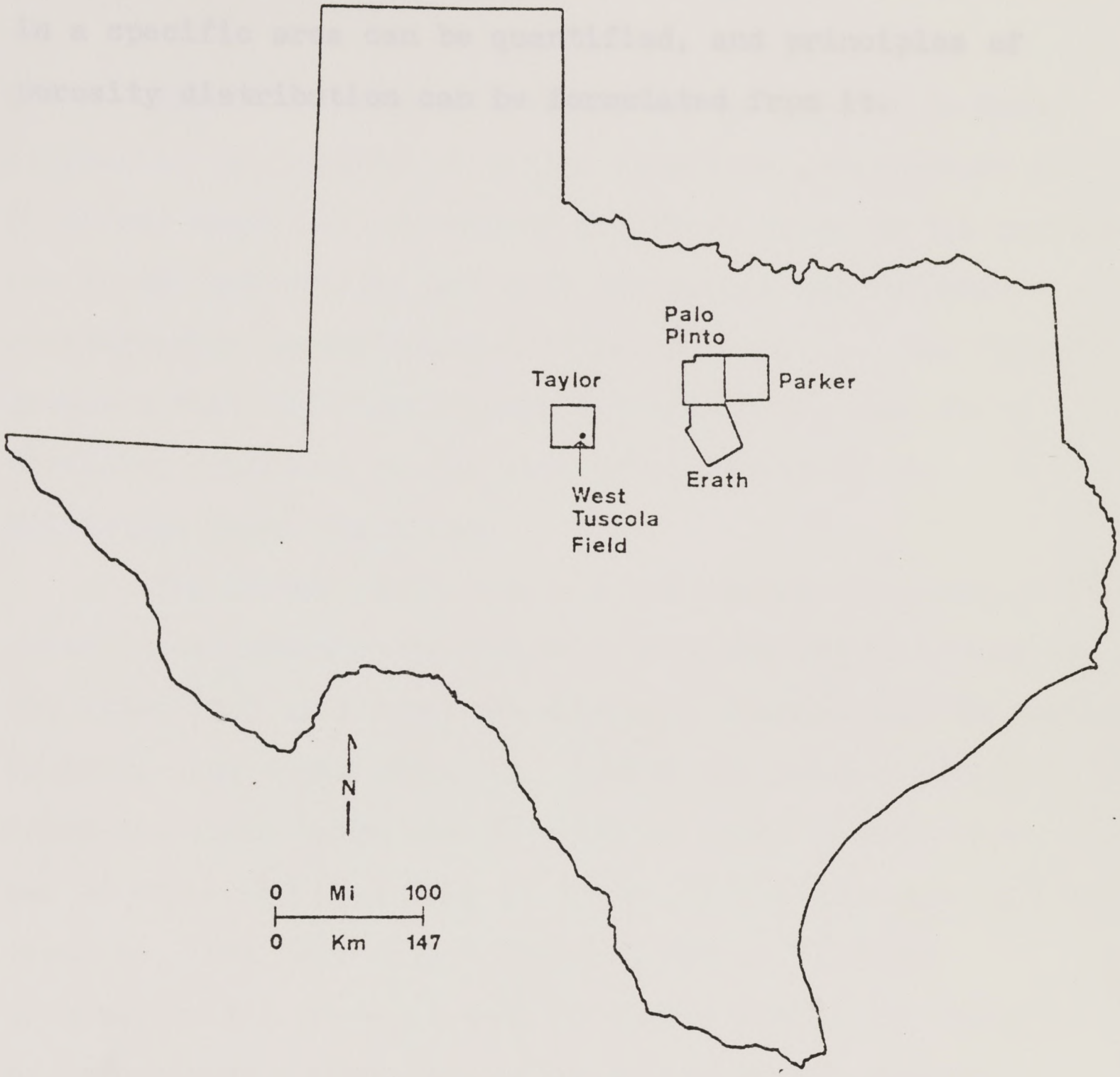

Figure 1. Location of West Tuscola field, Taylor County, Texas. The location of Erath, Palo Pinto, and Parker counties, where the "Gray" sandstone (Buck Creek Formation) crops out, is also shown.

been suggested as possible controls of porosity in sandstones. By studying one subsurface deltaic lobe with good well control, the effect of each of these different factors in a specific area can be quantified, and principles of porosity distribution can be formulated from it.

GEOLOGIC SETTING

Strawn Group Stratigraphy

The Strawn Group of the Late Desmoinesian to Early Missourian is composed of shale, sandstone, and carbonate. Different names have developed for these units on the surface and in the subsurface, and both the formal and informal stratigraphic nomenclature is shown in Table 1. The "Gray" interval that was studied here is an informal name for a producing sandstone in the Buck Creek Member of the Grindstone Creek Formation.

The Strawn crops out in North-central Texas in a northeast-southwest trending belt 20 miles (29 km.) wide and 140 miles (205 km.) long, in which the central part is covered by Cretaceous rocks (Fig. 2). Within the Strawn, the Buck Creek sandstone crops out in a belt 4 miles (6 km.) wide and 33 miles (48 km.) long in Erath, Palo Pinto, and Parker counties. The beds have a regional dip of 35 ft/mi (7 m/km) to the west, so that in Taylor County the "Gray" is approximately 4500 feet (1372 m.) below the surface.

Regional Structural Setting

The major structural elements of the Desmoinesian Epoch in Texas are shown in Figure 3. The Ouachita Fold Belt developed in the latest Early Pennsylvanian

Table 1. Surface and subsurface stratigraphic nomenclature, Upper Desmoinesian and Lower Missourian (Strawn Group), North-Central Texas. From Brown and Goodson (1972).

System			Surface		Subsurface
Pennsylvanian	Canyon Group	Missourian Series	Palo Pinto Fm.	Wiles Ls. Posideon Sh. Wynn Ls.	
			Mineral Wells Fm.	Turkey Creek Ss. Sandstone #2 Dog Bend Ls. Lake Pinto Ss.	Cross Cut Moran Morris
	Strawn Group	Desmoinesian Series		Village Bend Ls. Sandstone #1 Hog Mountain Ss.	Upper Fry
			Brazos River Fm.	Ss. and Congl.	Lower Fry
			Mingus Fm.	Thurber Coal Goen Ls. Dobbs Valley Ss. Santo Ls.	Jennings Gardner
			Grind-stone Creek	Buck Creek Ss. Brannon Bridge Ls.	Gardner Gray Gray
			Lazy Bend Fm.	Meek Bend Ls. Hill Creek Beds	

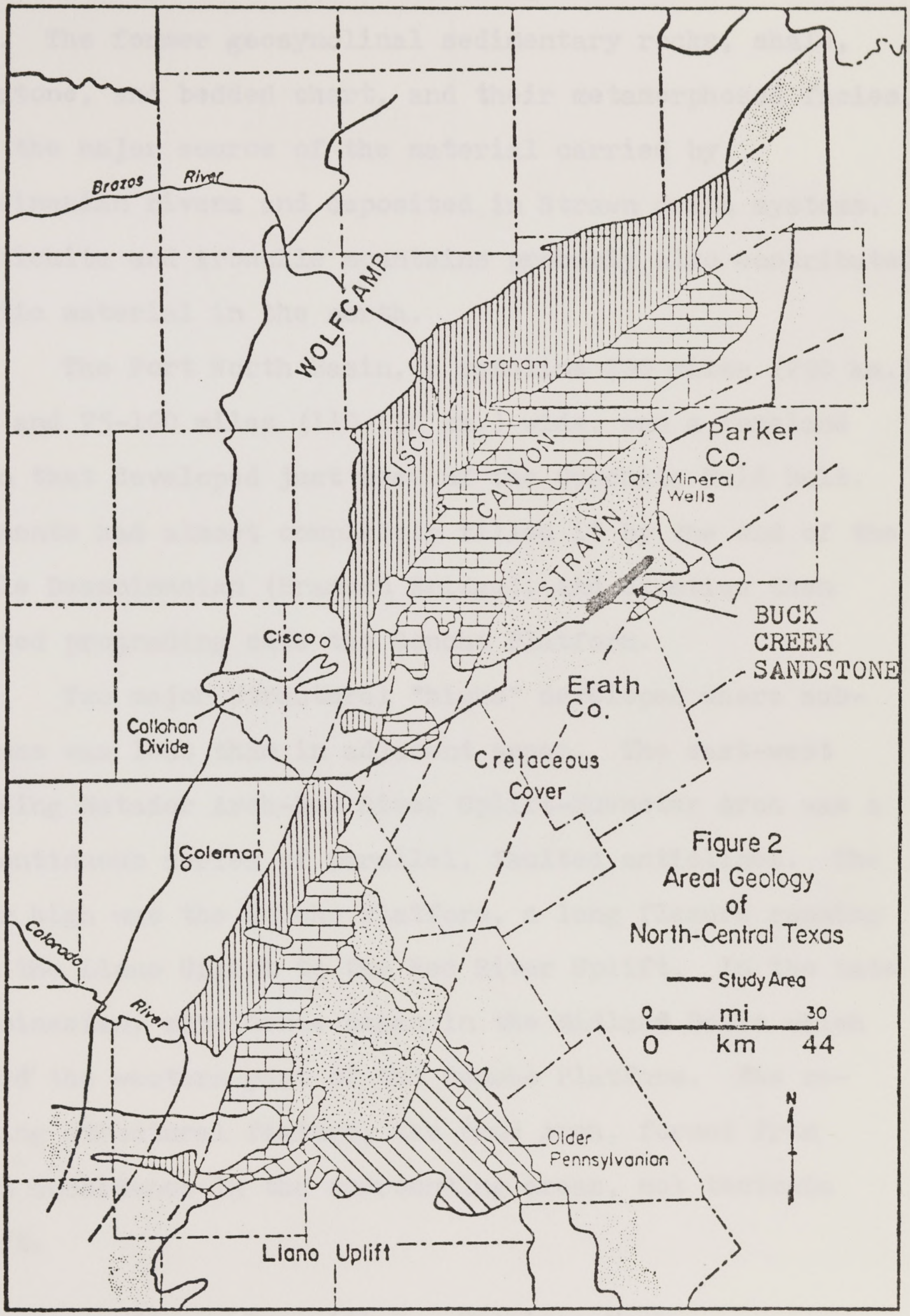

Figure 2. Areal geology of North-Central Texas showing the outcrop location of the Buck Creek sandstone. From Cleaves (1975).

(Cleaves, 1975), and started shedding clastic debris to the west. The former geosynclinal sedimentary rocks, shale, sandstone, and bedded chert, and their metamorphosed facies, were the major source of the material carried by Desmoinesian rivers and deposited in Strawn delta systems. The Wichita and Arbuckle mountains probably also contributed clastic material in the north.

The Fort Worth Basin, a syncline 200 miles (290 km.) long and 75-100 miles (110-150 km.) wide, was a foreland basin that developed just west of the Ouachita Fold Belt. Sediments had almost completely filled it by the end of the Middle Desmoinesian (Brannon Bridge), and clastics then started prograding onto the Concho Platform.

Two major structural "highs" developed where subsidence was less than in adjacent areas. The east-west trending Matador Arch-Red River Uplift-Muenster Arch was a discontinuous series of parallel, faulted anticlines. The other high was the Concho Platform, a long flexure running from the Llano Uplift to the Red River Uplift. In the Late Desmoinesian, subsidence began in the Midland Basin which tilted the western part of the Concho Platform. The resulting structural feature, the Bend Arch, formed from basin subsidence in the surrounding areas, not tectonic uplift.

Strawn Deposition - Previous Work

The most complete study of the Strawn in both the

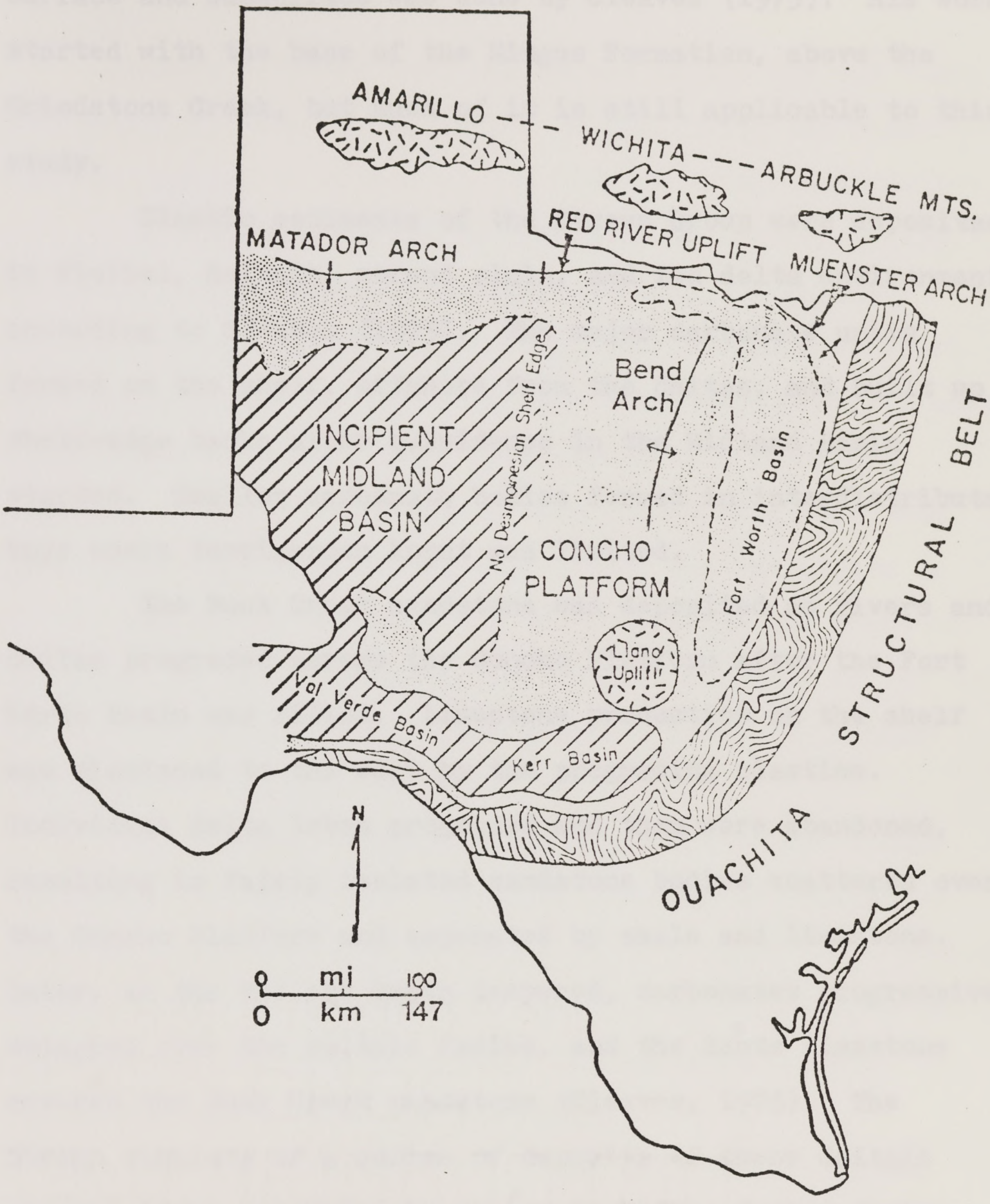

Figure 3. Tectonic setting of North-Central Texas during the Desmoinesian Epoch. Modified from Cleaves (1975).

surface and subsurface was done by Cleaves (1975). His work started with the base of the Mingus Formation, above the Grindstone Creek, but much of it is still applicable to this study.

Clastic sediments of the Strawn Group were deposited in fluvial, deltaic, strand plain, and fan delta environments, according to Cleaves (1975). The major carbonate units formed on the shelf, offshore from the deltas, and built up shelf-edge banks after subsidence in the Midland Basin started. Smaller carbonate bodies formed in interdistributary bays where terrigenous input was limited.

The Buck Creek sandstone was deposited as rivers and deltas prograded across the Concho Platform after the Fort Worth Basin was filled. Limestone production on the shelf was displaced to the west by the prograding clastics. Individual delta lobes prograded and then were abandoned, resulting in fairly isolated sandstone bodies scattered over the Concho Platform and separated by shale and limestone. Later, as the Midland Basin deepened, carbonates progressively onlapped over the deltaic facies, and the Santo limestone covered the Buck Creek sandstone (Cleaves, 1975). The Strawn consists of a series of deposits of these deltaic progradations separated by carbonate bodies formed during transgressions.

Depositional Environments

Cleaves believes that the Strawn deltas are all high-constructive, elongate or lobate deltas, using the classification system of Fisher et al. (1969). High-constructive deltas are mainly composed of fluvially influenced facies, which are progradational and aggradational. Elongate deltas develop when there is a high rate of sediment input that prevents marine reworking, the sediment contains a large amount of mud, and the sand progrades over a thick mud sequence. High-constructive lobate deltas also form when there is a high rate of sediment input, but when there is little mud in the sediment and the underlying mud sequence is thin. By these criteria, the deltaic deposits in the area of the West Tuscola field were probably formed by a high-constructive elongate delta.

On a stable cratonic platform there is not enough subsidence to allow thick vertical stacking of facies, so rapid progradation results (Brown et al., 1973). The sediment package deposited in one whole cycle of delta progradation, aggradation, and abandonment may be only 100-200 feet (30-60 m.) thick at its central axis.

The major deltaic facies are the prodelta, delta front slope, channel mouth bar crest, distributary channel, interdistributary bay, and marsh (Cleaves, 1975). The prodelta deposits are largely unfossiliferous shale and silty shale, with rare burrows and silty laminations. Well

macerated plant debris is common, and the high organic content makes these good hydrocarbon source beds. Seaward, the prodelta facies grades into normal shelf deposits, and toward the delta it grades into the slope facies.

The delta slope deposits consist of interbedded shale and siltstone or very fine sandstone with common burrows, load structures, and convolute bedding. Toward the delta crest the lenses of sand and silt become thicker and more numerous. Shale laminae become thinner until they are just partings between sandstone.

The channel mouth bar crest facies consists of clean sandstone with parallel laminae or low-angle trough cross-beds. Parallel laminations form in upper flow regime conditions in the shallow water over the bar; troughs form during floods when the bar is scoured by the channel. Plant debris is common, especially concentrated along bedding planes.

Distributary channel sand deposits are the coarsest in the delta system. They have an erosional base, and large-scale trough cross-beds that form when the channel is active. After channel abandonment, silt and clay fill it in, providing an impermeable seal.

As the delta progrades, these facies form a vertical upward-coarsening sequence.

Marsh deposits are highly organic shale and silty shale, with very abundant plant material. The organic content is higher than in prodelta deposits, and the plant material is not so finely disseminated. Interdistributary

bay deposits are also composed of shale and silty shale, but there are thin layers of laterally continuous, highly burrowed sandstone and siltstone, as well as marine and brackish-water fossils.

West Tuscola Field

The "Gray" sandstone interval in the West Tuscola and adjacent fields was interpreted by Shannon and Dahl (1971) to be of deltaic origin. Electric logs and cores were used to delineate the boundaries of the deltaic facies. Figure 4, from Shannon and Dahl (1971), is an isopach map of the delta front facies, which includes deposits of the slope and channel mouth bar crest. Delta progradation was generally to the west, but individual lobes spilled out toward the north and south. An isopach map of just the bar crest facies (Fig. 5) gives the outline of the clean sandstone, the main producing unit.

Vertical and lateral facies relations are shown in cross sections perpendicular to the direction of delta growth (Fig. 6,7). Datum is a limestone marker bed about 100 feet (30 m.) above the top of the "Gray" sandstone. In the lower part of the section, in the slope facies, sand lenses are separated by impermeable shale and siltstone lenses, but at the top of the bar crest facies, sandstones are more laterally continuous. The relatively thick section of bar crest sandstone beds results from the settling and compaction

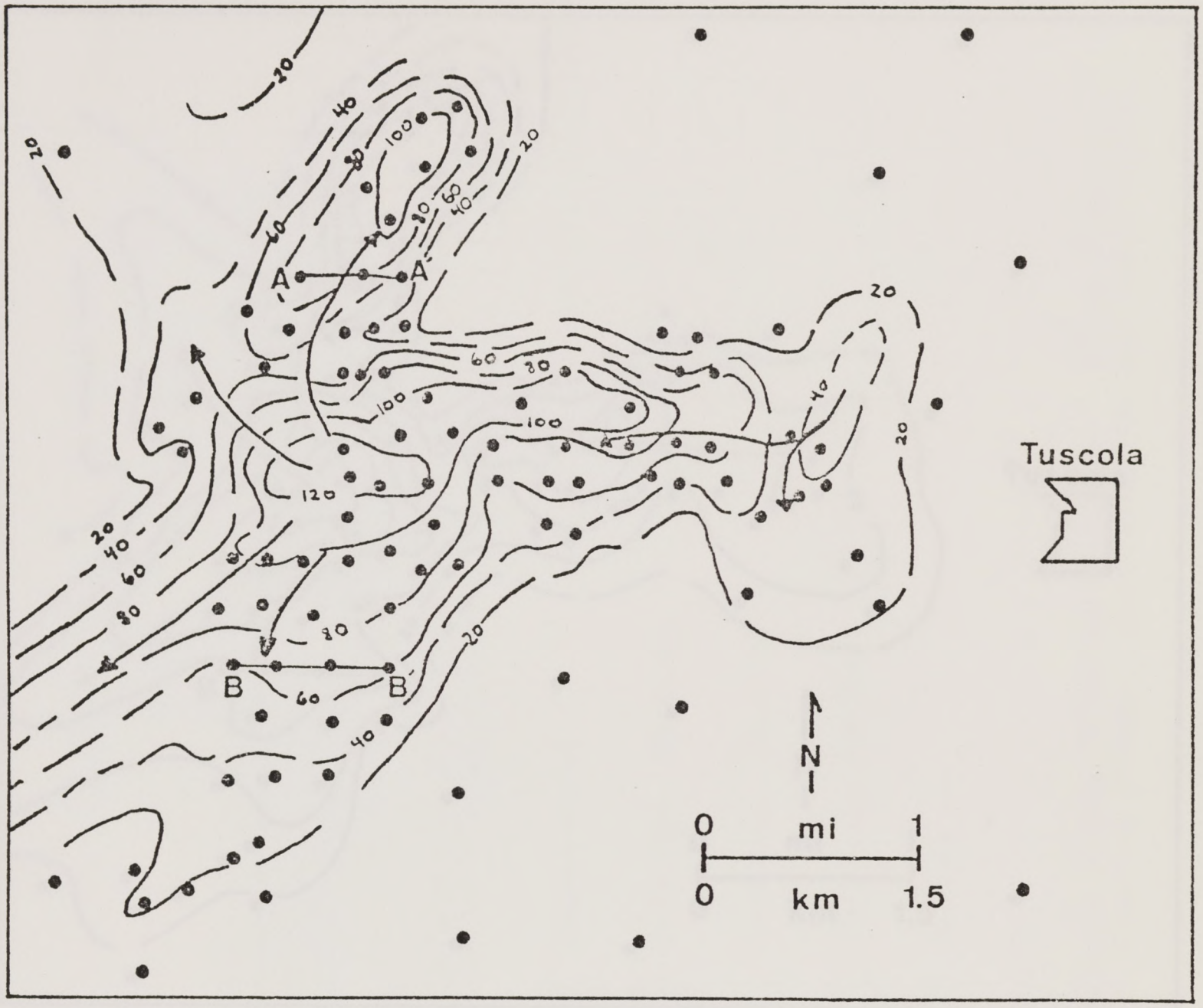

Figure 4. Isopach map of delta front facies, West Tuscola field. From Shannon and Dahl (1971).

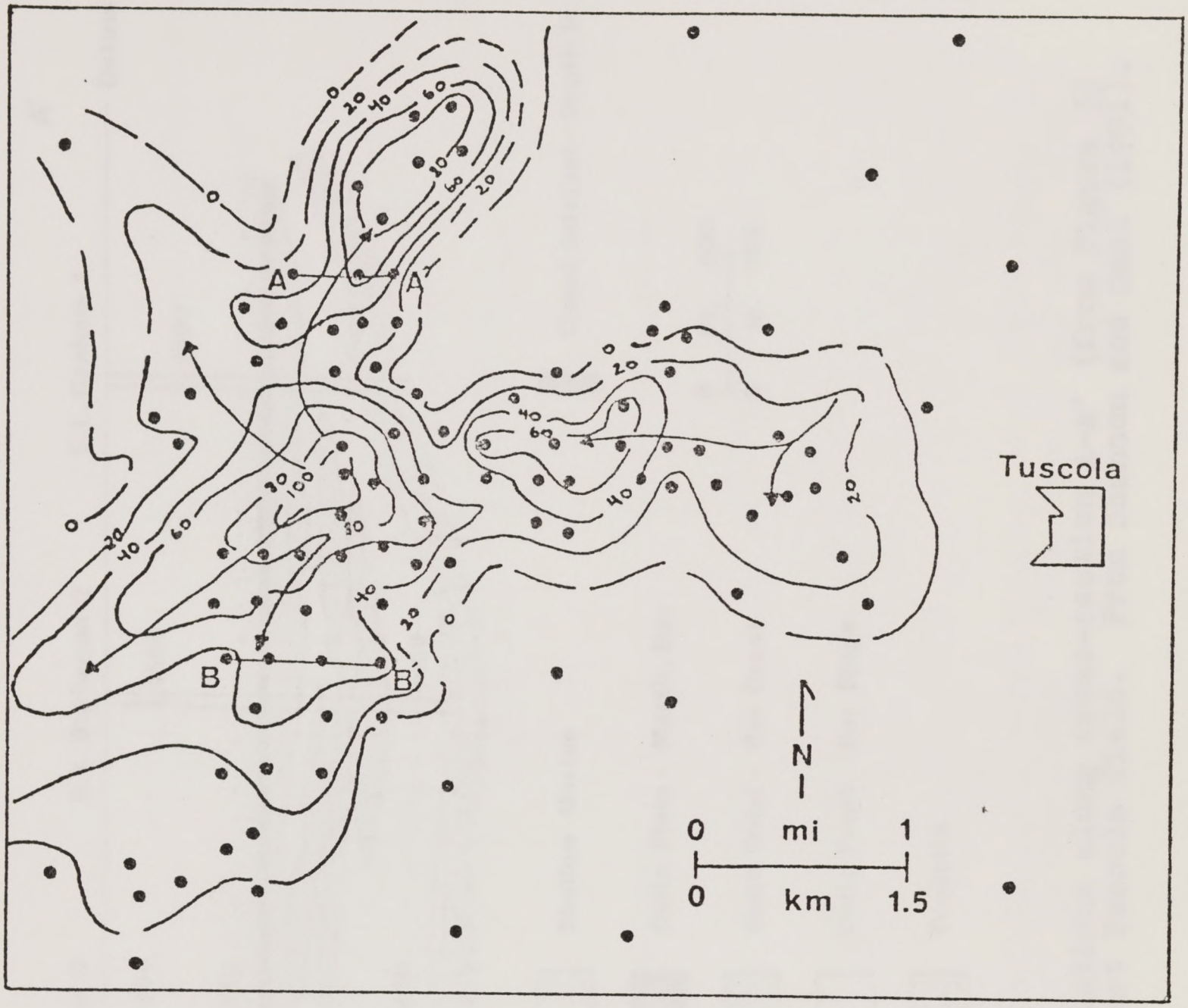

Figure 5. Isopach map of clean sandstone zone, West Tuscola field. From Shannon and Dahl (1971).

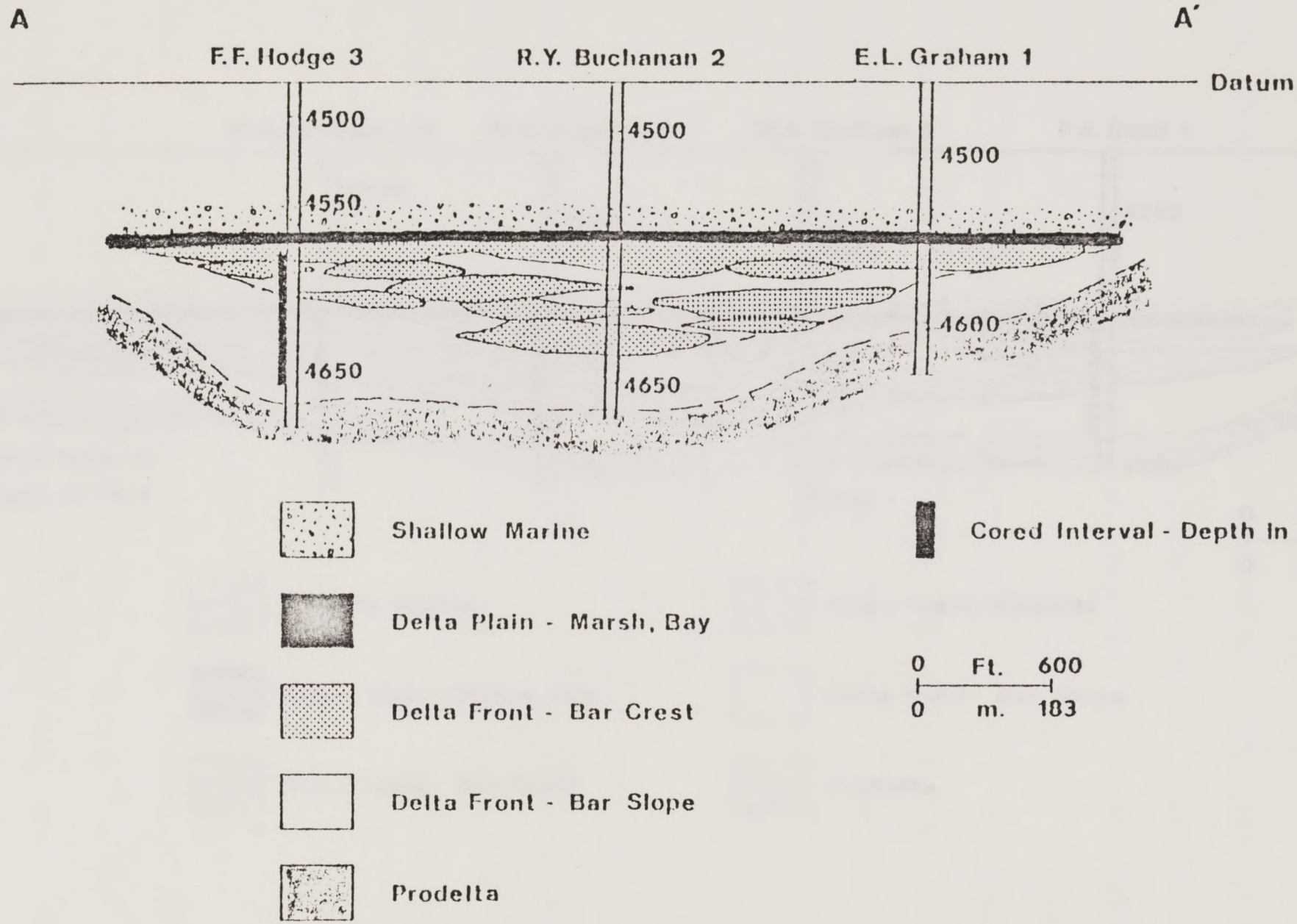

Figure 6. Facies relations along cross-section A-A' (from Figure 5) through West Tuscola field. From Shannon and Dahl (1971).

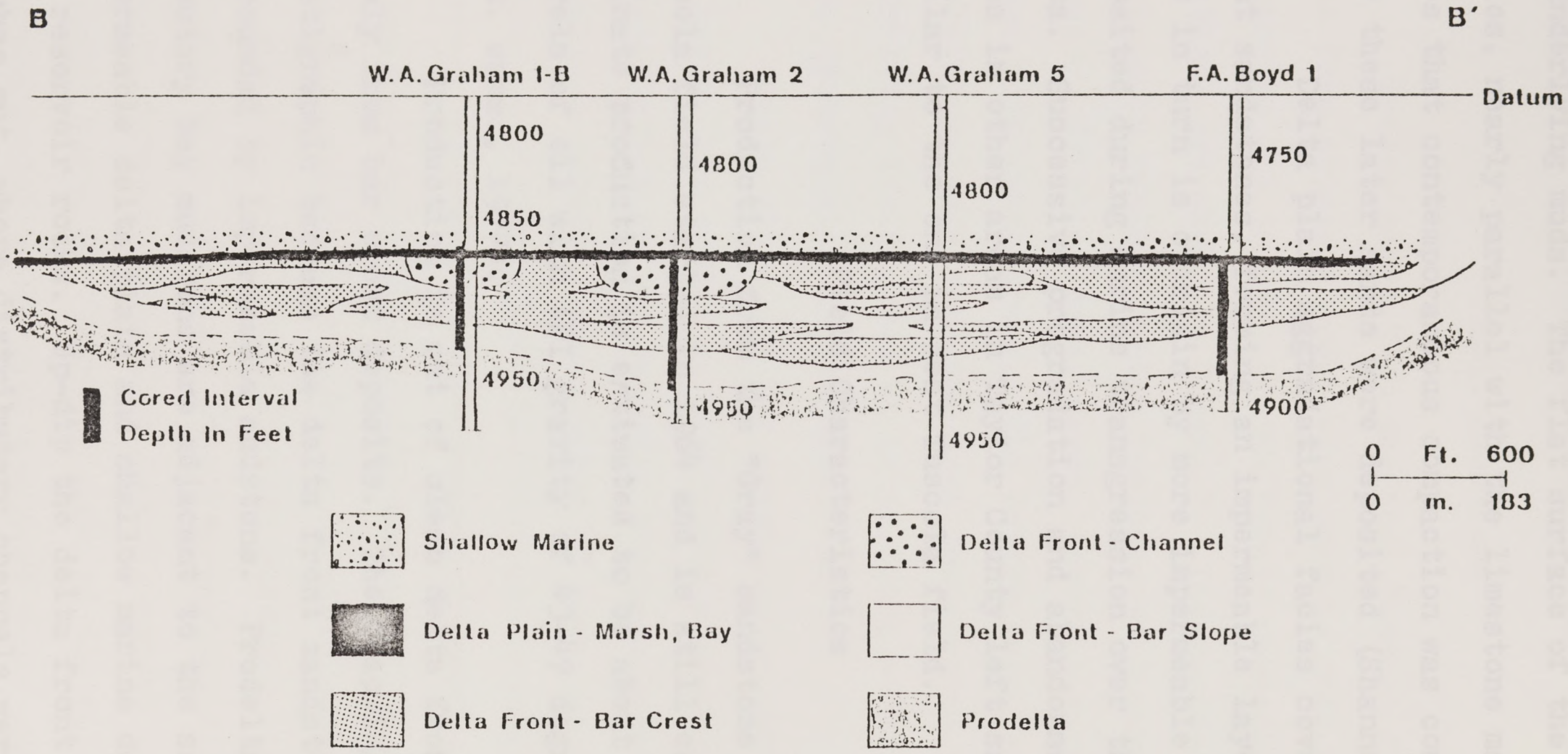

Figure 7. Facies relations along cross-section B-B' (from Figure 5) through West Tuscola field. From Shannon and Dahl (1971).

of underlying muds. The flat surface of the delta front facies, nearly parallel with the limestone marker bed, indicates that contemporaneous compaction was completed by the time these later sands were deposited (Shannon and Dahl, 1971).

Delta plain aggradational facies cover the delta front sandstones, forming an impermeable layer over the top. This in turn is overlain by more impermeable strata that were deposited during marine transgression over the abandoned delta. Successive progradation and abandonment of the delta lobes in other areas in Taylor County left sandstone bodies similar to the one in West Tuscola field.

Field Characteristics

Production from the "Gray" sandstone in the West Tuscola field started in 1964 and is still continuing. The ultimate production is estimated to be about one million barrels of oil with API gravity of 43-47 degrees (Shannon, pers. comm., 1977).

Production is out of clean delta front sandstone, mainly from bar crest deposits. The trapping mechanism is stratigraphic because the delta front sandstone bodies are surrounded by impermeable mudstone. Prodelta and interdistributary bay mudstone are adjacent to the sandstone, and impermeable delta plain and shallow marine deposits cover the reservoir rocks. Up-dip the delta front sandstone pinches out, where distributary channels were plugged with

silt and clay after abandonment (Shannon and Dahl, 1971).

Well Locations

Twelve cores from the West Tuscola field and five cores from adjacent areas were used in this study; each core penetrated all or most of the "Gray" sandstone. Their locations are shown in Figure 8. Information about each well is given in Table 2, which includes well name and location, operator, drilling date, depth, interval cored, and measured bottom hole temperature. The bottom hole temperature given is slightly lower than the true temperature because of cooling by drilling fluids, but it is probably within 5% of the true value (Schoeppel and Gilarranz, 1966).

Delta slope and bar crest facies comprise the bulk of the cores, but prodelta, distributary channel, marsh, and interdistributary bay deposits are also present. Appendix 1 contains a detailed description of each core. The different facies are distinguished by vertical stratigraphic sequence, texture, sedimentary structures and fossil content. Although the complete prograding delta sequence is not found in each core, the composite picture is an upward-coarsening sequence from prodelta mudstones, through burrowed, interbedded shale and sandstone, to clean, parallel-laminated bar crest sandstones. Cross-bedded distributary channel sequences with erosional bases are found in some of the wells. Marsh deposits of organic-rich shale with abundant plant material, and fossiliferous interdistributary bay deposits cap the sequence.

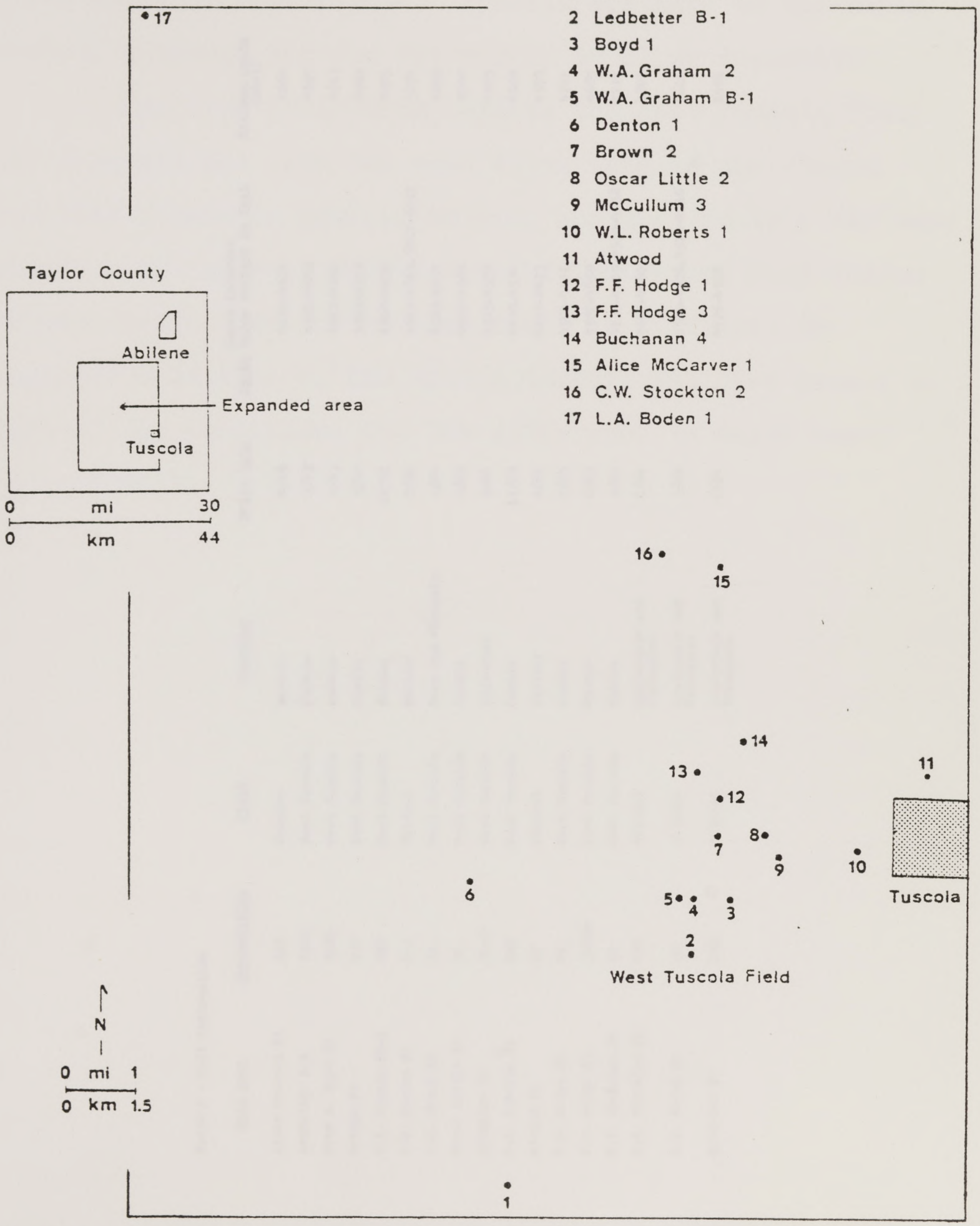

Figure 8. Location of wells used in this study. Table 2 gives information about each well.

Table 2 - Well Information

Well Name	Abbreviation	Field	Operator	Drill Date	Cored Interval Depth below surface in feet	Maximum Depth (feet)	Maximum Temperature (°F)
Alton Roberts #1	ALR	Proctor	Humble	4/66	4614-4664	4664	116
Ledbetter B-1	LB-1	West Tuscola	Humble	3/63	4781-4818	4890	120
Fred A. Boyd #1	BOYD	West Tuscola	Humble	4/63	4811-4882	4913	120
Graham #2	G-2	West Tuscola	Humble	9/62	4861-4939	4980	120
W.A. Graham #B-1	WAG	West Tuscola	Humble	10/62	4868-4930	4985	120
J.M. Denton #1	D-1	Wildcat	Humble	8/64	4815-4865, 5017-5037	5174	122
J.C. Brown #2	2B	West Tuscola	Hope and Champlin	1/64	4585-4632	4699	118
Oscar Little #2	OL	West Tuscola	Humble	6/64	4527-4564	4700	120
McCullum #3	MC-3	West Tuscola	Sojourner	9/64	4515-4558	4605	118
W.L. Roberts #1	ROB	West Tuscola	Humble	11/63	4438-4534	4608	117
Atwood #1	A1	Wildcat	Frazier	4/64	4422-4473	4578	117
F.F. Hodge #1	HO	West Tuscola	Humble	2/63	4564-4621	4701	118
F.F. Hodge #3	3-HOD	West Tuscola	Humble	6/63	4582-4659	4685	118
R.Y. Buchanan #4	BH	West Tuscola	Humble	9/63	4139-4169, 4550-4658	4714	117
C.W. Stockton #2	C#S	Wildcat	Lauderdale and Straughan	6/64	4642-4680	4801	119
L.O. Boden #1	BO	Wildcat	Lauderdale and Straughan	3/64	4519-4526, 4573-4616	4616	110
McCarver #1	AMC	Wildcat	Lauderdale and Straughan	2/64	4476-4526	4696	117

Fossils found in the bay facies include brachiopods, gastropods, pelecypods, bryozoans, crinoids, foraminifers, green algae, and ostracods. Fossils are rare in the other facies, although burrows are common in slope deposits.

The five wells from outside the West Tuscola field are probably not from the same delta lobe as the others, but they formed in similar deltas, and they contain the same sequence of facies. Correlation of individual sand bodies between wells even in the same field is difficult or impossible because of the discontinuous, isolated nature of most of the sandstones and the difference in depth cored in each well.

METHODS

Each core was measured and described (Appendix 1), and on the basis of this information, the electric logs, and the previous work by Shannon and Dahl (1971), a depositional environment was inferred for every part of the core. Samples were chosen from sandstone and coarser siltstone deposited in the different environments. 43 samples are from bar crest deposits, 29 from delta slope deposits, 15 from channel deposits, 2 from delta plain marsh deposits, and 2 from interdistributary bay deposits. The number of samples reflects the relative abundance of sandstones in each environment in these cores.

Porosity and Permeability

From each sample a 1-inch diameter plug was cut and used to determine porosity and permeability. A Nitrogen Compression Permeameter was used to measure the permeability of the samples. The flow rate and pressure of the gas coming out of the sample, as well as the difference in pressure between the gas entering and leaving the sample, are measured. With this information plus the length and cross-sectional area of the sample plug, and the viscosity of the gas, Darcy's Law may be used to calculate the permeability in darcies. The values obtained by this method are best used as relative comparisons among the samples, not as an absolute measure of

the permeability.

Porosity was measured in a Nitrogen Compression Porosimeter, which determines effective pore volume using the principle of Boyle's Gas Law. A known volume of gas at a known pressure is released into an unknown volume, the connected pore space within the sample. The new pressure is measured, and the volume can be calculated. Temperature is assumed constant throughout.

The values of porosity (in percent) and permeability (in millidarcies) are given in Table 3, which is a compilation of the data for each sample. Porosity ranged from 0 to 15.1%, with a mean of 7.3% and standard deviation of 2.8%. Permeability ranged between 0 and 387 md; the log mean of the permeability plus one was 0.73 md and the log standard deviation was 0.78 md. Mineralogical composition, texture, and depositional environment are also included in this table.

A second method was used to determine the porosity of the samples, in which a thin section was made from each plug and point-counted for 400 points on an evenly spaced grid. Porosity is calculated as follows:

$$\text{Porosity} = \frac{\text{No. of pore spaces counted}}{\text{Total no. of points counted}} \times 100$$

Petrographic methods are explained in more detail in the next section.

Generally, the two methods for calculating porosity

Table 3. Petrographic information about each sample.

WELL		QTZ	POLY	OR	PLAG	SCP	SIL	SHR	BRF	QCEM	CARB	KAO	MTX	FOR	SEC	Other	CEM	FPOR	FCP	Φ	PERM	ENV	DIST	Q:R	R	$\bar{x}$	σ	CAL
ALR	4616	59.5	2.5	1.5	1.3	.5	.5	6.5	.5	15.5	4.0	0	0	3.5	3.0	1.3	19.[illegible]	6.5	23.0	12.2	0	CH	4	75:[illegible]	19	3.5	.76	
ALR	4623	57.0	3.5	1.8	.5	1.5	.8	3.0	.5	9.0	9.3	.8	.5	9.8	1.5	.8	18.[illegible]	10.5	28.1	12.6	8	CH	2	88:[illegible]	7	2.8	.62	
ALR	4630	62.3	1.8	1.3	.3	.3	.5	2.8	1.0	17.5	3.0	1.0	1.0	6.5	2.0	0	20.[illegible]	7.5	27.0	13.7	211	CH	3	91:[illegible]	6	2.0	.72	
ALR	4639	65.2	2.7	.7	1.0	.7	.3	3.2	2.5	6.4	0	2.9	4.7	6.9	2.0	1.0	6.4	7.8	13.2	11.5	6	CH	3	88:[illegible]	8	3.0	.77	
ALR	4642	64.8	3.5	.3	0	1.5	.8	1.0	.3	5.8	.3	0	3.8	12.8	4.8	.8	6.4	15.2	18.[illegible]	15.1	387	CH	6	91:[illegible]	3	1.7	.52	
ALR	4648	69.9	2.8	.5	0	.3	1.3	1.8	.8	8.5	.8	.5	.5	12.0	1.3	.3	9.[illegible]	12.6	21.3	14.3	125	CH	12	94:[illegible]	5	1.7	.69	
ALR	4652	70.5	3.5	.5	.3	0	.5	1.2	.5	7.4	0	.3	2.0	11.4	1.5	.5	7.4	12.2	18.8	12.1	265	CH	12	96:[illegible]	4	2.0	.78	
ALR	4661	57.3	1.8	1.0	.3	.5	.5	1.8	.5	21.3	2.8	1.0	1.4	8.0	1.6	.5	24.0	8.9	32.9	13.0	73	CH	3	92:[illegible]	4	2.5	.52	
LB1	4782	66.3	1.0	.5	.8	0	.3	2.0	0	2.8	23.0	.3	3.0	0	0	0	25.[illegible]	0	25.8	0	0	SL	2	95:[illegible]	3	4.2	.72	+
LB1	4793	50.3	0	.3	.5	0	.5	24.3	.3	.3	9.8	0	12.3	0	0	1.3	10.[illegible]	0	10.0	1.6	0	SL	1	65:[illegible]	33	4.5	.79	+
LB1	4798	57.3	0	1.0	.5	0	0	2.3	.3	1.9	36.0	0	1.5	0	0	.3	37.[illegible]	0	37.0	7.9	0	SL	6	93:[illegible]	4	3.8	.89	+
LB1	4808	53.8	0	1.5	1.0	0	0	5.5	0	3.3	27.3	0	4.5	1.3	0	2.0	30.[illegible]	1.3	31.8	13.8	1	SL	10	80:[illegible]	9	4.0	.64	
LB1	4813	55.5	.5	.8	.5	0	0	15.5	0	3.8	13.8	0	7.8	.8	0	1.3	17.[illegible]	.8	18.3	11.1	5	SL	5	76:[illegible]	21	4.3	.69	+
LB1	4816	41.3	0	.5	.8	0	.8	4.0	0	0	3.0	0	45.5	0	0	4.3	3.[illegible]	0	3.0	0	20	SL	2	80:[illegible]	9	4.4	.61	+
BOYD	4824	61.8	3.3	2.5	1.0	.5	.5	0	0	19.3	4.0	1.0	.3	5.5	.3	.3	23.[illegible]	5.6	28.8	6.7	5	CH	7	93:[illegible]	1	3.0	.69	
BOYD	4835	62.8	3.0	1.3	.5	0	.3	1.8	0	22.3	.3	1.8	1.8	2.8	1.5	.3	22.[illegible]	3.5	25.3	4.5	0	CR	18	94:[illegible]	3	3.1	.67	
BOYD	4849	63.3	1.3	1.8	0	.3	.5	1.0	.3	12.3	5.0	.3	.3	10.3	3.8	0	17.[illegible]	12.2	27.6	11.5	93	CR	30	95:[illegible]	3	2.6	.57	
BOYD	4865	64.5	3.8	1.8	.5	0	.3	4.5	0	12.3	1.5	0	6.0	2.0	1.0	2.0	13.[illegible]	2.5	15.8	5.6	11	SL	14	90:[illegible]	6	3.0	.53	
G2	4862	62.3	0	.5	.5	.3	0	9.1	0	3.7	.7	2.9	8.1	2.4	3.0	.5	4.4	10.2	13.8	10.6	9	CH	2	85:[illegible]	12	3.7	.78	
G2	4895	59.8	2.8	.3	.3	0	.3	4.5	.3	17.8	.5	2.5	1.8	8.8	.8	0	18.[illegible]	9.1	27.1	9.5	106	SL	25	92:[illegible]	7	2.5	.66	
G2	4932	59.9	1.0	.5	1.0	.5	.5	26.1	0	2.3	.8	0	7.4	0	0	0	3.[illegible]	0	3.0	3.9	7	SL	7	68:[illegible]	30	3.9	.74	
G2	4938	57.5	.5	1.0	.5	0	0	1.0	.5	4.8	33.5	0	0	0	0	.8	38.[illegible]	0	38.3	0	0	SL	2	94:[illegible]	3	2.6	.55	
WAG	4877	53.7	1.2	2.0	1.5	0	.5	10.3	0	0	0	0	31.1	0	0	.7	0	0	0	7.1	4	LR	1	79:[illegible]	16	4.1	.75	
WAG	4887	60.5	3.5	.8	.3	.3	.5	3.8	.8	13.5	2.3	1.5	0	9.5	2.8	.3	15.8	10.5	25.3	10.4	52	CH	10	91:[illegible]	7	2.1	.71	
WAG	4893	57.3	3.2	1.2	.7	0	0	5.2	.7	25.2	0	.7	2.2	2.2	1.2	0	25.[illegible]	2.2	27.4	6.9	0	SL	16	88:[illegible]	9	2.9	.69	
WAG	4899	61.9	3.7	1.0	.7	1.0	1.2	4.2	.7	18.6	.5	.5	1.0	5.7	3.2	0	15.[illegible]	7.3	20.8	9.6	13	CR	19	86:[illegible]	8	2.5	.58	
WAG	4906	62.0	3.8	1.3	0	0	.5	.3	0	.3	31.8	0	0	0	.3	0	32.[illegible]	0	32.2	.5	0	CR	18	97:[illegible]	1	1.8	.56	
WAG	4909	71.0	2.3	.8	.3	0	.3	6.0	1.0	7.3	.8	.3	4.8	3.8	1.5	.3	8.0	4.5	11.5	10.4	15	CR	15	90:[illegible]	9	2.7	.67	
WAG	4912	71.8	2.5	.8	.5	0	.3	.5	.5	8.3	.3	.3	2.0	10.5	2.0	0	8.[illegible]	11.[illegible]	19.[illegible]	12.4	151	CR	12	97:[illegible]	2	2.2	.58	
WAG	4915	66.1	2.2	1.0	.5	.3	.5	4.5	.5	10.1	.5	.7	1.7	5.7	2.0	0	10.[illegible]	10.[illegible]	16.3	11.5	37	CR	9	90:[illegible]	7	2.4	.52	
D1	4834	50.7	5.0	1.2	.5	1.0	0	1.0	.3	17.6	14.9	.7	.3	5.4	1.0	.5	32.[illegible]	5.9	37.9	.3	0	CR	6	93:[illegible]	2	3.1	.50	+
D1	4844	52.5	1.3	1.8	1.5	.3	1.3	10.3	.3	.5	.8	1.3	23.3	2.0	.5	2.8	1.3	2.3	3.3	7.7	58	SL	4	76:[illegible]	17	4.1	.66	
D1	4853	60.5	3.7	1.7	1.2	.5	1.7	2.0	.2	11.5	5.4	1.5	.5	8.5	1.0	.2	16.[illegible]	9.0	25.4	6.5	38	SL	0	89:[illegible]	6	3.6	.64	+
D1	4865	50.5	1.8	.3	.5	.8	.8	.8	0	.3	34.3	0	5.0	0	0	5.3	34.[illegible]	0	34.6	0	0	SL	1	86:[illegible]	3	3.4	.74	+
D1	5017	57.8	4.7	.5	.5	1.0	.7	3.4	.5	10.5	1.7	.7	1.7	11.3	4.9	.3	12.[illegible]	13.8	23.5	5.7	9	CH	7	90:[illegible]	7	2.9	.67	
D1	5038	60.0	2.5	.8	1.0	.5	.8	1.5	.3	26.5	2.3	.3	1.0	1.0	1.5	.3	28.8	1.5	29.8	0	0	SL	3	93:[illegible]	4	2.7	.70	
2B	4585	61.2	2.5	1.0	.7	.7	.7	8.4	.5	9.6	0	0	2.5	7.2	4.7	.3	9.[illegible]	2.5	16.8	6.2	0	CR	7	89:[illegible]	13	3.2	.67	
2B	4590	65.4	2.5	2.0	.7	1.5	.5	3.7	.3	13.8	0	.5	.5	3.7	4.9	0	13.8	6.2	17.5	5.5	0	CR	12	89:[illegible]	6	2.7	.71	
2B	4594	62.3	3.7	.7	.5	.7	.7	2.5	.5	22.4	0	.3	.5	3.5	1.0	.7	22.[illegible]	4.0	25.9	0	0	SL	0	94:[illegible]	6	2.9	.46	
2B	4603	67.8	2.5	1.3	.3	.5	.3	1.0	.3	13.3	.8	1.3	0	10.0	1.0	0	14.[illegible]	10.5	24.6	5.7	100	CR	3	93:[illegible]	2	2.1	.64	
2B	4620	44.2	1.2	.7	.3	.5	.7	4.0	.3	1.5	35.8	0	0	5.4	3.5	1.0	37.[illegible]	7.2	42.7	11.0	10	CR	20	81:[illegible]	11	3.0	.35	+
2B	4629	57.1	5.4	1.0	.7	.7	.7	1.7	1.0	16.9	0	.3	.3	9.3	4.7	.3	16.[illegible]	11.6	26.[illegible]	12.2	10	CR	29	91:[illegible]	5	2.7	.65	
AMC	4491	57.5	1.3	.5	.8	0	0	0	.8	1.8	36.5	0	0	0	0	1.0	38.[illegible]	0	38.3	0	0	SL	1	97:[illegible]	1	3.9	.58	+
AMC	4526	48.1	1.5	1.8	2.2	0	.3	19.0	.5	0	0	0	22.4	0	0	4.2	0	0	0	0	3	SL	4	68:[illegible]	27	3.8	.70	
BO	4594	70.2	1.2	.5	.5	0	.7	.5	.5	12.0	5.2	0	.7	0	0	1.0	24.[illegible]	0	24.2	9	9	CR	2	85:[illegible]	3	2.9	.63	
BO	4599	69.6	1.9	.5	.5	0	0	2.5	0	14.1	2.0	1.7	.3	3.0	4.7	.3	16.[illegible]	5.3	19.[illegible]	4.9	0	SR	7	95:[illegible]	3	2.9	.56	

Table 3. Petrographic information about each sample.

WELL		QTZ	POLY	OR	PLAG	SCP	SIL	SRF	MRF	QCEM	CARB	KAO	MTX	POR	SEC	Other	CEM	TPOR	PCP	Φ	PERM	ENV	DIST	QF:R	$\bar{x}$	σ	CAL
OL	4536	57.0	3.2	1.0	.7	.5	.3	2.7	.7	18.3	.7	5.1	0	5.6	3.9	.2	19.0	7.6	24.6	7.6	0	SL	5	91:1:6	2.9	.55	
OL	4544	60.1	3.0	.5	.5	.3	.3	1.0	1.2	30.5	0	1.0	0	.7	.7	0	30.5	1.1	31.2	4.8	0	CR	0	96:2:4	2.5	.59	
OL	4550	67.4	3.2	1.0	.3	0	0	1.0	.5	17.8	1.2	.3	.5	4.4	2.2	.3	19.0	5.6	23.4	3.3	0	CR	6	96:2:2	2.8	.58	
OL	4551	65.3	1.2	1.2	1.0	0	1.0	11.5	.7	2.0	0	.3	3.4	6.9	4.9	.7	2.0	9.3	11.3	10.1	0	CR	7	81:1:16	3.8	.50	
OL	4562	68.8	2.0	1.9	.5	.5	.3	4.7	.3	11.5	4.2	.3	.5	1.5	1.2	1.0	17.7	2.1	19.8	0	0	SL	2	90:1:8	3.0	.45	
MCJ	4517	46.3	.5	0	.3	.5	.3	.5	0	0	31.5	0	8.3	0	0	1.0	31.5	0	31.5	0	0	BR	0	95:2:2	3.4	.49	+
MCJ	4529	66.6	1.7	1.0	.3	0	.5	0	.3	14.6	5.5	.7	0	8.7	.3	0	20.1	8.8	28.9	5.5	14	BAY	4	97:1:1	2.2	.62	
MCJ	4531	68.4	1.2	.5	.3	.3	.3	.7	.3	17.0	.3	1.0	0	7.7	2.2	0	17.3	8.8	25.0	8.9	6	CR	11	97:1:2	2.9	.46	
MCJ	4549	65.3	1.8	.3	0	1.0	0	1.8	0	20.0	.3	.3	.5	6.8	2.0	.3	20.3	7.8	27.1	1.8	26	CR	13	95:2:2	2.3	.41	
MCJ	4557	71.0	1.7	.7	.7	0	1.0	4.2	2.0	15.6	0	0	2.2	.5	0	.5	15.6	.5	16.1	4.3	0	SL	5	89:2:9	3.3	.51	
ROB	4447	61.8	1.7	.5	.7	0	0	.7	.5	2.3	29.7	0	.7	0	0	1.5	31.9	0	31.9	1.1	0	CR	1	94:1:2	3.0	.56	+
ROB	4457	63.0	1.3	1.3	.3	.8	0	1.0	.3	25.0	2.5	.5	0	2.8	1.5	0	27.5	3.5	30.3	5.6	0	CH	2	95:1:2	2.3	.42	
ROB	4479	50.8	.5	.5	.5	0	.5	0	0	.3	46.8	0	0	0	0	.3	47.1	0	47.1	0	0	CR	4	97:1:1	3.3	.42	
ROB	4483	56.4	.7	1.5	.5	.5	.3	3.9	.3	5.7	15.5	0	1.5	8.9	3.7	.7	21.1	10.7	30.3	12.7	0	CR	15	88:4:7	3.1	.45	
ROB	4489	64.5	1.7	1.2	1.0	.5	1.7	.5	.5	23.3	.7	.7	0	2.5	2.2	.5	23.9	3.6	26.4	4.2	0	SL	13	94:1:2	2.8	.65	
ROB	4495	59.5	1.8	.8	0	.3	.5	0	.8	25.3	1.5	.3	0	6.0	3.3	.3	26.8	7.6	32.8	4.5	8	CR	7	96:1:2	2.1	.60	
A1	4422	60.1	1.7	1.2	.5	.7	1.7	1.2	.7	14.9	2.9	.7	1.7	5.6	5.6	.5	17.8	8.4	23.4	7.1	0	CR	12	90:3:5	3.0	.44	
A1	4453	67.0	.5	1.5	.7	0	1.0	3.0	.2	0	0	0	23.6	0	0	2.7	0	0	0	0	63	SL	2	92:1:5	4.6	.60	
A1	4456	61.8	2.0	.8	.3	0	0	.3	.3	21.8	9.0	.3	0	3.3	.5	0	30.8	3.5	34.1	1.3	0	CH	5	98:1:1	2.1	.45	
A1	4469	55.8	2.5	1.2	.7	.3	1.2	2.2	.5	16.5	2.7	4.7	.7	6.6	4.4	0	19.2	8.8	25.8	10.2	61	CR	4	90:1:6	4.0	.59	
A1	4476	60.0	1.3	1.5	.5	0	0	3.8	0	11.0	11.5	.8	.5	6.6	2.8	.5	22.5	7.4	28.5	3.5	5	SL	3	91:1:6	3.6	.63	
HO	4569	63.3	2.2	1.0	1.2	.2	1.0	1.7	.7	15.4	9.0	.2	3.2	0	.7	.2	24.4	.4	24.4	.7	0	CR	1	91:1:5	4.5	.49	
HO	4582	58.1	1.5	.3	.3	.3	1.2	1.5	0	5.4	14.0	.5	12.6	1.2	3.0	.3	29.4	2.7	30.6	7.2	287	BAY	3	90:1:4	3.7	.75	
HO	4586	64.5	2.0	1.7	.5	0	.3	1.7	.7	18.0	1.7	1.7	.3	4.9	3.2	0	19.7	6.1	24.6	13.4	9	CR	7	93:1:4	4.2	.54	
HO	4601	68.3	3.5	.5	.8	.8	.3	.8	.3	11.8	0	1.5	.3	6.8	4.5	0	11.8	9.0	18.6	9.3	24	CR	21	86:1:2	4.8	.71	
HO	4611	74.1	4.0	1.3	.5	.5	1.3	2.3	0	9.5	1.3	1.0	1.0	.3	2.5	.5	10.8	1.5	11.1	7.7	0	SL	11	93:1:4	4.4	.50	
MOD	4584	66.1	3.0	1.0	.3	.3	.3	1.2	.3	20.0	.5	.7	0	4.7	1.2	.5	20.5	5.3	25.2	5.0	9	CR	6	95:2:3	3.2	.59	
MOD	4586	59.1	5.4	0	0	0	.3	1.2	0	15.5	3.7	4.2	0	5.2	4.2	0	23.0	1.5	23.7	3.4	125	CR	12	97:1:2	3.4	.59	
MOD	4590	69.4	3.0	.3	.5	.3	.7	.5	.3	22.5	.5	0	0	.7	1.5	0	5.8	7.4	10.4	10.5	0	SL	18	84:1:10	3.6	.52	
MOD	4596	62.1	2.2	.5	1.2	.2	1.0	8.5	1.0	5.6	.3	0	7.3	4.6	5.6	.2	22.2	3.7	24.3	4.3	3	CR	23	90:2:8	2.6	.60	
MOD	4601	61.6	3.2	.5	.3	.5	1.0	4.4	.7	20.0	2.2	0	.7	2.0	3.4	0	22.6	.1	22.6	1.4	0	SL	31	97:1:3	3.9	.54	
MOD	4629	65.0	4.5	.3	0	0	1.5	.5	0	7.0	20.6	0	.5	0	.3	.5	28.3	3.7	29.8	6.0	0	SL	14	97:1:2	3.6	.66	
MOD	4646	67.8	2.7	.3	.3	0	.5	.5	0	19.1	3.2	.3	0	2.5	2.5	1.2	19.2	7.3	24.4	8.9	0	CR	8	86:1:4	2.6	.56	
BH	4554	60.6	2.5	.7	1.5	0	1.0	11.9	0	0	0	.3	15.8	2.7	2.0	1.0	0	3.7	2.7	9.3	46	CR	6	80:1:16	4.6	.55	
BH	4561	73.9	2.9	.7	1.5	0	0	2.9	1.2	4.6	0	0	3.2	3.2	5.1	.7	4.6	5.7	7.9	9.8	5	CH	13	92:1:6	4.4	.54	
BH	4575	67.8	1.8	.3	.5	.8	.8	1.8	.5	20.5	.3	.8	0	1.3	2.8	.5	20.8	2.6	22.1	3.3	0	CH	27	93:2:5	3.4	.63	
BH	4618	68.7	1.7	0	.3	0	.5	1.0	0	17.1	0	.5	.3	6.0	3.7	.3	17.1	7.0	23.5	10.1	2	CR	24	97:1:2	2.3	.62	
BH	4630	69.9	3.0	1.0	.3	.3	.3	1.7	0	12.1	0	0	.5	6.9	4.2	0	12.1	9.0	18.6	9.7	21	CR	12	95:1:3	2.3	.71	
BH	4657	62.6	1.0	.3	.5	0	.3	0	0	0	34.3	0	0	0	1.0	.3	34.8	.5	34.9	5.6	0	CR	3	93:1:1	2.2	.66	+
CWS	4645	54.2	.5	1.2	.8	0	.8	15.7	0	0	.3	0	25.1	0	0	1.5	.3	0	.3	2.1	3	SL	3	84:1:14	4.2	.63	
CWS	4653	64.7	1.2	1.5	.5	.3	.5	8.3	0	2.9	2.5	.5	6.8	4.0	6.8	.5	4.4	7.4	8.4	11.6	10	CR	3	79:2:14	2.8	.64	
CWS	4655	65.6	1.7	.7	1.0	0	.7	10.8	0	1.3	0	.7	12.5	0	0	4.9	1.2	0	1.3	4.1	0	SL	5	90:2:14	3.0	.81	
CWS	4660	69.2	1.2	1.7	1.0	.7	.3	2.2	0	3.0	1.7	.3	1.0	7.9	8.7	1.2	4.7	12.3	13.2	8.2	4	CR	10	91:1:3	2.7	.62	
CWS	4665	61.7	1.7	.8	.8	.5	.5	5.2	0	15.3	.3	.3	.3	7.1	4.9	.3	15.5	9.6	22.4	10.3	15	CR	15	89:1:8	2.8	.54	
CWS	4679	65.0	2.2	.8	.8	.5	.3	2.7	.3	12.5	0	.3	.3	6.0	6.7	.3	12.5	7.0	19.2	3.7	3	CR	1	92:1:4	2.8	.55	

give similar results. Figure 9 is a plot of thin section porosity vs. porosimeter porosity for all samples; the linear regression line and equal value line are shown also. The correlation coefficient is 0.69, which is significant at P = 0.01. Values of porosity measured by porosimeter tend to be higher than those determined by point counts, a phenomenon also noticed by Stanton and McBride (1976). Microporosity between clay flakes in matrix, shale clasts, and clay cements cannot be seen in thin section, but it can be measured by the porosimeter, which accounts for some of the differences. In Figure 10, only the samples with a mean grain size of medium or fine sand, which generally have less clay matrix, were plotted. The correlation coefficient here is higher, 0.76, and the linear regression line is quite close to the line of equal values.

The relationship between thin section porosity and log permeability is shown in Figure 11. The correlation coefficient is 0.53. The plot of porosimeter porosity vs. log permeability is very similar, with a correlation coefficient of 0.51. These are both significant at P = 0.01.

Thin Section Point Counts

Thin sections were made from each of the sample plugs after the porosity and permeability had been measured by porosimeter. The plugs were impregnated with blue epoxy to enhance pore space. Before cover slips were added, the

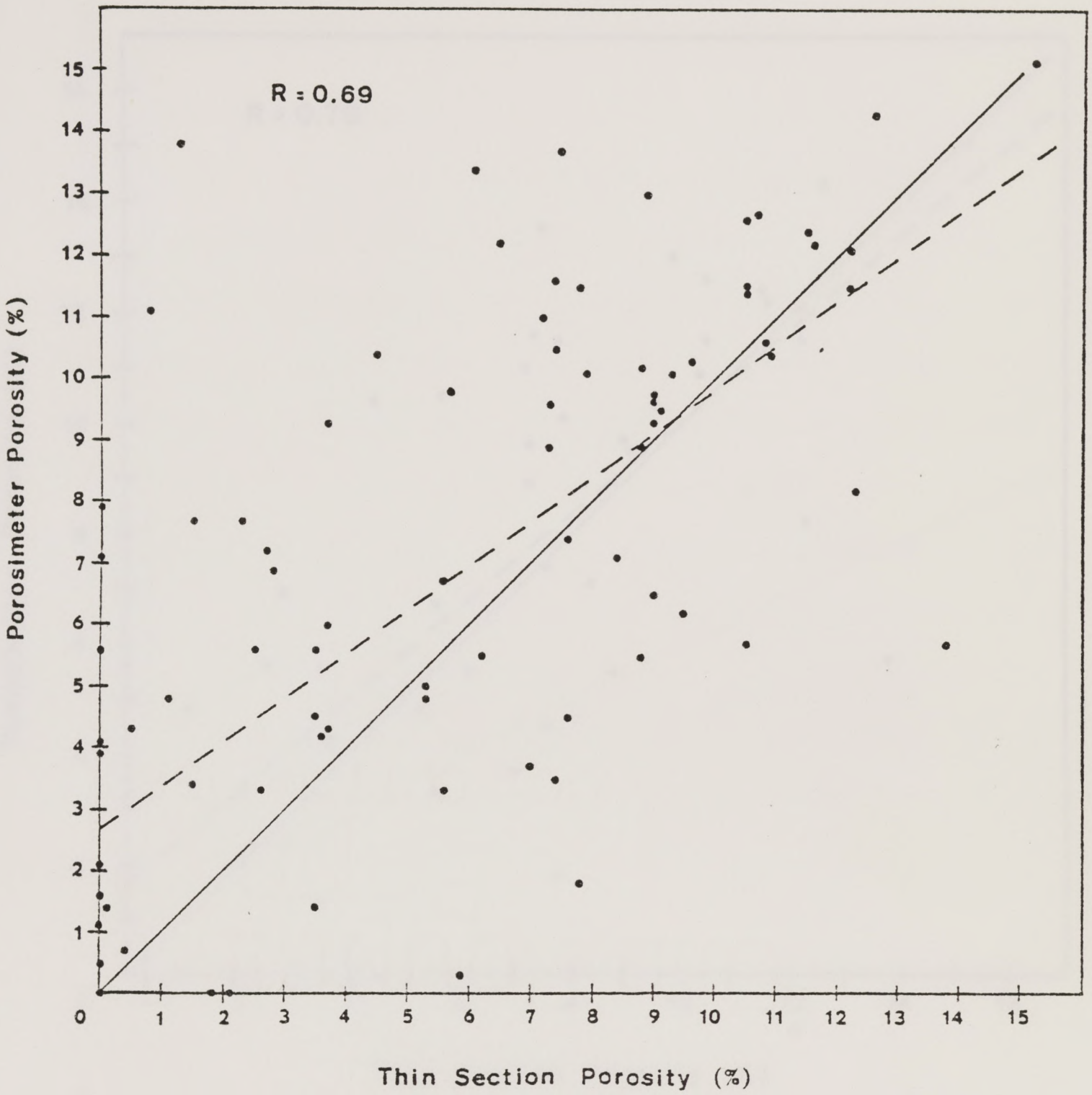

Figure 9. Plot of thin section porosity versus porosimeter porosity. Solid line is equal-value line, dashed line is linear regression line, R = 0.69.

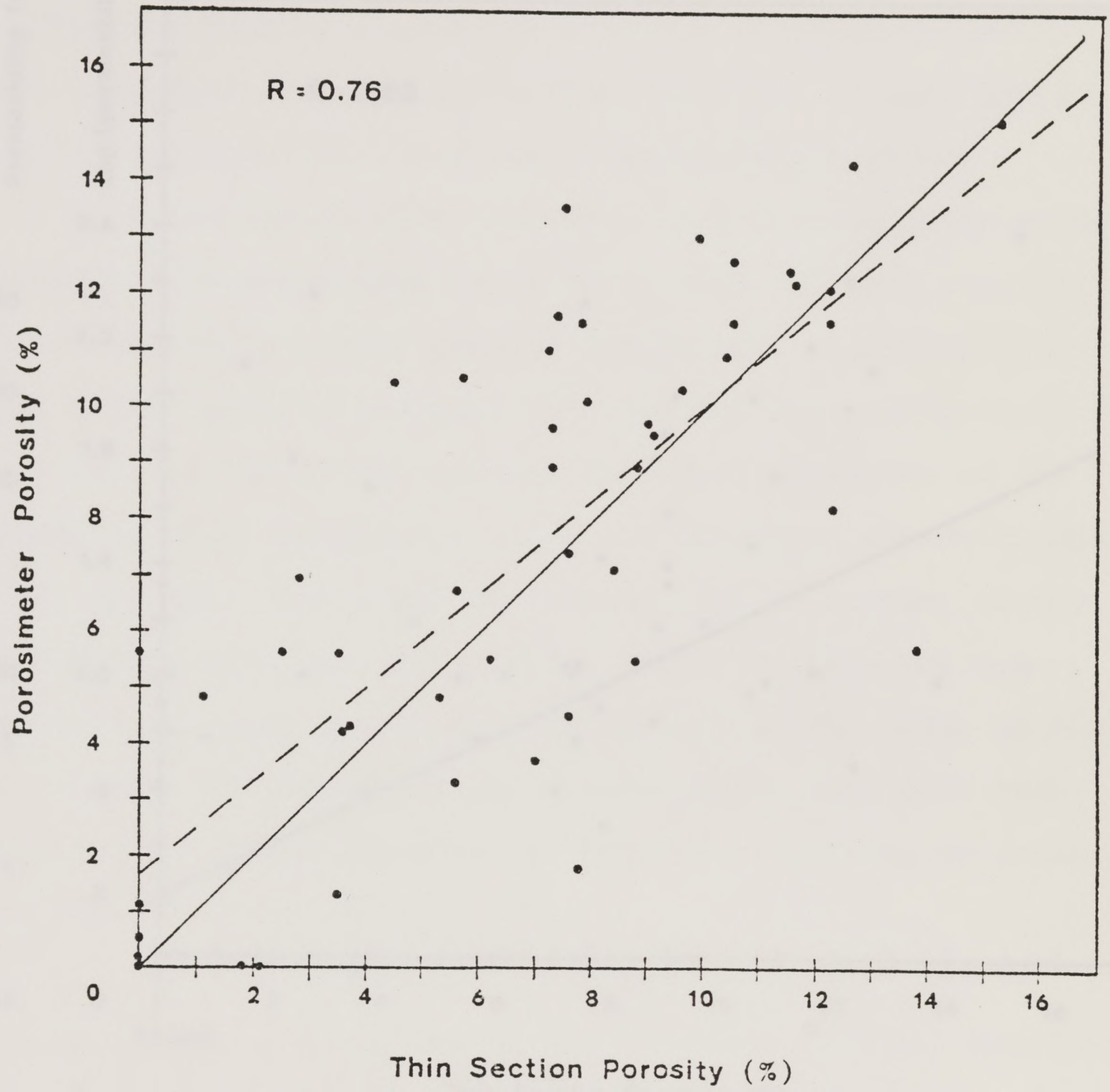

Figure 10. Plot of thin section porosity versus porosimeter porosity for medium and fine sandstone samples. Solid line is equal-value line, dashed line is linear regression line, R = 0.76.

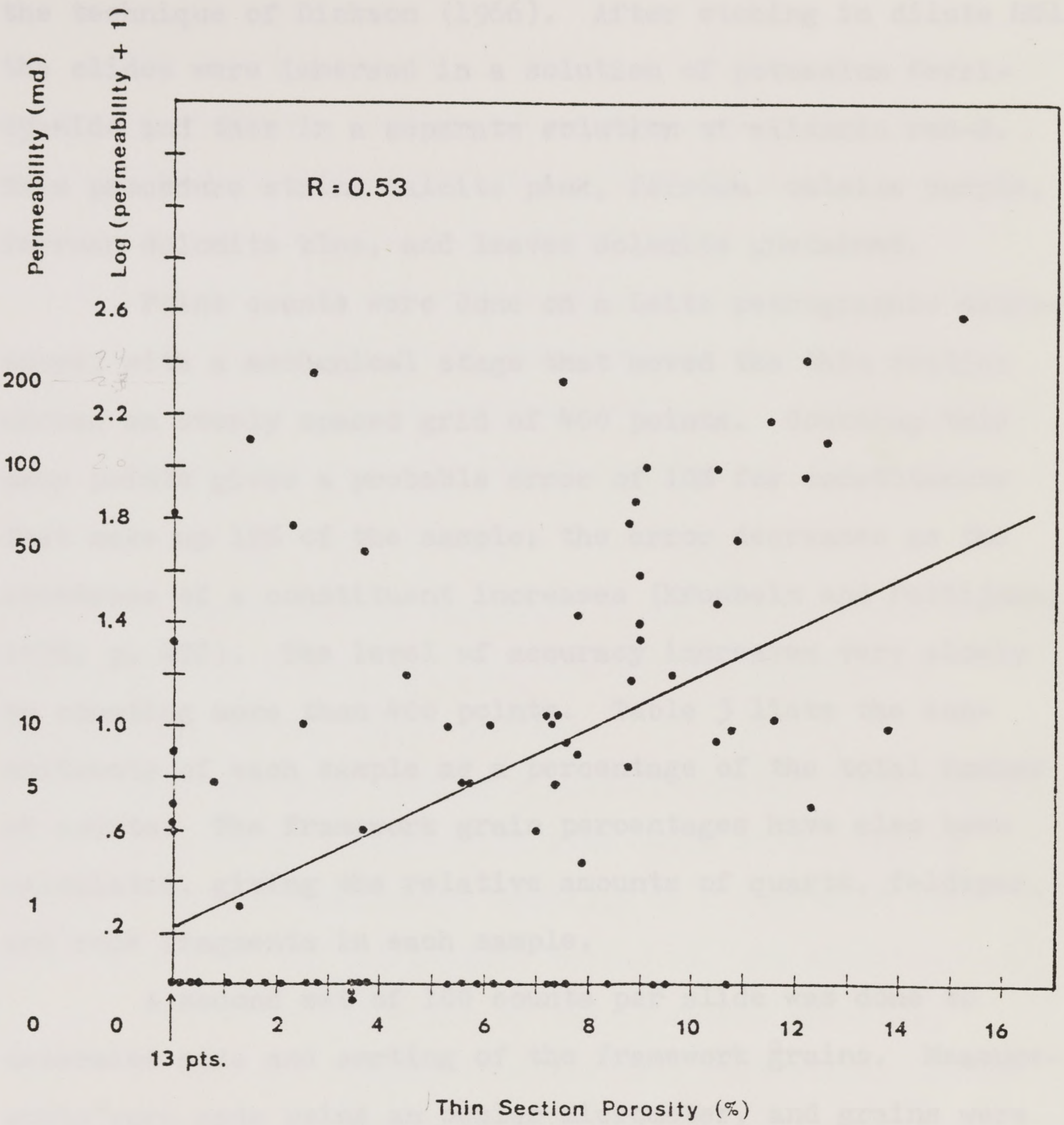

Figure 11. Relationship between thin section porosity and log (permeability +1). Linear regression line has correlation coefficient of R = 0.53.

slides were stained to differentiate carbonate minerals using the technique of Dickson (1966). After etching in dilute HCl, the slides were immersed in a solution of potassium ferricyanide and then in a separate solution of alizarin red-S. This procedure stains calcite pink, ferroan calcite purple, ferroan dolomite blue, and leaves dolomite unstained.

Point counts were done on a Leitz petrographic microscope, with a mechanical stage that moved the thin section across an evenly spaced grid of 400 points. Counting this many points gives a probable error of 10% for constituents that make up 10% of the sample; the error decreases as the abundance of a constituent increases (Krumbein and Pettijohn, 1938, p. 472). The level of accuracy increases very slowly by counting more than 400 points. Table 3 lists the constituents of each sample as a percentage of the total number of counts. The framework grain percentages have also been calculated, giving the relative amounts of quartz, feldspar, and rock fragments in each sample.

A second set of 100 counts per slide was done to determine size and sorting of the framework grains. Measurements were made using an ocular micrometer, and grains were assigned to $\frac{1}{2}$ phi-unit size classes. Mean and standard deviation were calculated for each sample by the method of moments (Folk, 1974), using a Wang 2200 Series Program for mean, variance, and standard deviation of grouped data. This textural information is listed in Table 3.

Multiple Regression Analysis

The percentages of porosity, pre-cement porosity, and quartz and carbonate cement collected by point counting were analyzed statistically using multiple regression. Multiple regression describes the relationship between any number of independent variables and one dependent variable, analyzing how much of the variation in the dependent variable is explained by each of the independent variables. The relationship is summarized in a regression equation of the form:

$$Y = B_o + B_1X_1 + B_2X_2 + ... + B_mX_m$$

where Y is the dependent variable, $X_1, X_2 .... X_m$ are the independent variables, and $B_o, B_1 .... B_m$ are partial regression coefficients (Davis, 1973, p. 415).

This equation defines a multidimensional surface, and it is analogous to a regression line which statistically relates a single independent variable to a dependent one. For given values of the independent variables, the equation can be used to predict the value of the dependent variable.

A computer program from the SPSS Statistical Package for the Social Sciences (Nie et al., 1975) was used to perform the multiple regression. The variables were entered in an order determined by the programmer (the computer will enter them in a random order if desired), and after each one was entered the regression equation was printed. The correlation coefficient, r, and coefficient of determination, r^2, were

also printed after each step for each variable. The correlation coefficient measures how well the data fit the regression surface. In multiple regression, r varies between -1 and 1, a correlation coefficient of 1 indicating a perfect fit, -1 a perfect inverse correlation, and 0 meaning there is no correlation at all. The coefficient of determination has a value between 0 and 1, and measures how much of the variation in the dependent variable is explained by the independent variables entered up to that point. Besides the total r^2, the r^2 for each variable alone is printed so that the influence of every variable can be seen clearly.

After all the variables have been entered, the final regression equation is printed, and a summary table presents the correlation coefficient and coefficient of determination for all of the variables. Statistics for testing the significance of each variable's contribution are also given.

If the so-called "independent" variables are not truly independent of each other, the order in which they are entered will affect the coefficient of determination assigned to each one. If two independent variables are closely related to each other, the one entered first will explain their mutual effect on the dependent variable, so that when the second one is entered, its effect will have already been assigned to the first variable. It will have a low coefficient of determination, whereas if it had been the first variable entered, it would have had the larger r^2. The more closely the variables are related, the larger is the overlap between

them. The partial regression coefficients, however, do not change with the order in which the variables are entered, so the regression equation is always the same.

Porosity, pre-cement porosity, quartz and carbonate cement were all analyzed as dependent variables, and the results are discussed in later sections. The independent variables used were detrital quartz, quartz cement, total cement, pre-cement porosity, shale and matrix, distance from shale, phi mean grain size, and phi sorting.

PETROGRAPHY

Classification

A complete list of the composition of each sample is given in Table 3. Appendix 2 explains all the categories and their abbreviations used in this tabulation.

The samples were all classified by framework grain composition using Folk's (1974) classification. Sublitharenites are the most abundant sandstones, but quartzarenites, litharenites, and subarkoses also occur (Fig.12). Most rock fragments are clay clasts which were probably ripped up from and redeposited in the deltaic environment. Except for these clasts the samples are very mature, and nearly all would be called quartzarenites. The slope samples tend to have more clay clasts than either the channels or crest. The latter two are higher energy environments and the weak clasts were more easily destroyed in them.

The percent quartz vs. matrix of each of the samples was plotted to see if this would separate samples from different environments, a technique suggested by Ethridge and others (1975). However, there was so much overlap among samples from the different environments that this was not a satisfactory method of discrimination.

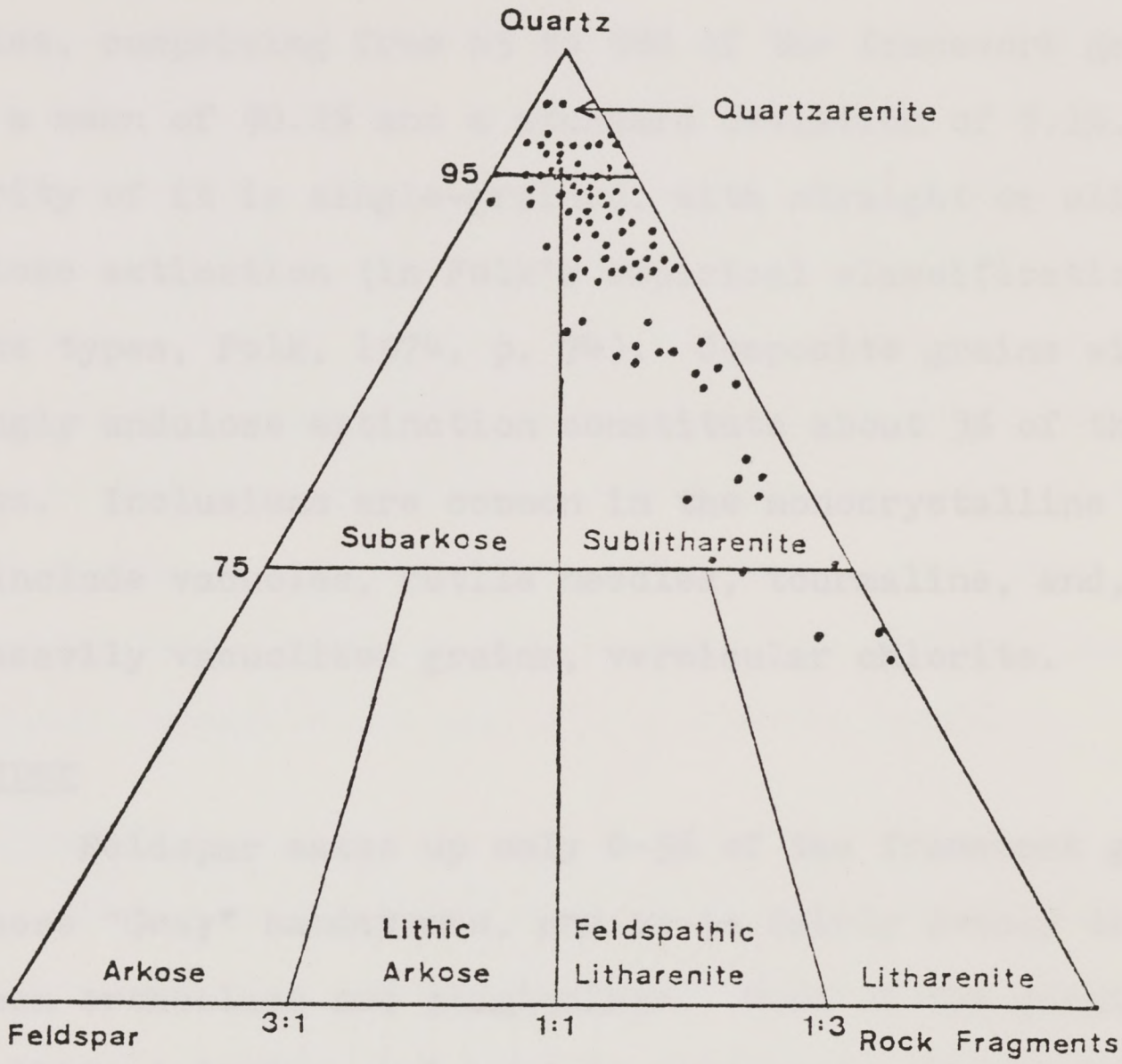

Figure 12. Classification of "Gray" sandstone samples using Folk's (1974) classification.

Detrital Mineralogy

Quartz

Quartz is the most abundant mineral in all of the samples, comprising from 65 to 98% of the framework grains, with a mean of 90.2% and a standard deviation of 7.1%. The majority of it is single-grained, with straight or slightly undulose extinction (in Folk's empirical classification of quartz types, Folk, 1974, p. 74). Composite grains with strongly undulose extinction constitute about 3% of the total quartz. Inclusions are common in the monocrystalline quartz, and include vacuoles, rutile needles, tourmaline, and, in a few heavily vacuolized grains, vermicular chlorite.

Feldspar

Feldspar makes up only 0-5% of the framework grains in these "Gray" sandstones, and it is fairly evenly divided between orthoclase and plagioclase. Most of the plagioclase has albite twinning, but some is untwinned. The maximum extinction angle of albite twins, determined by the Michel-Levy method, was 17°, indicating a sodic plagioclase. Potassium feldspar comprises 0-2% of the framework grains; there is a trace of microcline, but the majority is orthoclase.

The feldspars show a wide range in alteration. Some grains appear fresh and completely unaltered, while others have been vacuolized, or, rarely, sericitized. Calcite replacement of feldspars was common. Most of the calcite cement has since been removed, but in a few samples there are

still inclusions of it within feldspar grains (Fig. 13). Skeletal wreckage remains from grains that were not completely replaced by calcite (Fig. 14). These "Swiss cheese" feldspar grains have ragged boundaries and corroded interiors, and in some plagioclase grains the holes tend to follow extinction bands. Feldspar wreckage like this was also found by Lindquist (1976) and Stanton (1977) in Tertiary Gulf Coast sandstones.

In many samples the only evidence of an original framework feldspar grain is a pore space too large to have formed during deposition (Fig. 15). These pores must have originally been framework grains that were entirely replaced by calcite cement which was itself removed later.

Rock Fragments

Clay clasts ripped up from mud layers near the site of deposition are the most abundant rock fragments. Many of these clasts have been partially or completely replaced, like the feldspars, and only remnants of the original grains remain (Fig. 16). This secondary porosity was also probably caused by replacement and removal of calcite cement.

There are rare grains of detrital chert and chalcedony, true sedimentary rock fragments. There are also a few metamorphic rock fragments, which constitute 0-3% of the framework grains. Most of the latter are fine-grained, low-rank metamorphic rocks such as slates or phyllites, but there are some unusual grains of quartz with "beards" of muscovite

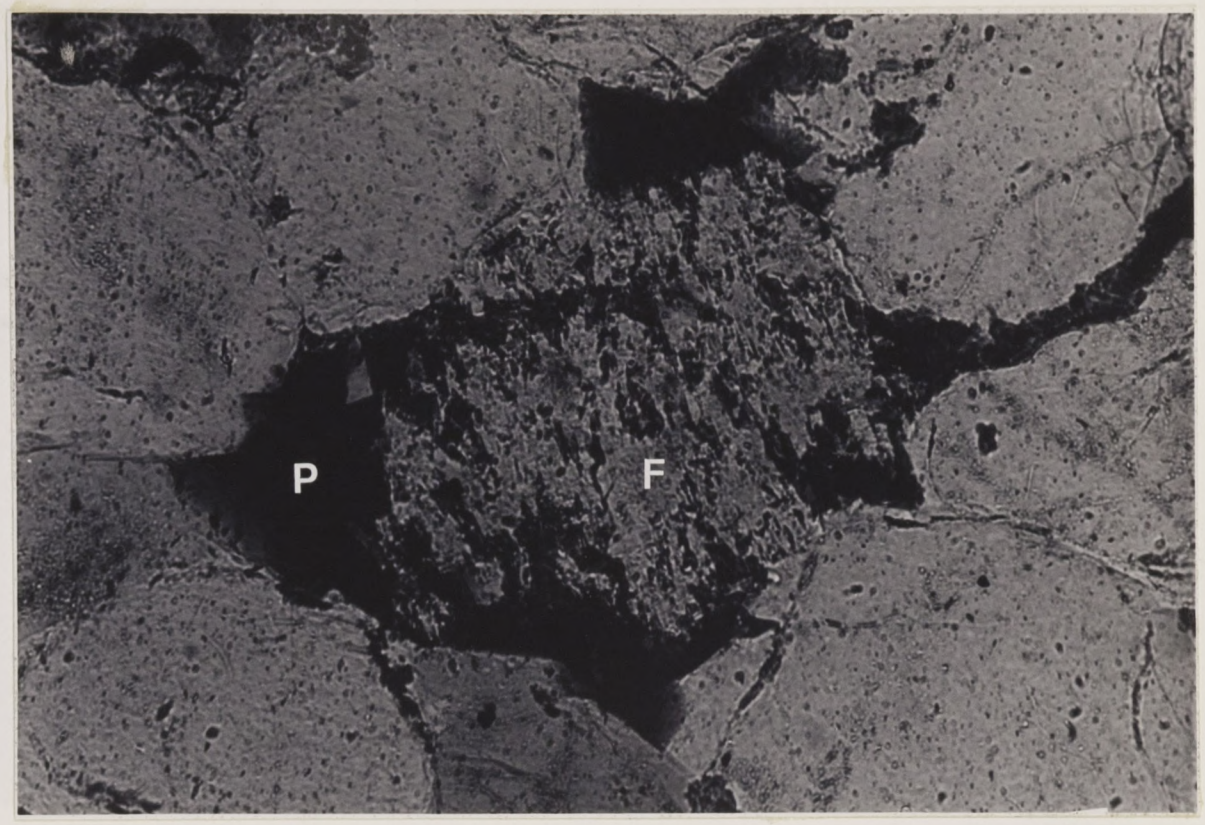

Figure 13. Calcite cement inside feldspar grain in sample BH 4657. The dark material labeled C is calcite cement; the feldspar grain is labeled F. Bar = 0.1 mm.

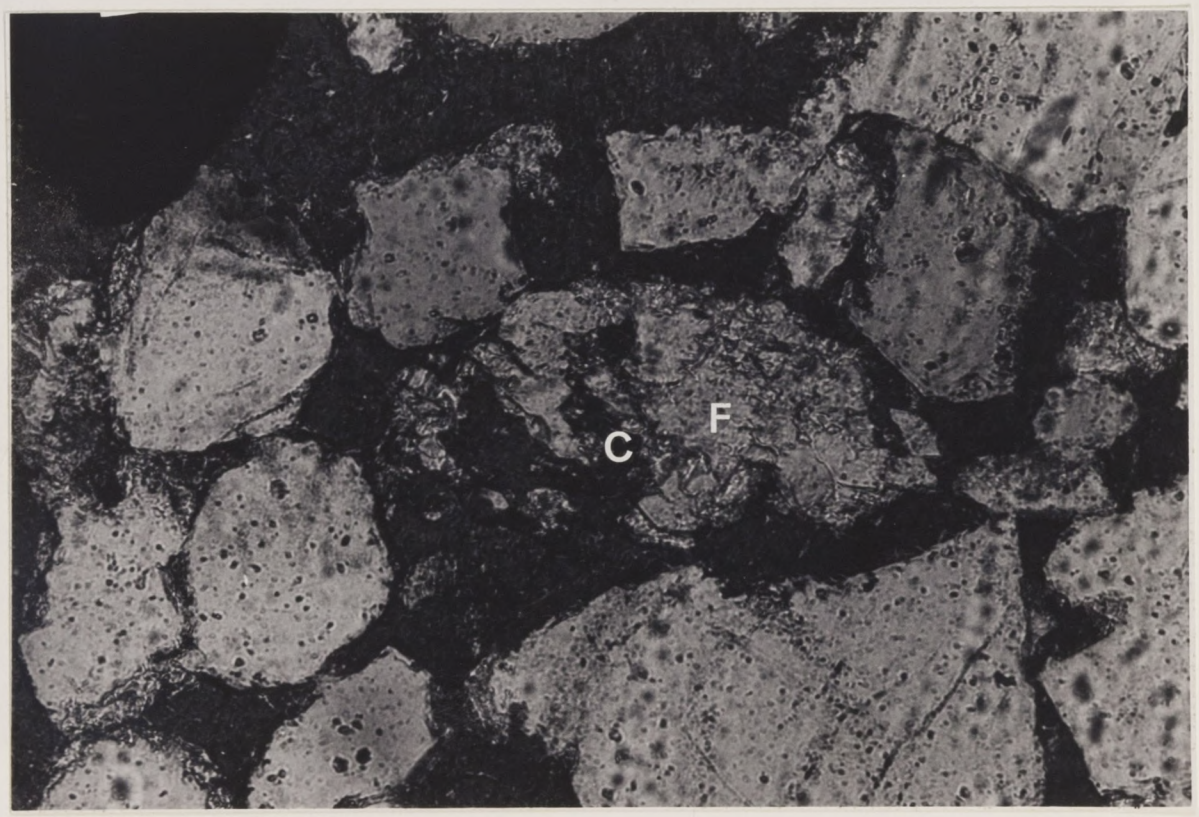

Figure 14. "Swiss cheese" feldspar grain (F) in sample 3-HOD. Pore space is labeled P. Bar = 0.1 mm.

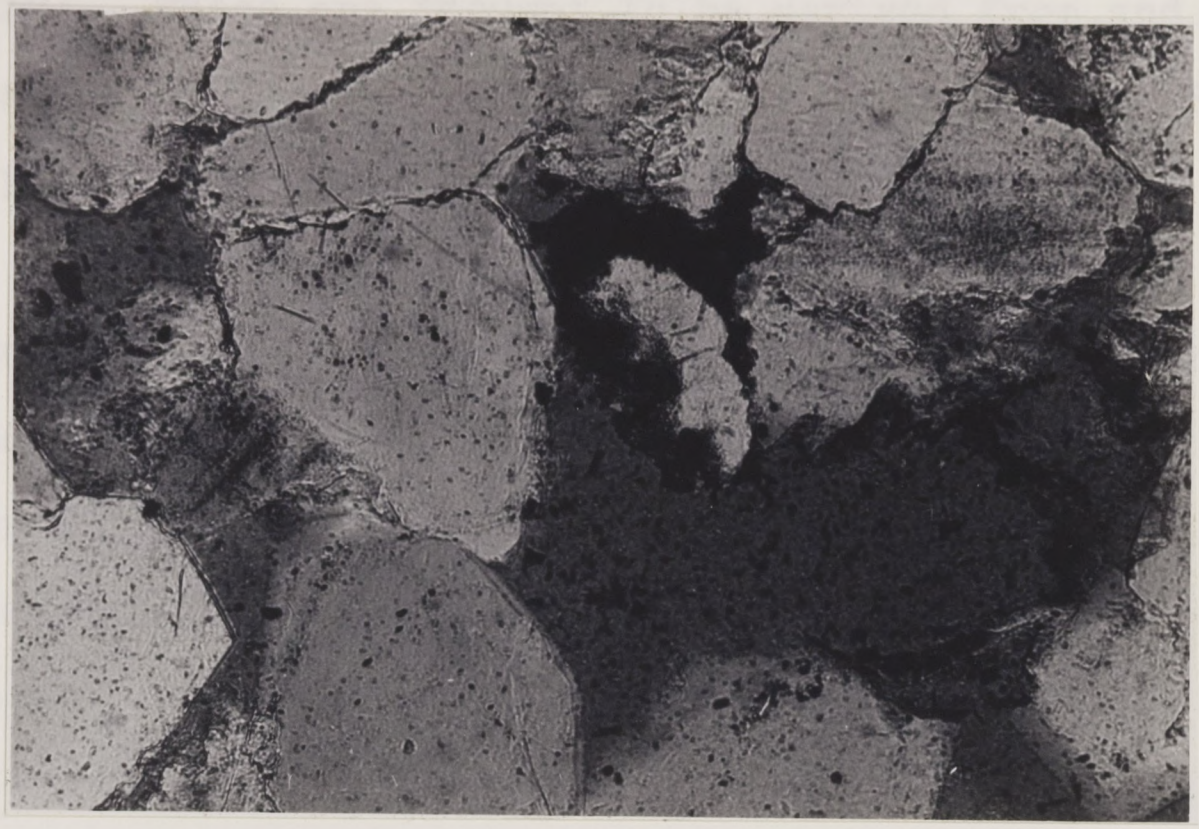

Figure 15. Secondary porosity in sample 2B 4603. Bar = 0.1 mm.

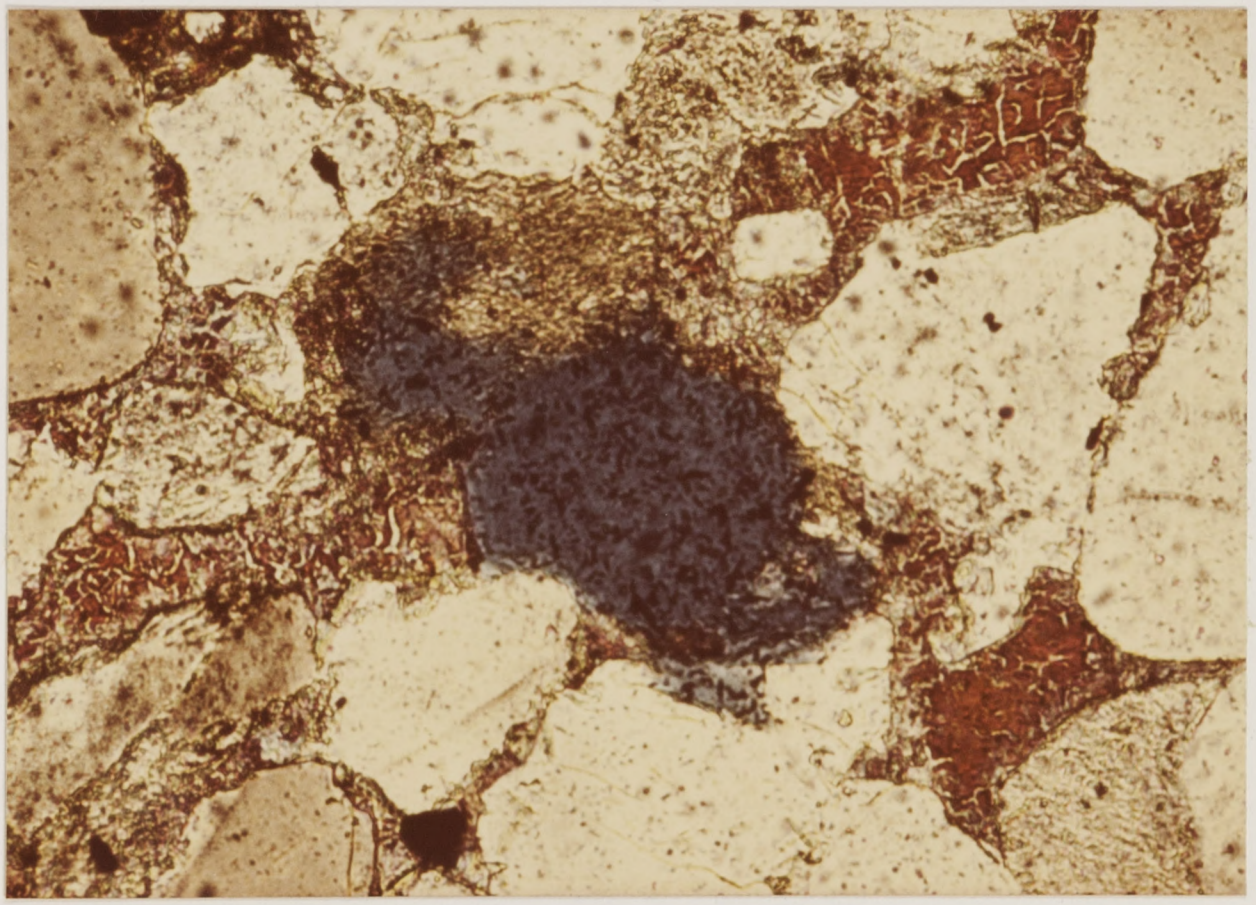

Figure 16. Leached clay clast in sample BH 4657. Bar=0.1mm.

(Fig. 17). These are thought to be derived from and characteristic of detritus from the Ouachita Fold Belt (Folk, 1976, pers. comm.).

Most of the samples contain a trace of "very fine-grained siliceous rock fragments". Their origin is not known, but they appear to be either metamorphosed fine siltstone or metamorphosed chert whose grain size increased during metamorphism. Some of these grains, as well as a few polycrystalline quartz grains, appear to have been partially replaced by calcite cement. Many pores contain fine, angular, siliceous wreckage (Fig. 18). These chips are too small to be identified positively, but they look like quartz, not feldspar, and they may be the disintegrated remains of siliceous rock fragments and polycrystalline quartz replaced by calcite that was later dissolved. Stanton and McBride (1976) have suggested that these silt-sized chips are free to migrate, and that they may cause a reduction in permeability by blocking the throats of some of the pores.

Other Framework Grains

There are trace amounts of heavy minerals present in most of the samples - zircon, tourmaline, magnetite, hornblende, and biotite.

The samples from interdistributary bay environments contain fossil fragments of brachiopods, gastropods, pelecypods, bryozoans, crinoids, foraminifers, green algae, and ostracods. Plant material is common in all of the rocks.

Figure 17. Detrital metamorphic rock fragment with a "beard" of muscovite, sample BOYD 4824. Bar = 0.05 mm.

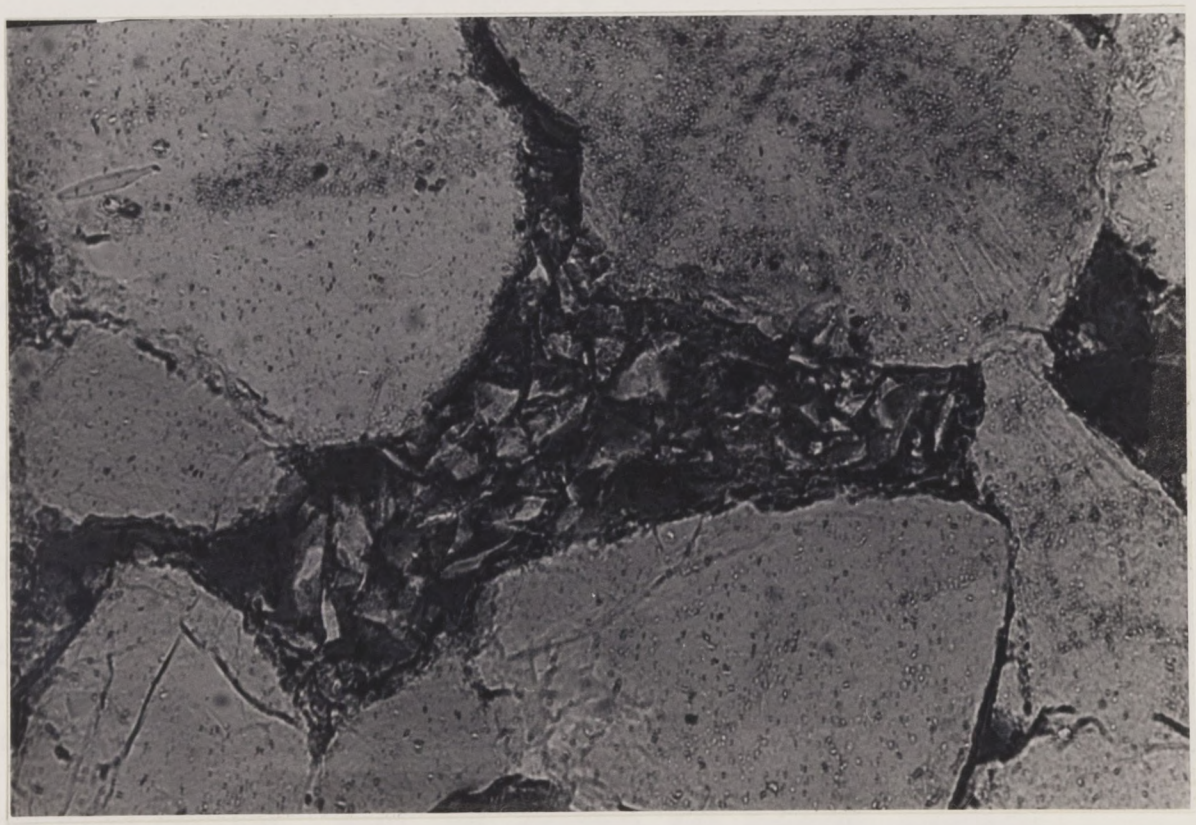

Figure 18. Angular quartz chips inside pores, sample ALR 4642. Bar = 0.05 mm.

It is quite fine and evenly disseminated in the slope samples, but is found in larger pieces, about 0.1 mm, in the crest, channel, and marsh samples.

Diagenetic Mineralogy

Diagenetic cements are abundant in these sandstones, comprising up to 47% of the total volume of the rock as determined by point counting (Table 3). The cement types found in these samples are chlorite, quartz, calcite, kaolinite, barite, ferroan dolomite, and pyrite.

Chlorite

About one-third of the samples contain chlorite rims around some of the quartz grains (Fig. 19). Where they are well-developed the cutans are about 0.01 mm thick, and continuous around the grain. More often though there are gaps in the chlorite which leave portions of the quartz exposed to the surrounding pore space. In these samples cutans have never been seen around any framework grain other than quartz. In some samples there are minor amounts of authigenic chlorite on top of quartz overgrowths. Cutans are most easily recognized and are most abundant in samples without any detrital matrix. They do not fill pores, as matrix would, but form a thin rim around the quartz. The chlorite has weak birefringence, and is green in plane light.

Quartz

Quartz overgrowths, in optical continuity with the

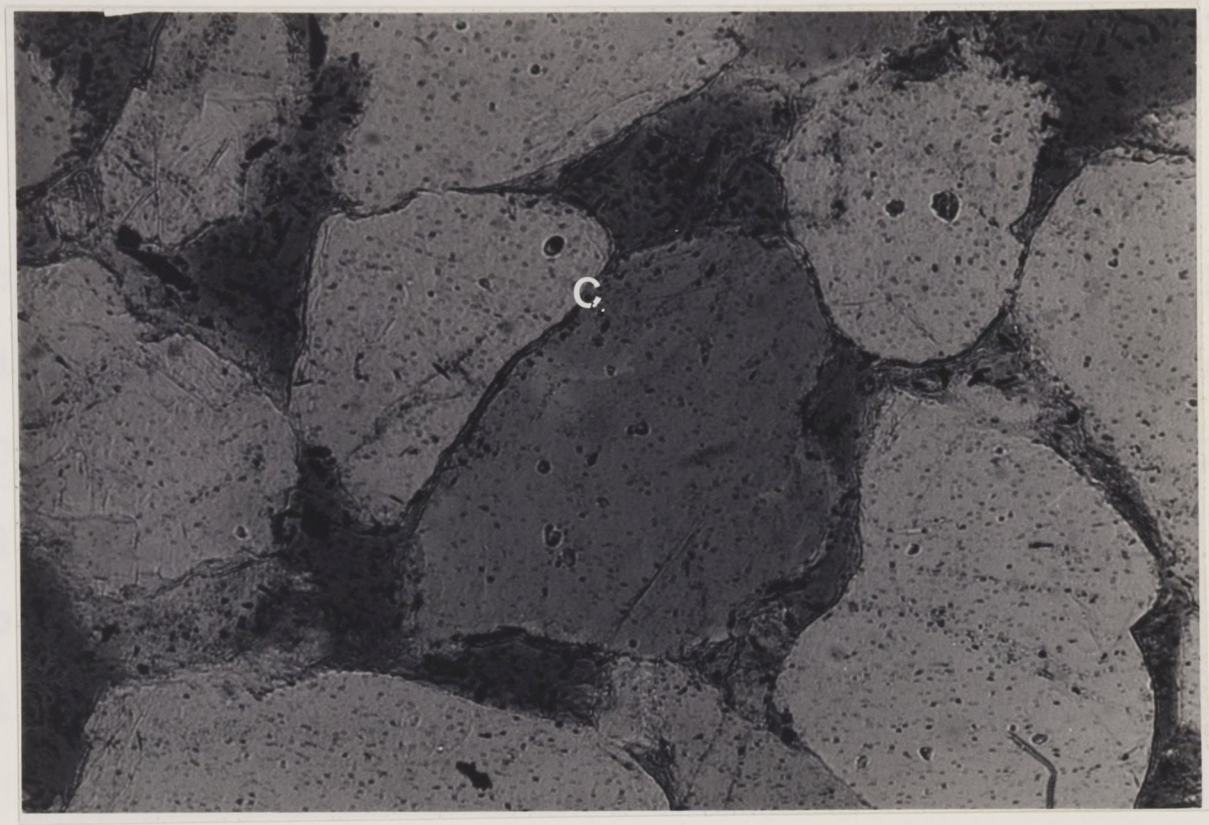

Figure 19. Authigenic chlorite rims around quartz grains, sample ALR 4642. Chlorite labeled C. Bar = 0.1 mm.

Figure 20. Euhedral quartz overgrowths, sample ALR 4630. Bar = 0.1 mm.

detrital quartz grains, are found in all samples except those with large amounts of matrix. Overgrowths constitute up to 31% of the volume of the rock, and the average volume in all samples is 11%. Many overgrowths would have beautiful euhedral faces if there was enough room for them to grow without running into another grain or other cement (Fig. 20,21). Where quartz cement completely filled pores, it forms an interlocking mosaic (Fig. 22). Overgrowths are generally easy to distinquish from detrital grains because of "dust rings" around the grains and the lack of inclusions in the overgrowths.

Quartz cement could not precipitate on detrital grains that were covered by chlorite cutans. Where there were breaks in the chlorite, small, isolated patches of quartz cement formed, leaving "bumps" on the grain surface (Fig. 23, 24). This type of influence of grain coatings on quartz cementation was first reported by Heald and Larese (1974).

Calcite

Only thirteen samples contain calcite cement, in amounts from a trace to 37% of the rock. However, most of the thin sections do show evidence that it was present at one time, in the form of skeletal feldspars and clay clasts, and suspiciously large pore spaces. The remaining cement is present as equant crystals of spar that completely fill what pore space survived after the precipitation of quartz overgrowths (Fig. 25). The average crystal size is 0.08 to 0.3 mm wide.

Figure 21. Quartz overgrowths in sample CWS 4665. Bar = 0.1 mm.

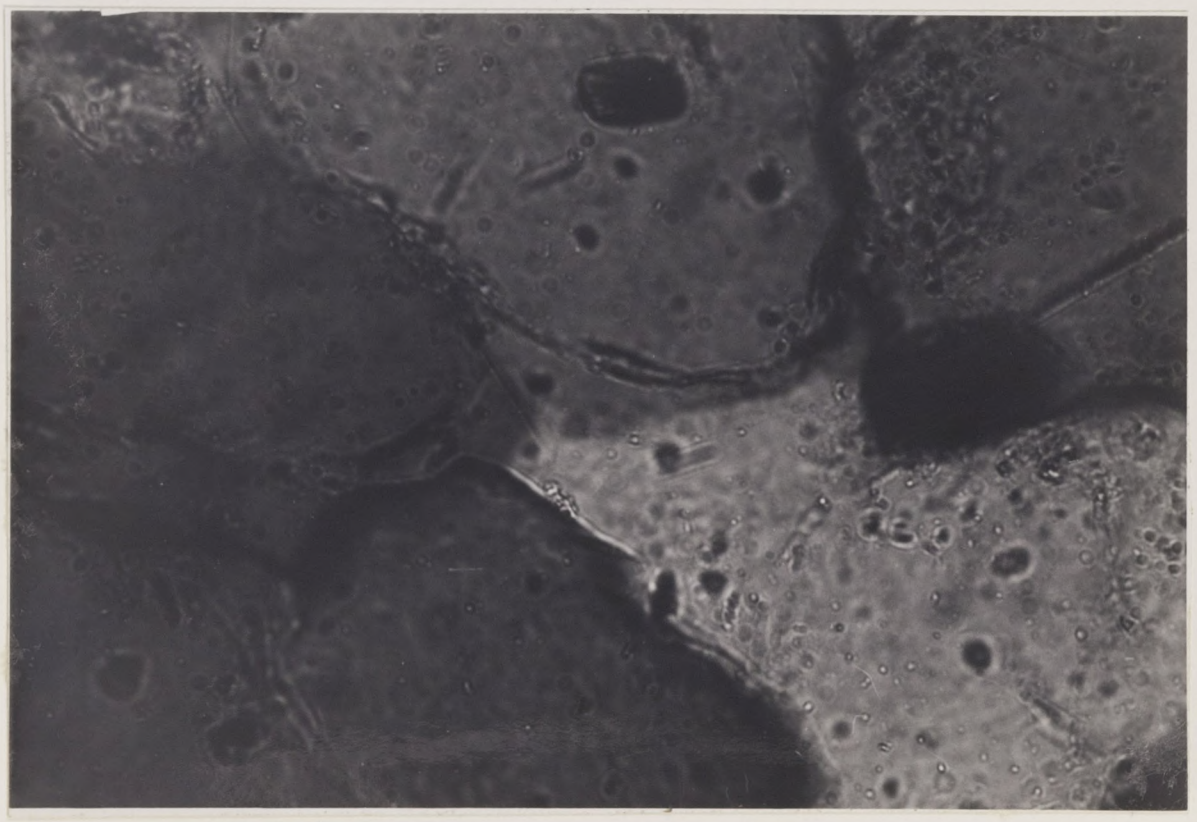

Figure 22. Complete loss of porosity by quartz cementation in sample WAG 4893. Bar = 0.05mm.

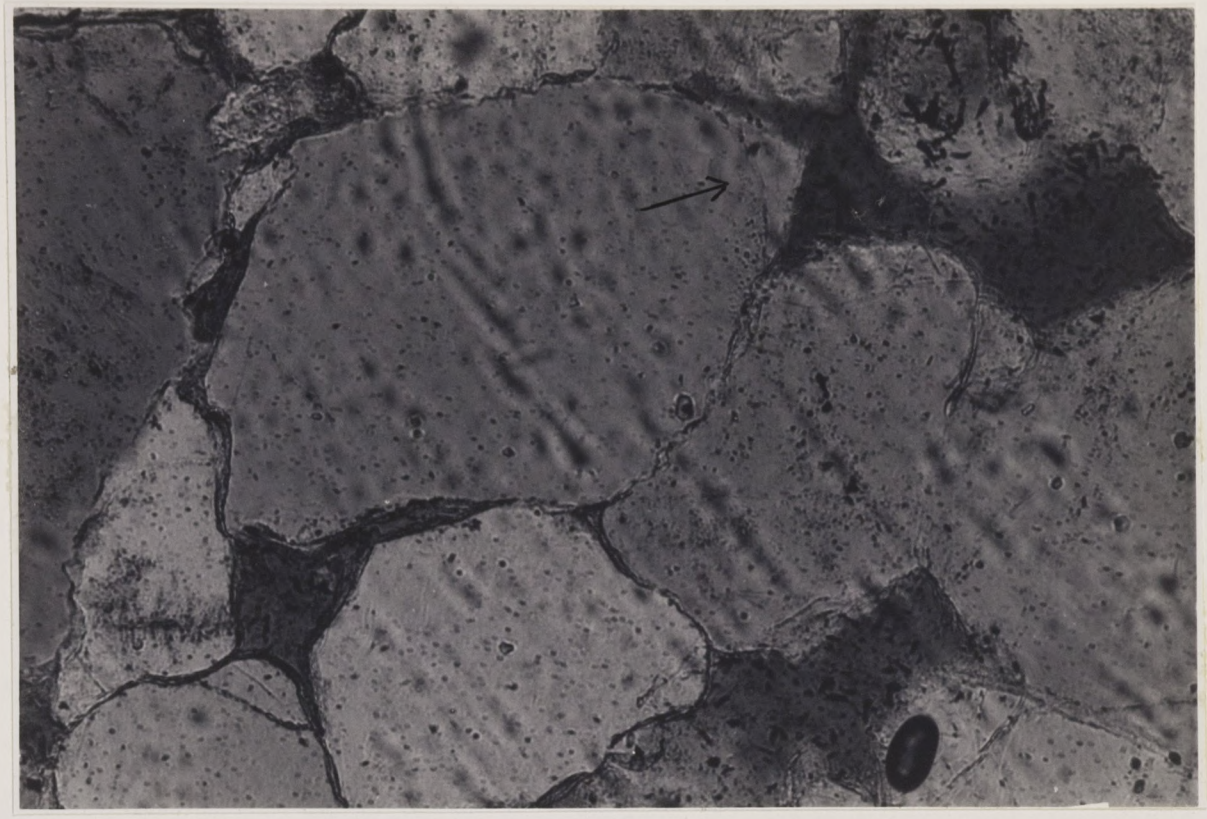

Figure 23. Quartz overgrowths present only where chlorite rims are absent, sample ALR 4642. Bar = 0.1 mm.

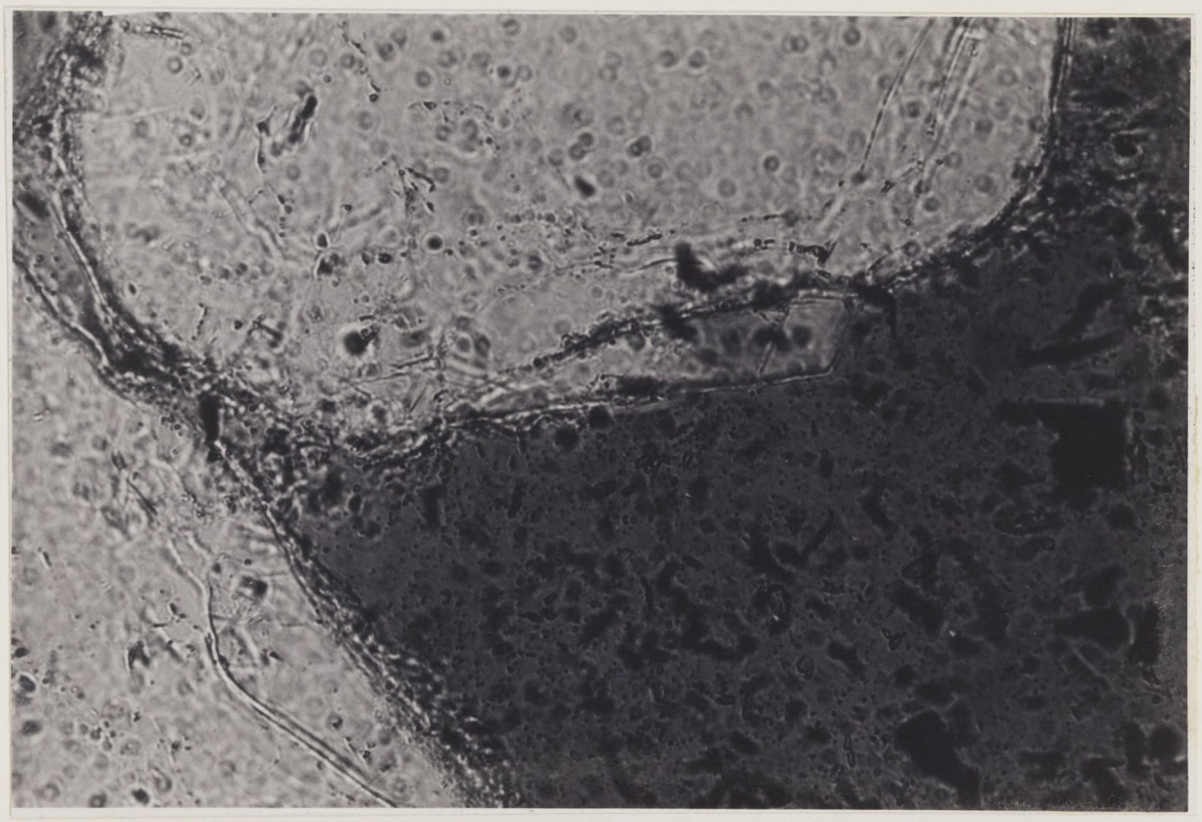

Figure 24. Location of quartz overgrowths controlled by authigenic chlorite, sample ALR 4642. Bar=0.05mm.

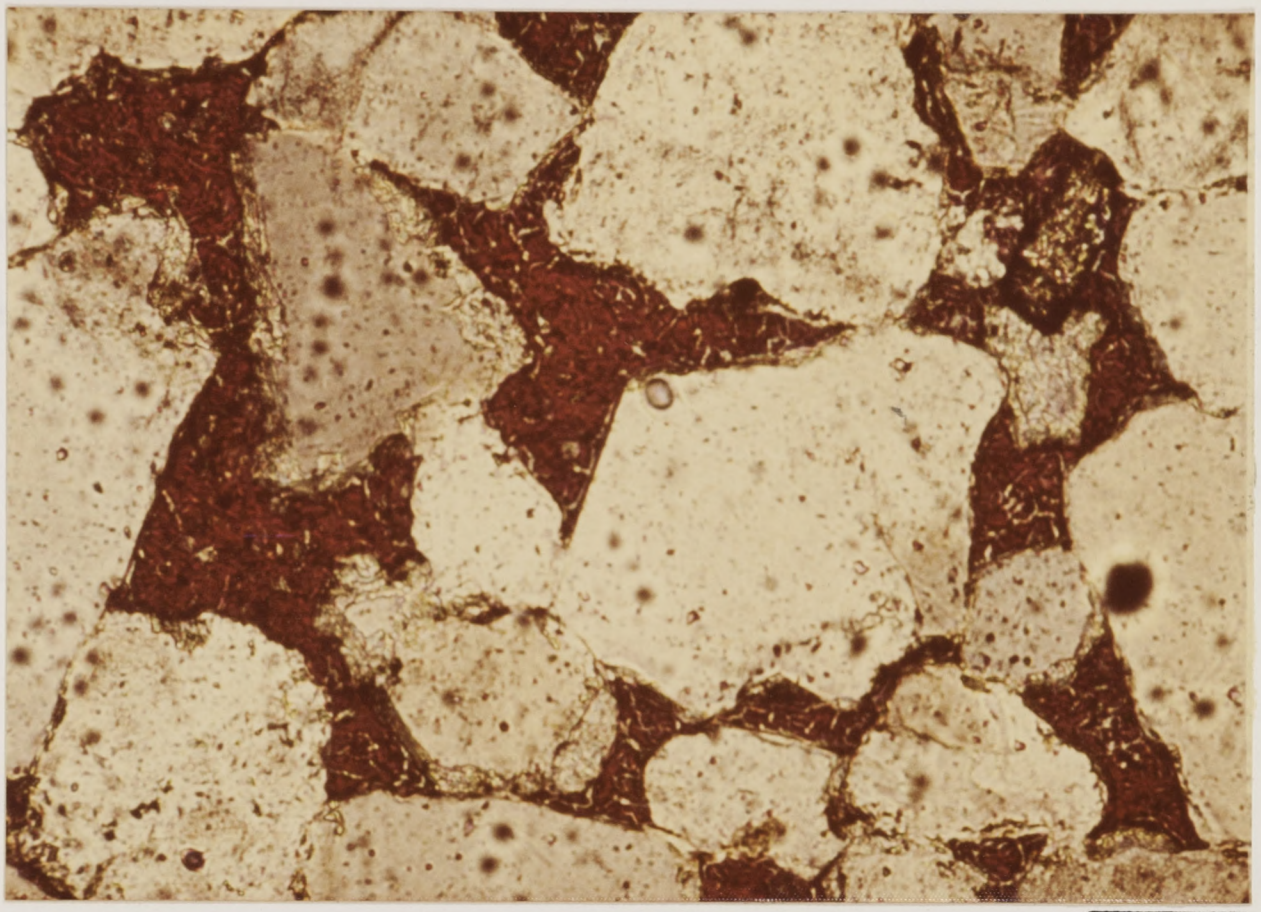

Figure 25. Calcite pore filling cement (red) in sample BH 4657. Bar = 0.1 mm.

Figure 26. "Canals" through quartz grains, sample ALR 4630. Bar = 0.1mm.

There are some patches of cement with poikilitic texture.

Further evidence of removed calcite cement may be provided by thin canals between fragments of quartz grains (Fig. 26). The outlines of the separated fragments and the patterns of inclusions on both sides of the canals indicate that a single grain has been divided. This fabric may have formed when calcite cement forced or replaced its way along a hairline fracture in the quartz grain (McBride, 1976, pers. comm.). Figure 27 illustrates this suggested process.

Kaolinite

Kaolinite cement occurs in isolated patches in most samples, making up from 0-5% of the volume. It precipitates as stacks of flakes that look like worms or books. The kaolinite is almost always found inside secondary pores which formed by the removal of feldspars or clay clasts (Fig. 28).

Barite

Rare, isolated patches of barite cement are found in some thin sections. Barite too seemed to precipitate mostly inside secondary pores. Barite is anhedral in contact with quartz and calcite cement (Fig. 29), but euhedral next to ferroan dolomite (Fig. 30, 31).

Ferroan Dolomite

Ferroan dolomite is the most common carbonate cement in the samples. It comprises 0-47% of the volume of the rocks, with an average volume of 7%. It occurs as poikilotopic

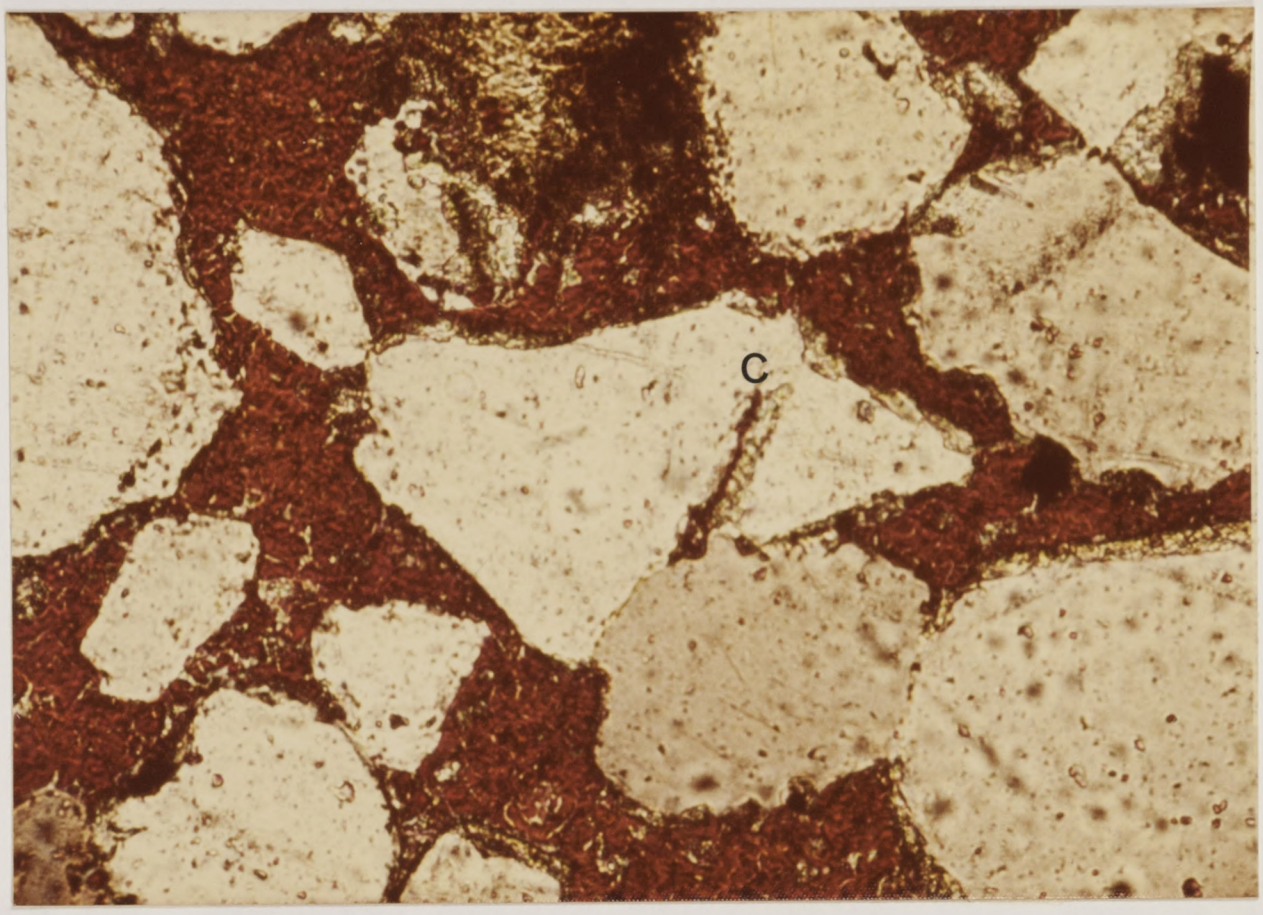

Figure 27. Quartz grain with a thin line of calcite cement (C) through it, sample BH 4657. Bar = 0.1 mm.

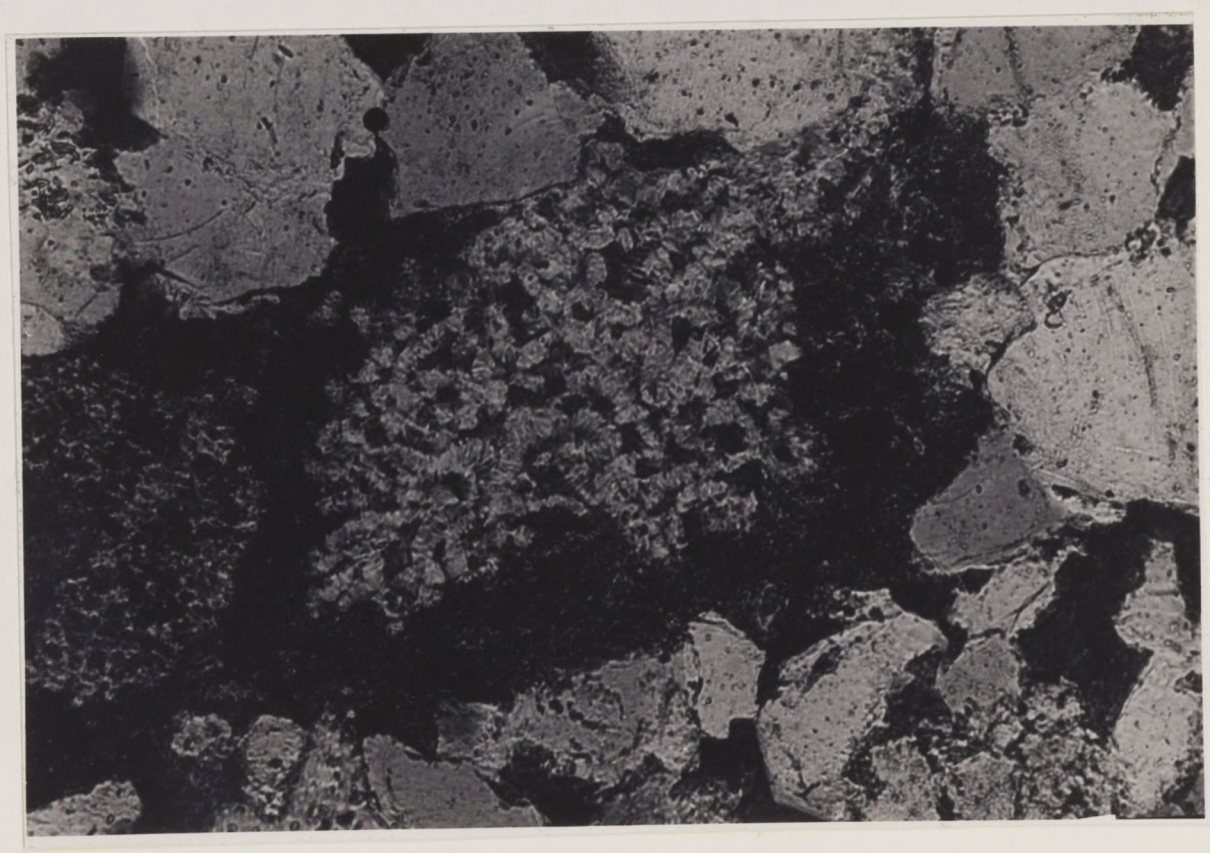

Figure 28. Authigenic kaolinite inside a secondary pore, sample WAG 4896. Bar = 0.1 mm.

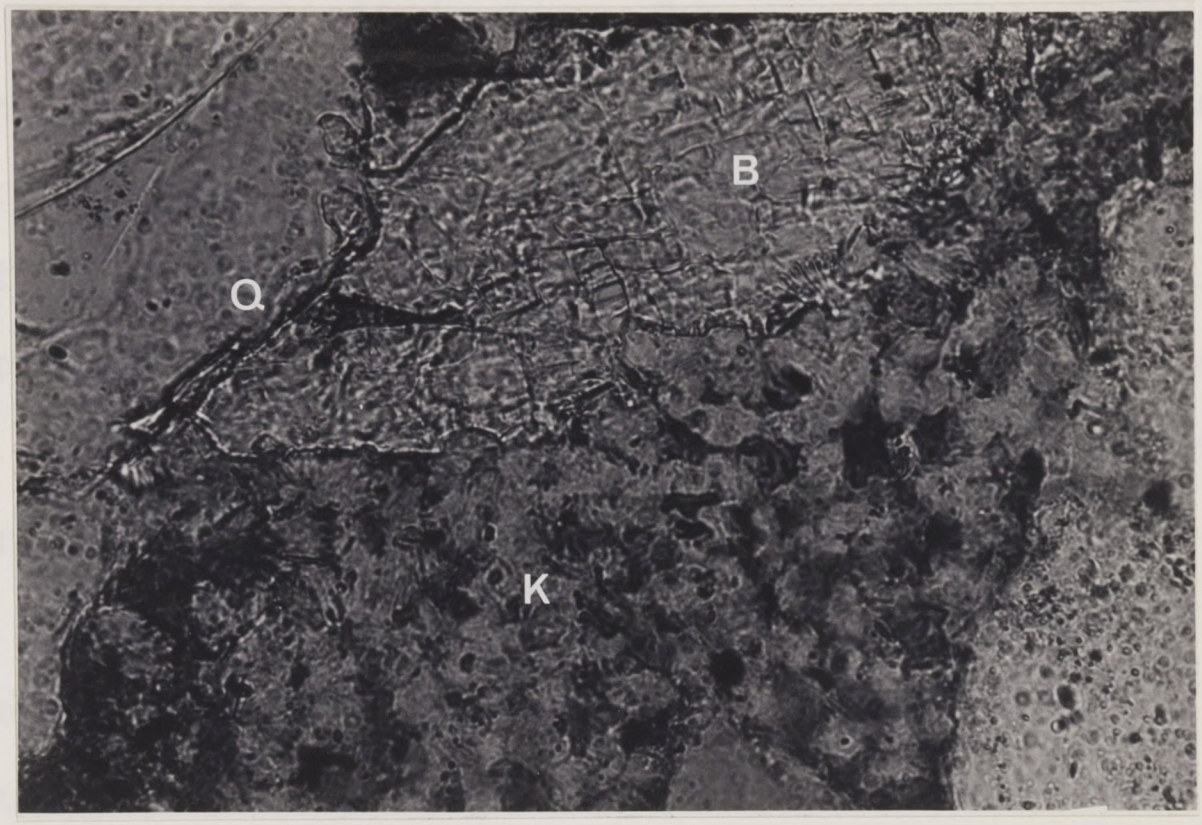

Figure 29. Euhedral quartz overgrowths (Q), barite (B), and kaolinite (K) cement in sample WAG 4887. Bar = 0.05 mm.

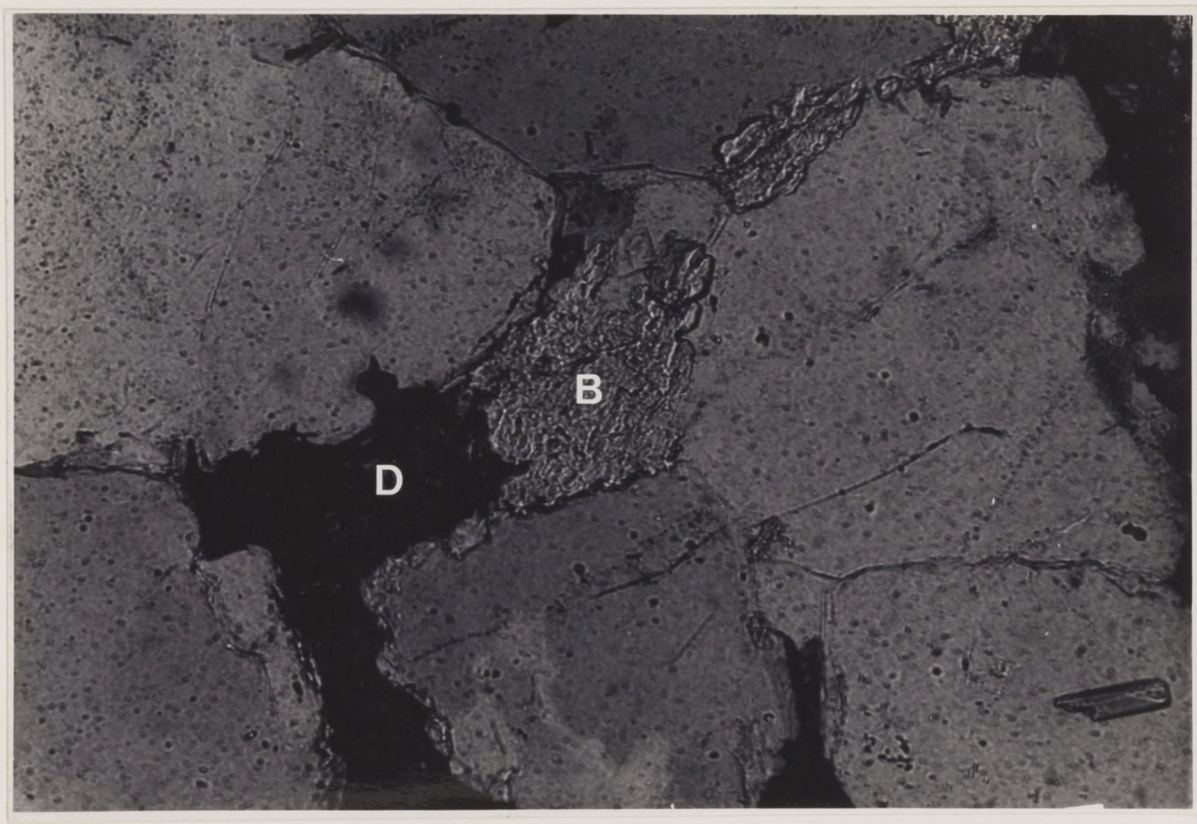

Figure 30. Barite(B) and ferroan dolomite(D) cement in sample ALR 4630. Bar = 0.1 mm.

patches up to a few millimeters wide that have undulose extinction (Fig. 32). Some crystal faces are curved. Usually the ferroan dolomite is found in small patches scattered around the slide, but in some samples it completely fills the pore space. Framework grains are commonly surrounded by ferroan dolomite, and in places only small fragments of the grains remain within the cement (Fig. 33).

Ferroan dolomite was differentiated from calcite by its blue color after staining. A minor amount of the carbonate cement, perhaps 5-10%, seemed to have a purplish color, which would indicate ferroan calcite. No difference in occurrence could be found between the purple and blue cements. The presence of a minor amount of ferroan calcite in some of the samples was suggested by x-ray analysis.

Pyrite

Cubes and irregular masses of pyrite occur in trace amounts in many samples. It is found in pore space and replacing either framework grains or cement.

Porosity

Thin section porosity in these "Gray" sandstones ranges from 0-15.2%, with a mean of 5.3% and standard deviation of 4.2% (Table 3). Total porosity was calculated by adding the value for intergranular porosity to half the value tabulated for secondary porosity. Secondary pores are those which either are too large to have been formed at the time

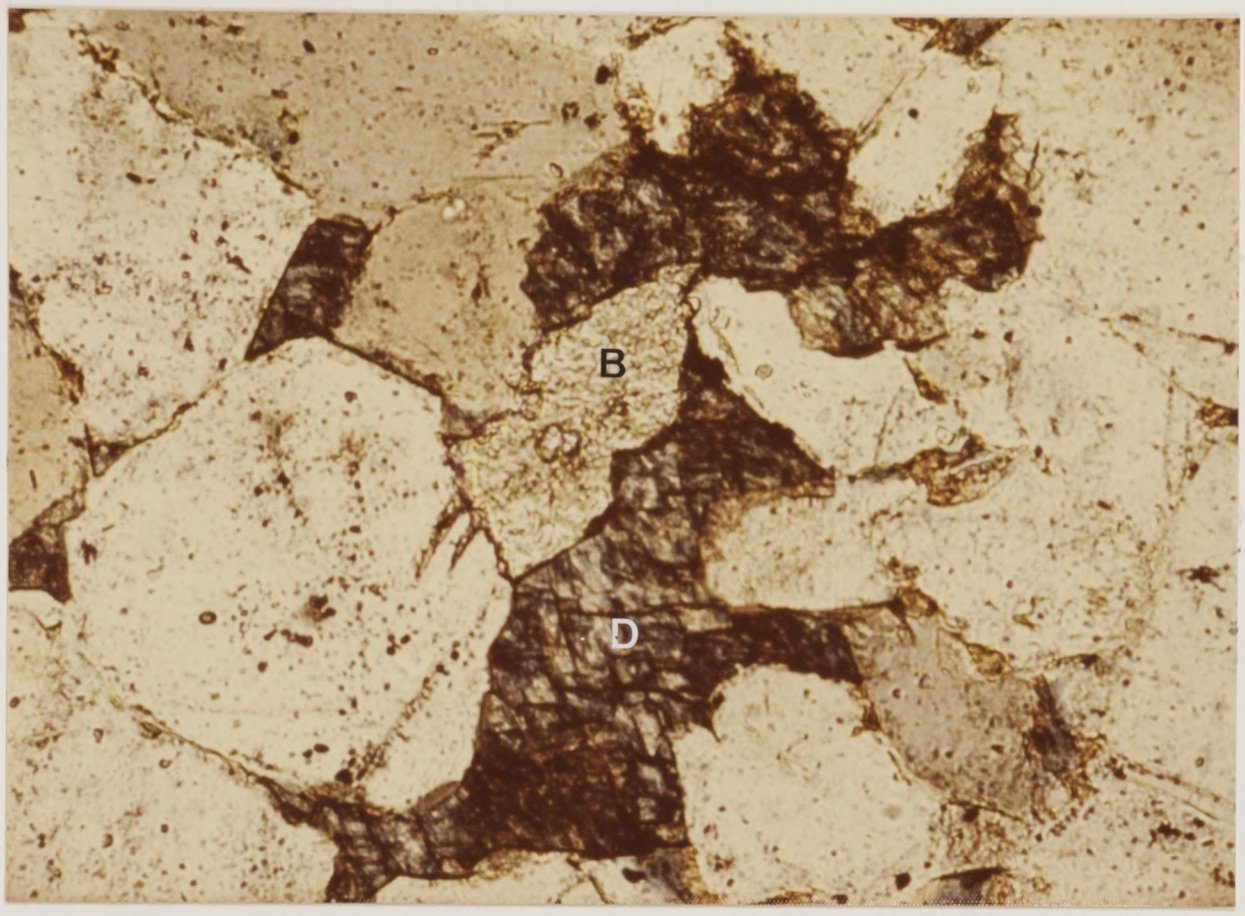

Figure 31. Barite(B) and ferroan dolomite(D) cement, sample ROB 4495. Bar = 0.1 mm.

Figure 32. Ferroan dolomite with undulose extinction, and euhedral quartz, sample G2 4938. Bar = 0.05 mm.

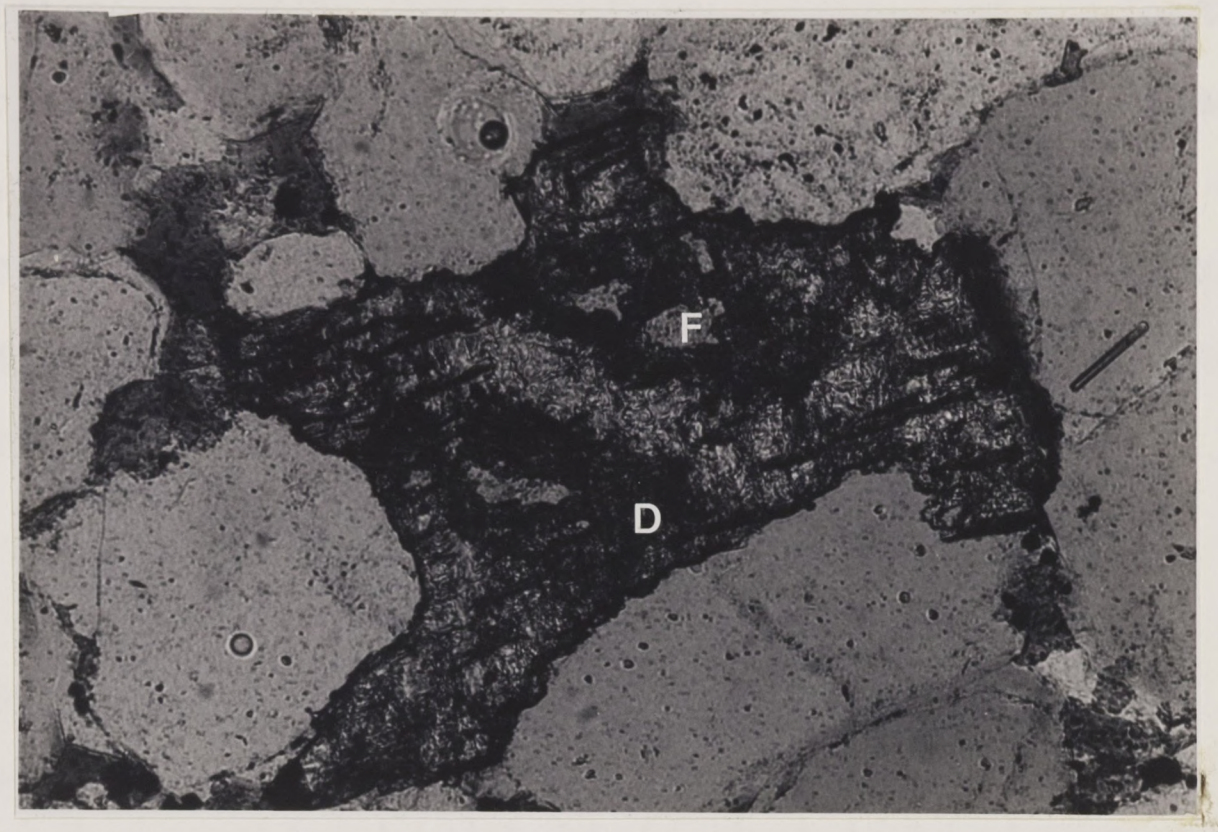

Figure 33. Ferroan dolomite(D) with framework grain inclusions (F) in sample WAG 4887. Bar = 0.1 mm.

Figure 34. Pressure solution of quartz (arrow) in sample ALR 4642. Bar = 0.1 mm.

of deposition or which still contain wreckage of unidentifiable framework grains. This latter group was not totally porosity, but still contained some framework material. So, to get a more accurate figure for the porosity, only one-half the volume counted as secondary porosity went into calculating total porosity.

Pre-Cement Porosity

Pre-cement porosity (or minus-cement porosity of Rosenfeld, 1949) is the amount of porosity remaining after compaction but before cementation. It is the sum of the present porosity, excluding secondary porosity, and the total amount of cement. The difference between pre-cement porosity and initial porosity should tell how much porosity was lost by compaction.

The West Tuscola field samples have an average pre-cement porosity of 22% (σ = 10.2%). The values of pre-cement porosity for all the samples were calculated and are presented in Table 3. The averages for each of the three major environments, slope, crest, and channel, are 19.2%, 23.6%, and 23.3% respectively, values which are quite similar. (The slope values are somewhat lower because a few of the samples have no present porosity or cement because of their abundant clay matrix.) If these sediments started with an initial porosity of 45% at deposition, an average figure suggested by McBride (in Jonas and McBride, 1977, p. 42), they lost an

average of 23% porosity by compaction. Ten percent of this, from 45% to 35%, was probably lost during the first few feet of burial. The loss of the other 13% occurred during deeper burial.

Several factors contribute to the loss of porosity during burial, the most important of which is grain rotation. Overburden pressure causes the grains to shift into a more compact packing arrangement, reducing the pore space. Deformation of ductile grains also destroys porosity by squeezing the soft grains into the adjacent pore space. This could be an important factor in these sediments, because some samples contain greater than 25% clay clasts. A third factor which may cause a reduction of porosity is pressure solution of framework grains. Solution takes place at points of contact between grains where the effective lithostatic pressure is very high. There are a few samples in which this appears to have occurred (Fig. 34). Interlocking quartz cement often gives the appearance of pressure solution, but examination of the slides under cathodoluminescence will reveal the true grain boundaries (Sippel, 1968). In these samples, essentially all the contacts seen under cathodoluminescence were of interlocking cement, not framework grains. If pressure solution occurred at all in these samples, it was of very minor importance in reducing the porosity. Breakage of brittle grains may also lower porosity, but there is no evidence that it occurred in these samples.

Pre-cement porosity shows a good correlation with mean grain size, the finer grain sizes having a lower pre-cement porosity (Fig. 35). (Figure 35 plots only 79 of the samples; the other 12 thin sections have large amounts of carbonate cement which replaced some of the framework grains. Their calculated values of pre-cement porosity are too high because of this replacement, so they were omitted.) This correlation means either that the finer-grained sediments underwent more compaction than the coarser ones, or that they started with less initial porosity. The latter is the more likely explanation, because many fine-grained slope, marsh, and interdistributary bay samples have a lot of detrital clay matrix in them.

This hypothesis is borne out by the multiple regression analysis of pre-cement porosity. The first variable entered was shaleand matrix, which is the sum of the sedimentary rock fragments and detrital matrix. This gave a correlation coefficient (r) of 0.75 and a coefficient of determination (r^2) of 0.56, which means that 56% of the variance of the pre-cement porosity is explained by the amount of shale and matrix (Table 4). Mean grain size was the next variable put into the equation, and it added only 0.002 to the total coefficient of determination. Sorting was added last, and it only contributed another 0.009 to the total r^2. The good correlation between pre-cement porosity and mean grain size shown in Figure 35, therefore, is due to the close relation

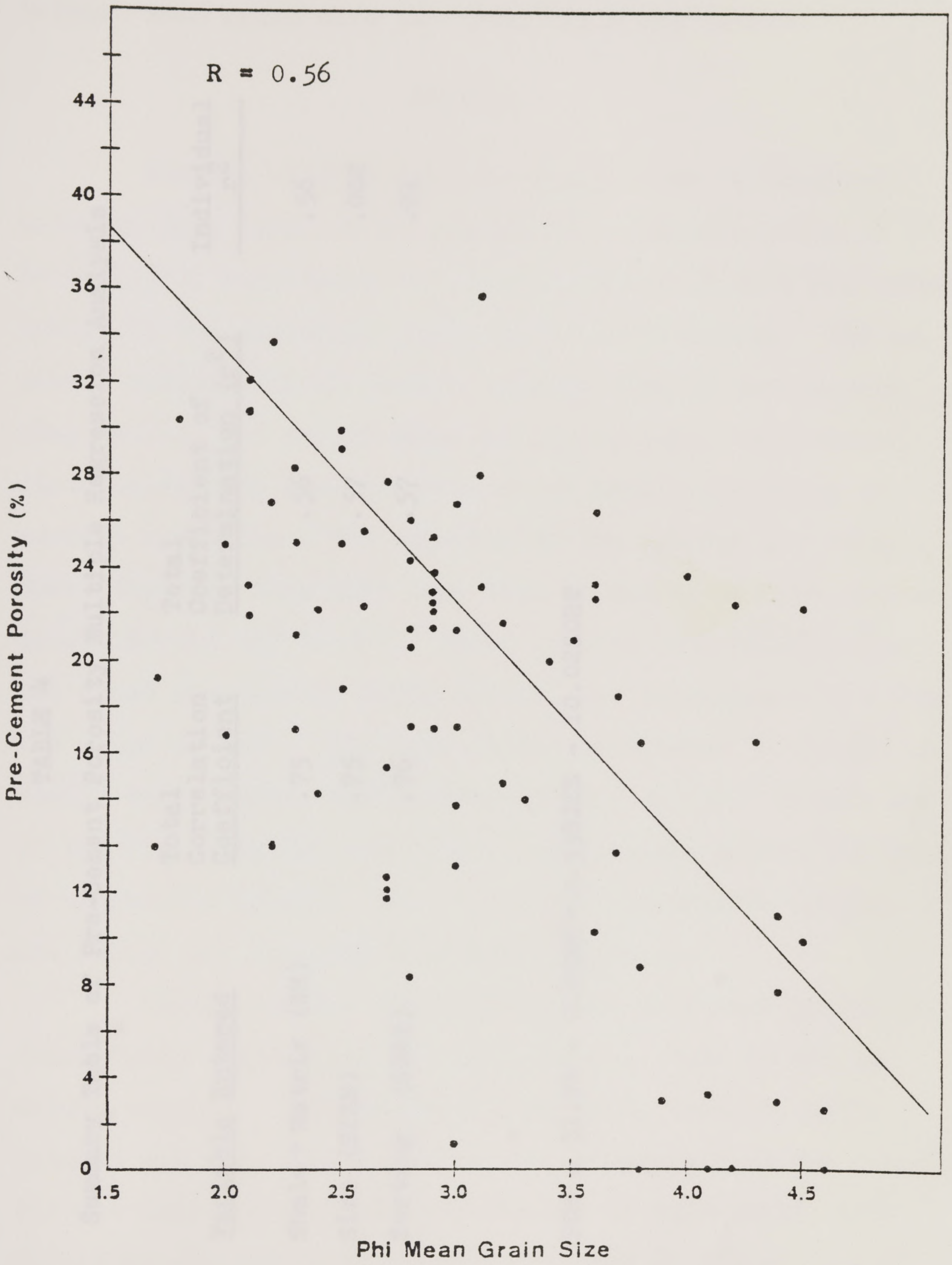

Figure 35. Plot of mean grain size versus pre-cement porosity. Linear regression line has R = 0.56.

TABLE 4

Summary Table of Pre-Cement Porosity Multiple Regression Analysis

Step	Variable Entered	Total Correlation Coefficient	Total Coefficient of Determination (r^2)	Individual r^2
1	Shale + Matrix (SH)	.75	.56	.56
2	Size (SIZE)	.75	.57	.002
3	Sorting (SORT)	.76	.57	.01

PCP = 31.74 - 0.69SH + 0.53SIZE - 10.02SORT

between mean grain size and total shale and matrix.

Texture

Samples studied span the whole range of textural maturity from immature to supermature (classification of Folk, 1974), reflecting the wide variation in wave and current energy in the different depositional environments. The immature samples, which contain greater than 5% terrigenous clay matrix, are mostly from the slope, marsh, and interdistributary bay environments, which have a low level of current winnowing. The majority of the samples are submature, that is, they have less than 5% matrix but the sand is poorly sorted ($\sigma > 0.5\,\phi$). These samples come chiefly from the crest and channel environments, but there are a few from the slope as well. The best sorted sandstones ($\sigma < .5\,\phi$) are mostly supermature, having well-rounded grains. Only a few of the finer-grained rocks have more angular grains and would be considered mature. The mature and supermature samples are almost all from the crests and channels.

Except for the finest fraction, most sand grains in these "Gray" sandstones are well-rounded, even in the immature samples. This textural inversion, that is, well-rounded but only moderately sorted, suggests that the rounding did not take place in the environment of deposition, but during an earlier cycle. The difference in energy levels among the different deltaic environments is best indicated by

the amount of terrigenous clay matrix that is present.

Size

The mean grain size of samples studied ranges from 1.7 to 4.6 ϕ (0.6 to 0.04 mm), or medium sandstone to coarse siltstone. The coarsest samples are chiefly from the channel and crest facies, and the finest ones from the slope and marsh facies.

Sorting

Framework grains of the samples are all moderately to well-sorted (0.35 to 0.8 ϕ) on the index set up by Folk (1974, p. 105), which has a verbal scale corresponding to ranges of phi standard deviation of grain size. Because the percent of matrix in each sample was already found in the first set of point counts, the second set measured only the grain size and sorting of the framework grains. A scatter plot of framework grain size vs. sorting shows essentially no correlation between the two, $r = 0.08$. This suggests that currents which were strong enough to winnow out the clay matrix could not effectively sort the sand.

Provenance

The predominance of well-rounded common quartz grains indicates that the main source rocks for the "Gray" sandstones were older sedimentary formations. The presence of some angular grains and of non-resistant clay clasts means

that the rounding of quartz did not occur in the final depositional environment but during an earlier cycle. Chert and well-rounded zircon and tourmaline, although minor in abundance, also indicate a sedimentary source.

There must have been low-rank metamorphic rocks in the source area as well, because slate and phyllite grains constitute up to 2% of the samples. The muscovite rimmed quartz grains, hornblende, and biotite were probably derived from metamorphic rocks also.

Orthoclase could have come from either silicic igneous rocks, like granite, or from high-rank metamorphic rocks such as gneiss. The twinned sodium-plagioclase could have had the same sources, but untwinned plagioclase is only characteristic of metamorphic rocks. Since there must have been a high-rank metamorphic source for the untwinned plagioclase, probably all the feldspars had the same, metamorphic origin. However, while their ultimate origin was probably metamorphic, the feldspars may have come from feldspathic sandstones in the source area.

Polycrystalline quartz grains could have come from either metamorphic rocks or from older, stressed granite, but their immediate source may also have been another sedimentary formation. Quartz grains with abundant vacuoles, and, rarely, vermicular chlorite, have probably come from pegmatites or hydrothermal veins (Folk, 1974, p. 70). The origin of the very fine-grained siliceous rock fragments is not known, but they are probably sedimentary grains that have been exposed

to metamorphism. The sedimentary rock fragments (clay clasts) are all locally derived.

According to Cleaves (1975), the Ouachita Fold Belt was the major source of the clastic debris shed to the west during the Desmoinesian (Fig. 36). Older sedimentary formations were eroded from the uplifted mountains and the detritus filled the Fort Worth Basin. The rivers then crossed the old basin and deposited their loads in deltas on the Concho Platform. The Buck Creek ("Gray") sandstone was deposited at the beginning of this progradation onto the platform.

In The Ouachita System Flawn (in Flawn et al., 1961) describes the rocks of the subsurface Ouachita Fold Belt in Texas. The Cambrian (?) to Pennsylvanian rocks are predominantly chert and siliceous shale, limestone and dolomite, shale, siltstone, and sandstone. In some areas they have been subjected to low-grade metamorphism and have developed foliation and slaty cleavage. Slate, phyllite, schist, metaquartzite, and marble, whose ages cannot be determined, have all been found in the subsurface Ouachitas. Based on position and composition of the Ouachita Fold Belt, it is very likely that it was the major source of the sediment deposited in the West Tuscola delta.

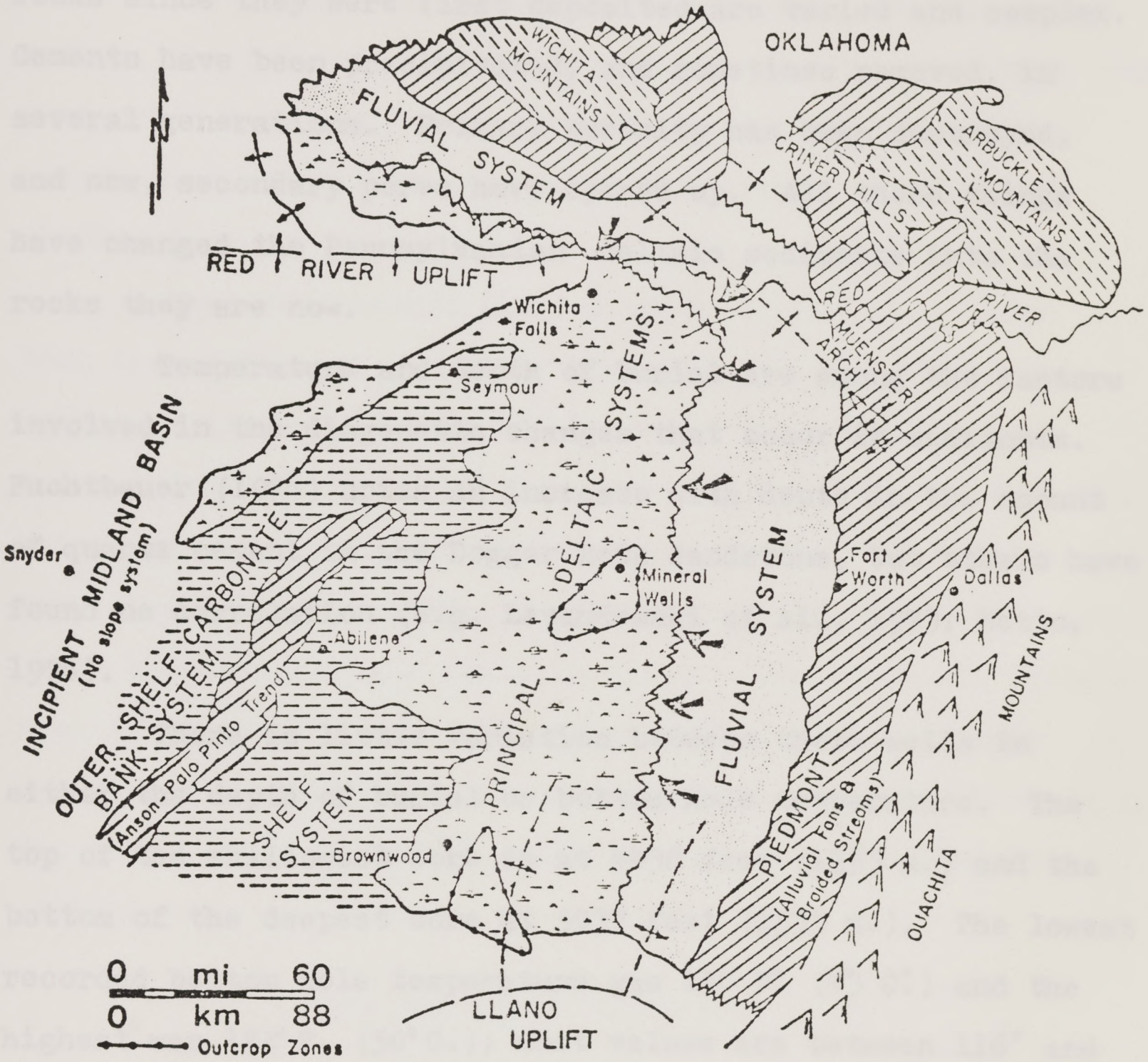

Figure 36. Late Desmoinesian sediment dispersal system, North-Central Texas. From Cleaves (1975).

DIAGENESIS

The diagenetic changes that have occured in these rocks since they were first deposited are varied and complex. Cements have been precipitated, and sometimes removed, in several generations. Primary porosity has been destroyed, and new, secondary pores have opened up. All these things have changed the Pennsylvanian deltaic sediments into the rocks they are now.

Temperature and depth of burial are among the factors involved in the diagenetic changes that occur in sediments. Fuchtbauer (1974) notes an increase with depth in the amount of quartz cement in the Dogger Beta sandstone, but others have found no correlation (e.g. Levandowski et al., 1973; Netto, 1974).

There is little variation between these wells in either the depth of burial or bottom hole temperature. The top of the shallowest core is at 4438 feet (1353 m.) and the bottom of the deepest core at 5037 feet (1535 m.). The lowest recorded bottom hole temperature was 110 F°. (43 C°.) and the highest was 122° F. (50° C.); most values are between 116° and 120° F. (47° - 49° C.). The observed variations between samples in the amount of cement that precipitated was most likely not controlled by differences in temperature or depth.

The "Gray" sandstone has in the past been buried more deeply than it is now. Erosion of overlying rocks has brought

it to its current level of about 4500 feet (1372 m.) below the surface, but it probably was once 7100 to 7600 feet (2160 to 2320 m.) deep (Brown, 1976, pers. comm.). These figures were estimated in two different ways. In the first method, the thickness of all the younger outcropping formations that would have covered the Buck Creek Formation in Taylor County were added together, yielding a value of 7125 feet (2172 m.).

The other method gives a depth of burial of about 7600 feet (2320 m.), which is probably more accurate. This method estimates only the thickness of the units that are younger than the basal Permian Clear Fork Formation, the unit which crops out over the West Tuscola field. The true thickness of formations older than the base of the Clear Fork is known because they are still in place. The estimated thickness of younger rocks is 3070 feet (940 m.), and assuming an average current depth of the "Gray" of 4500 feet (1372 m.), the total depth of burial would have been nearly 7600 feet (2320 m.).

Present Water Chemistry

An analysis of a water sample recovered from the "Gray" sandstone interval in the C.W. Stockton well indicates the present composition of the pore fluids (Table 5). The pH is slightly acid, and the brine has a very high total dissolved solids content. Calcium is highly enriched relative

Table 5. Present composition of pore water in the "Gray" interval, West Tuscola field, C.W. Stockton well.

Specific Gravity	1.123
pH	6.5
Sulfides	Negative
Total Dissolved Solids	191,800 ppm
Calcium (Ca)	14,136 "
Magnesium (Mg)	2,408 "
Chlorides (Cl)	107,830 "
Sulfates (SO_4)	270 "
Bicarbonates (HCO_3)	148 "

to magnesium (Mg/Ca = 1/6) compared to their concentration in seawater, which is Mg/Ca = 3/1 (weight ratios). The bicarbonate ion is also more concentrated in this brine than in normal sea water.

Sequence of Cementation

There are at least six different cement types in these rocks, and their relative age of formation is not always clear. However, by examining the textural relationships among them in all the thin sections, their sequence of formation could be determined. Chlorite was the first phase to precipitate, and where it occurs, it usually forms the innermost layer of cement around the grains.

The next cement to precipitate was quartz, and because the chlorite cutans are not widespread, it is usually found as the first cement around grains. The overgrowths are euhedral, so they must have been growing into open pore space where their crystal faces could develop. Where the chlorite cutans are thick and unbroken, they prevented the nucleation of quartz overgrowths. Some chlorite is found outside of quartz overgrowths, so limited precipitation of chlorite must have continued after quartz cementation started.

The third cement type was calcite, and it not only filled the remaining pore space but also partly or wholly replaced framework grains, especially feldspar and clay clasts. Where calcite is still present it is found next to

euhedral quartz overgrowths and fills the pore space. There are no inclusions of calcite inside the quartz overgrowths, so the quartz did not precipitate after the calcite and replace it. In most of the samples the calcite has been completely removed, leaving only skeletal grains as evidence of its former presence.

Two minor cements precipitated next, kaolinite and barite. They almost always occur inside secondary pores, so they must have formed after the dissolution of calcite cement. It has not been possible to determine which of these came first, or if they precipitated contemporaneously. They are both rare, so there are few places where they are found next to each other, and their age relation is not apparent. Barite has euhedral faces in contact with kaolinite, but barite did not necessarily form first; it may have been able to push the kaolinite aside by its force of crystallization.

The last cement to precipitate was probably ferroan dolomite, but the evidence regarding the age of its formation is not conclusive. It is found inside both secondary pores and primary ones which had probably been formed by the dissolution of calcite cement. In Figure 31, ferroan dolomite is in contact with euhedral barite, indicating that the barite probably precipitated into an open secondary pore, and the ferroan dolomite formed later in what space remained. Had the ferroan dolomite precipitated first, it should show good crystal faces. Most ferroan dolomite completely fills pores

so that crystal faces are not seen, but where it did not fill an entire space, it has good euhedral boundaries.

It is possible that the ferroan dolomite formed in what pore space remained after the calcite was precipitated but before it dissolved. McBride (unpub. mans.) believes that ferroan dolomite as well as calcite can replace framework grains, so the ferroan dolomite found inside secondary pores may be due to its own replacement of the grains. Then, when the calcite cement dissolved, the ferroan dolomite remained. The ferroan dolomite does not show evidence of dissolution.

The main evidence against this hypothesis is the presence of euhedral crystals of ferroan dolomite that do not fill secondary pores. It is not likely that they once filled the space and then dissolved to their current euhedral borders because, according to Pettijohn et al. (1972, p. 415) quartz and carbonate only form euhedral faces when they precipitate, not when they dissolve. Therefore, the ferroan dolomite must have been precipitated into an open secondary pore that formed by calcite replacement and dissolution. This situation is similar to one studied by Lindquist (1976, p. 85), who also concluded that the ferroan dolomite precipitated after calcite had been dissolved.

Ferroan calcite most likely formed at the same time as ferroan dolomite, because both minerals contain ferrous iron in their structure. There is no good evidence from which to deduce their relative ages.

This sequence of cementation is remarkably similar to the one found by Lindquist (1976) in the Oligocene Frio Formation of south Texas (Table 6). Her Frio samples were also from deltaic and marginal marine environments, but unlike the "Gray" sandstones, they were low in quartz and rich in volcanic rock fragments. The Frio samples were taken from an overpressured sandstone reservoir where pore fluid pressure exceeded normal pressure for that region. The sample depths ranged from 8,770 to 13,890 feet (2673 to 4235 m.) and temperatures were 212° to 302°F. (100° to 150°C.). Despite the different ages, physical conditions, and mineralogical composition of the samples, their diagenetic histories show some striking similarities. The major events - precipitation of quartz overgrowths, calcite cementation and replacement, dissolution of calcite, and precipitation of late cements including kaolinite and ferroan calcite and dolomite - are all the same.

Chlorite

Chlorite coatings are found on at least a few framework grains in about one-third of the samples; the cutans are well developed and fairly abundant in only nine of them. These nine are from channel, crest, and slope environments, but they all have in common low amounts of detrital clay matrix. The best chlorite grain coatings are from samples from the Alton Roberts well, but good cutans are found in

Table 6. Comparison of cementation sequences, Lindquist (1976) and this study.

Lindquist (1976)	This Study
1. Micritic calcite cement	1. Chlorite Cutans
2. Feldspar overgrowths	
3. Quartz overgrowths	2. Quartz overgrowths
4. Sparry calcite cement	3. Sparry calcite cement
5. Dissolution of calcite	4. Dissolution of calcite
6. Precipitation of kaolinite	5. Precipitation of barite, kaolinite
7. Precipitation of ferroan calcite, ferroan dolomite, analcime, zeolite crystals	6. Precipitation of ferroan dolomite, ferroan calcite

six other wells which have a wide geographic variation. The chlorite therefore, is not confined to one geographic location within the field or one particular depositional environment.

The chlorite in the "Gray" samples make thin, concentric fibrous rims around the grains. Where the rims have been compressed between adjacent grains by compaction, the crystals are well aligned, and have a high birefringence. Where the chlorite forms loose networks across pores (a morphology reported by Stalder [1973] for authigenic illite), it has a lower birefringence.

Authigenic clay minerals in sandstone have been reported frequently, with kaolinite, chlorite, and montmorillonite the most common types. The latter two seem to form mainly in sediments rich in volcanic rock fragments (Almon et al., 1976; Galloway, 1974). Almon and others (1976) studied volcaniclastic sandstone of the Horsethief Formation in Montana and found two distinct cement assemblages that could be related to the original depositional environments. Corrensite (an ordered mixed layer mineral of montmorillonite and chlorite) was found exclusively in delta distributary channel and distributary mouth bar sediments, and montmorillonite occurred in bay-beach, crevasse splay, lagoon, barrier island, and shallow subtidal deposits. They concluded that these clay were precipitated early in the diagenetic sequence, and their distribution reflects the differences in chemistry of the early pore fluids from the different environments.

The diagenetic environments represented in the "Gray" sandstone samples were probably similar enough that there was no difference in their pore fluid composition, and chlorite was able to precipitate in sediments from all of them.

Carrigy and Mellon (1964) report a difference in authigenic clay mineral assemblages related to the mineralogical composition of the sandstones as well as depositional environment. In marine and near-marine deposits illite, kaolinite, and quartz cements formed in sediments rich in feldspar and volcanic rock fragments, but only kaolinite and quartz formed in more quartzose sediments. In non-marine sediments, authigenic kaolinite and quartz formed in quartzose sandstone, chlorite, illite, and kaolinite formed in sandstone with a moderate amount of volcanic material, and chlorite-laumontite formed in sandstone with abundant volcanic debris. Carrigy and Mellon believe that the type of clay minerals that precipitate is controlled by the compostion of the pore fluids, which is itself related to the chemical composition of the sediment.

Neoformation of Chlorite

Neoformation of clay minerals is defined as the formation of clays entirely from products dissolved in water, as opposed to transformation, which is the addition of ions from solution to a material that is already a clay mineral, however disordered (Millot, 1970, p. 82). In studying natural examples of neoformation workers have distinguished between

leached and confined environments. A leached environment is one in which water can pass through easily, while a confined one has restricted exits, and the water level stays constant by evaporation or lateral drainage, so cations become concentrated there (Millot, 1970, p. 330). The dynamics of the solutions, whether they are leaching or confining, determine the pH, and the concentrations of cations, silica, and aluminum, and these conditions control the type of neoformation which occurs.

By using laboratory experiments that synthesize clay minerals at low temperatures, the chemical conditions necessary for the formation of particular minerals have been determined. Chlorite has not been successfully synthesized in low temperature experiments, but by comparison with similar minerals and from observations of natural systems in which it occurs, its conditions of formation can be determined. The neoformation of illite requires a confined environment with alkaline pH in water that is rich in potassium, aluminum, and silica (Millot, 1970, p. 351). Under the same conditions, but with abundant magnesium instead of potassium, montmorillonite will form; both magnesium and iron cations are necessary for the formation of chlorite.

Presumably, the chemical conditions during the early burial of the "Gray" sediments allowed the neoformation of chlorite rims on quartz grains. Magnesium, iron, silica, and aluminum must have been in solution in the pore waters in

sufficient quantity to cause the precipitation of chlorite. The ions probably came from the weathering of source rocks and were carried in solution by streams to the site of deposition, where they remained in the pore fluid. Plagioclase, biotite, potassium feldspar, and quartz could have supplied the silica. The weathering of biotite and chlorite in low-grade metamorphic rocks could have been the source of the iron and magnesium. Silica, iron, and magnesium are all fairly mobile in weathering (Goldich, 1938, p. 37). Aluminum is more stable, but intense weathering and leaching in the source area could have mobilized it as well, and provided enough aluminum for the formation of chlorite.

Solutions containing organic acids have increased solubility of Si, Al, Fe, Ca, and Mg (Huang and Keller, 1970), and humic and lignitic acids are likely to be present during soil weathering. In the presence of these acids, very intense weathering might not be needed to mobilize the aluminum. Without the acid, only a small amount of aluminum can be dissolved the water of pH 4.5-8, which is the range of most natural waters (Pettijohn et al., 1972, p. 411). It may be that the aluminum forms a soluble complex with other ions. Huang and Keller suggest that Al and Fe increase their solubility by complexing as salicylates and tartrates. Or, the Al may remain in aluminosilicate wreckage after weathering, and this precursor is built up to chlorite by the addition of magnesium and iron. Local variations in the pore water chemistry may have controlled where chlorite actually

precipitated, and where conditions were not right, perhaps because of insufficient iron, magnesium, or aluminum, it could not form.

Another possible source of the Fe, Mg, Si, and Al could have been the framework grains themselves. Galloway (1974) reports the formation of authigenic clay minerals under conditions of higher temperature and deeper burial than is assumed for the "Gray" authigenic chlorite. He believes that at a depth of 1,000 to 4,000 feet (300-1200 m.), there was chemical alteration of the unstable framework grains and volcanic debris. Silica and aluminum were mobilized and re-precipitated as clay coats on detrital grains. Chlorite and montmorillonite were the most common, but authigenic illite and kaolinite formed as well. Galloway believes the type of clay formed is determined by the mineralogy of the sandstone and the initial composition of the pore fluids.

Influence of Chlorite Cutans

Once the chlorite rims coated framework grains, they exerted control over later chemical precipitation. Quartz cement needs a quartz nucleus on which to precipitate, so where cutans are thick and unbroken, its nucleation was inhibited. Only a few samples had enough well-developed cutans to substantially affect the volume of quartz cement (i.e., ALR 4642, OL 4551, BH 4561). Figure 20, taken from ALR 4630, shows good euhedral quartz overgrowths. Figure 19 ia a photomicrograph from sample ALR 4642, just 12 feet (3.7 m.) below

ALR 4630; it shows good chlorite cutans and almost no quartz overgrowths. In sample ALR 4630 quartz cement makes up 17.5% of the volume, whereas in ALR 4642 authigenic quartz is only 1% of the total volume. This difference is apparently caused by the presence of well-developed chlorite coatings in ALR 4642 that inhibited quartz cementation. In other respects the samples are similar - they are both distributary channel deposits, and both have similar values of mean size and sorting. The porosity in the samples reflects the difference in quartz cementation; ALR 4630 has a total porosity of 7.5%, whereas ALR 4642 has more than twice that much, 15.2%. Where clay coats are well-developed, therefore, they can have an important influence on the porosity distribution in sandstones. Heald and Anderegg (1960) report a similar situation in the Tuscarora sandstone, in which considerable porosity was preserved where grains are coated with clay.

Where chlorite cutans are present but not thick or continuous, quartz cement may precipitate in peculiar patterns. Figures 23 and 24 show small, prismatic quartz overgrowths on parts of grains that were free of clay coatings. Heald and Larese (1974) describe other features that suggest a clay rim control of quartz cement distribution, including cement only on fractured grains, and framework grains in contact with overgrowths from other grains. Other minerals may be quartz cement inhibitors when they form grain coatings, including illite, chert, carbonate, and hematite.

If clay cutans are not thick, they may be replaced by secondary quartz (Heald, 1956). It is possible that more of the "Gray" sandstone samples originally had chlorite cutans, but they were thin enough that they were replaced and lost.

Quartz

Quartz overgrowths are well-developed in most of the samples, comprising between 0 and 31% of the volume. The mean secondary quartz volume is 11%, with a standard deviation of 8.2%. The average value of pre-cement porosity is 22%, so quartz cementation reduced the porosity by about half. The distribution of quartz cement is shown in Figure 37, a plot of the overgrowth volume frequency in all of the samples. The distribution of values is polymodal with the principal peak

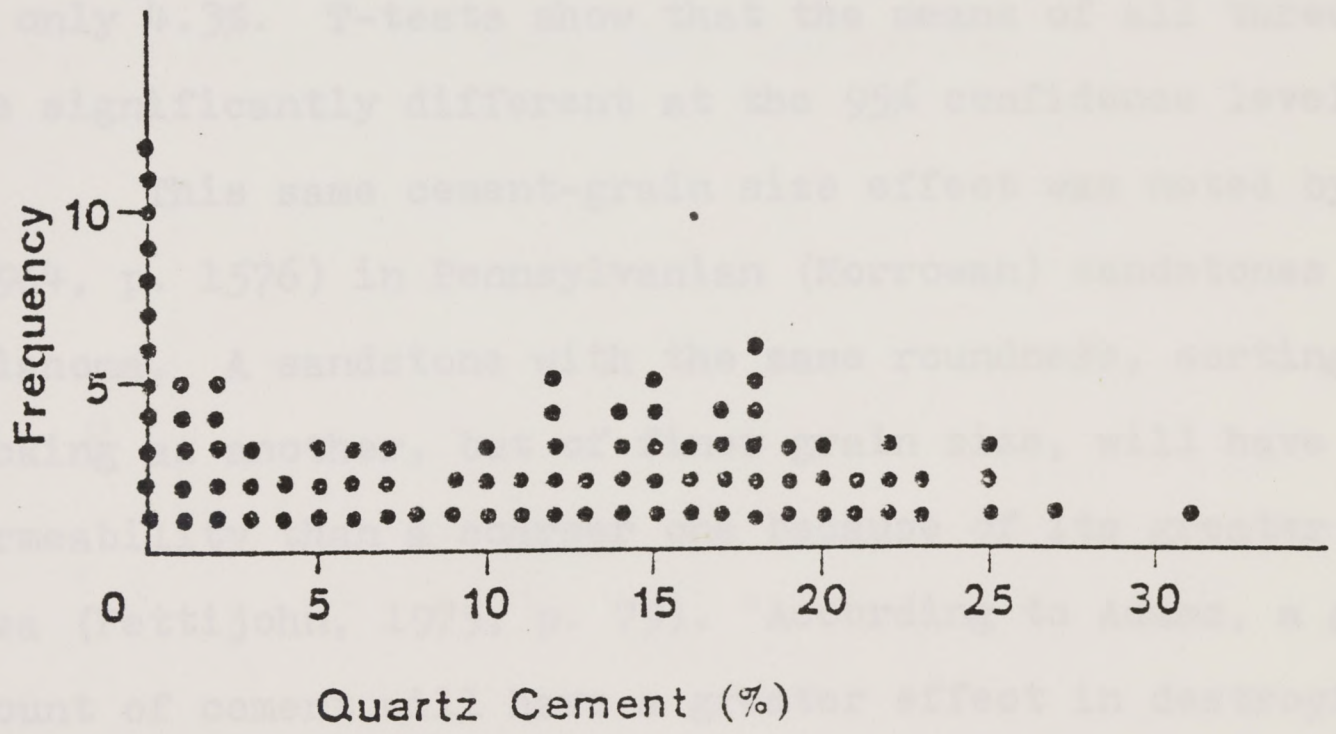

Figure 37. Frequency distribution of quartz cement, showing polymodal distribution.

at zero (meaning no quartz overgrowths present), and the secondary peak around 18%. All samples with less than 6% secondary quartz have a logical explanation for its scarceness, either there was a lot of detrital matrix, there were thick chlorite coatings, or there was replacement of quartz by carbonate cements. The remaining samples appear to be normally distributed around a mean of about 18%. These samples are clean sandstone and coarse siltstone, and presumably were free of impediments to the precipitation of quartz cement.

The effect of grain size on the amount of quartz cement found in the samples is shown in Figure 38. As the mean grain size increases, the average amount of quartz cement present also increases. Fine and medium sandstone samples have an average of 13.7% secondary quartz, very fine sandstones have an average of 9.4%, and siltstones an average of only 4.3%. T-tests show that the means of all three groups are significantly different at the 95% confidence level.

This same cement-grain size effect was noted by Adams (1964, p. 1576) in Pennsylvanian (Morrowan) sandstones of Oklahoma. A sandstone with the same roundness, sorting, and packing as another, but of finer grain size, will have less permeability than a coarser one because of its greater surface area (Pettijohn, 1975, p. 79). According to Adams, a given amount of cement will have a greater effect in destroying the permeability of a fine-grained rock than a coarser one. So, the finer-grained rocks end up with less quartz cement because

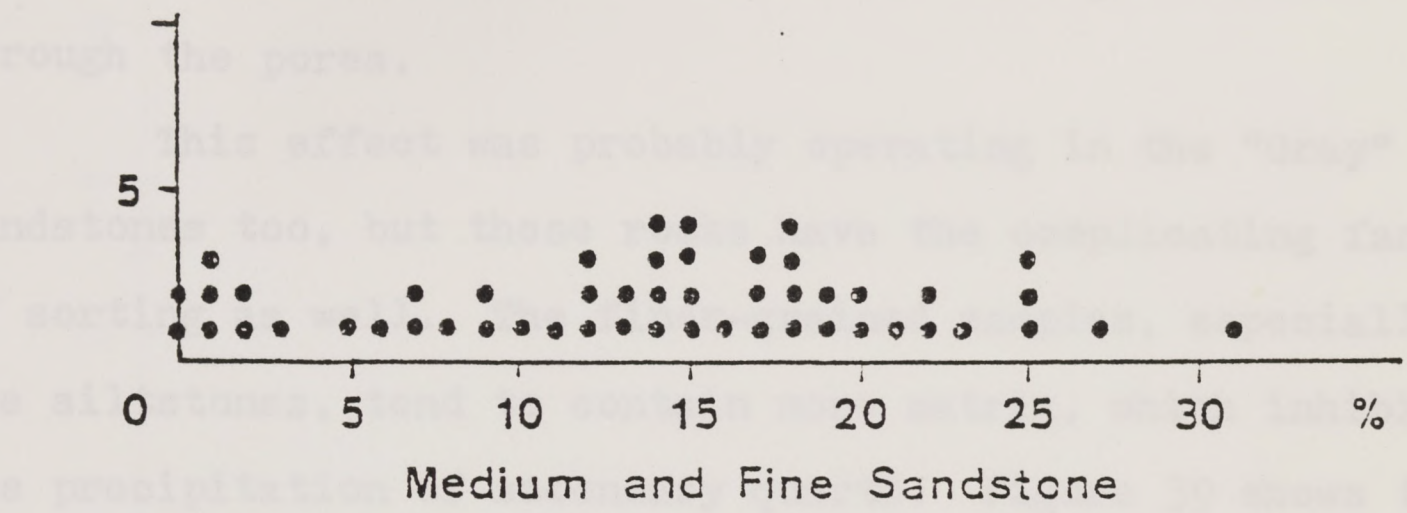

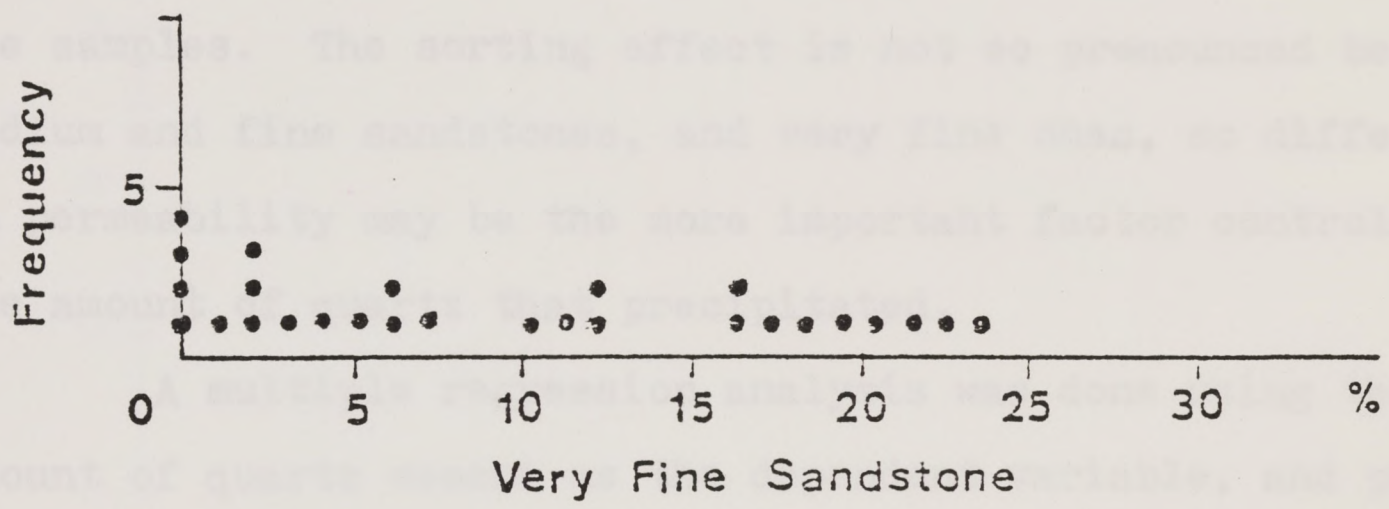

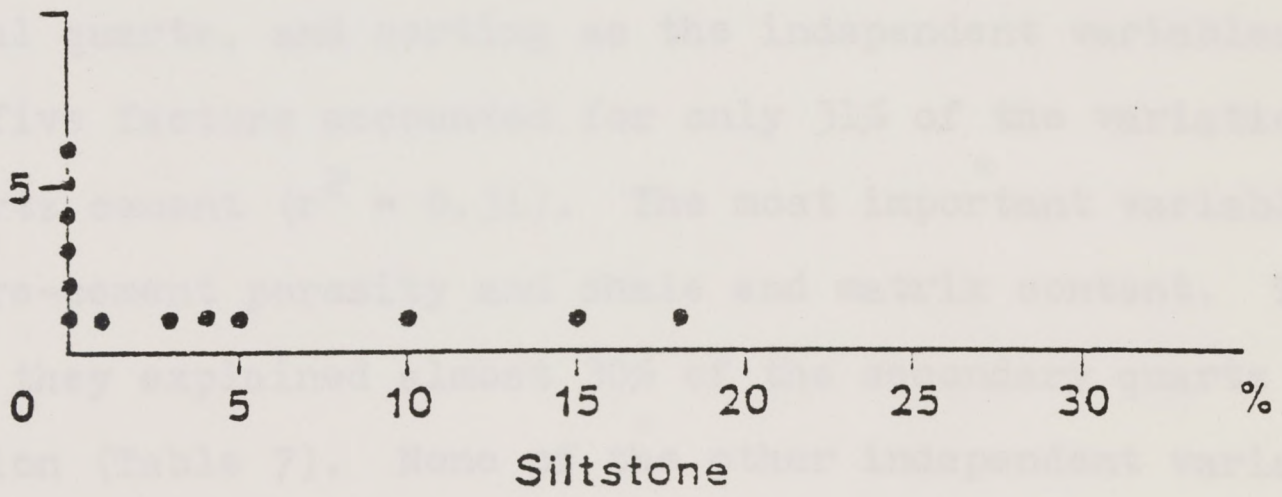

Figure 38. Distribution of quartz cement in different sandstone size classes.

they both start with lower permeabilities than coarser rocks, and what permeability they have is more easily lost, preventing further movement of silica-bearing solutions through the pores.

This effect was probably operating in the "Gray" sandstones too, but these rocks have the complicating factor of sorting as well. The finer-grained samples, especially the siltstones, tend to contain more matrix, which inhibits the precipitation of secondary quartz. Figure 39 shows the relationship between mean grain size and matrix content of the samples. The sorting effect is not so pronounced between medium and fine sandstones, and very fine ones, so differences in permeability may be the more important factor controlling the amount of quartz that precipitated.

A multiple regression analysis was done using the amount of quartz cement as the dependent variable, and pre-cement porosity, shale and matrix content, mean grain size, detrital quartz, and sorting as the independent variables. These five factors accounted for only 31% of the variation in quartz cement ($r^2 = 0.31$). The most important variables were pre-cement porosity and shale and matrix content. Together they explained almost 30% of the secondary quartz variation (Table 7). None of the other independent variables had a significant effect on the quartz cement variation.

Pre-cement porosity indicates how much pore space was present in the sediments before cementation began. It

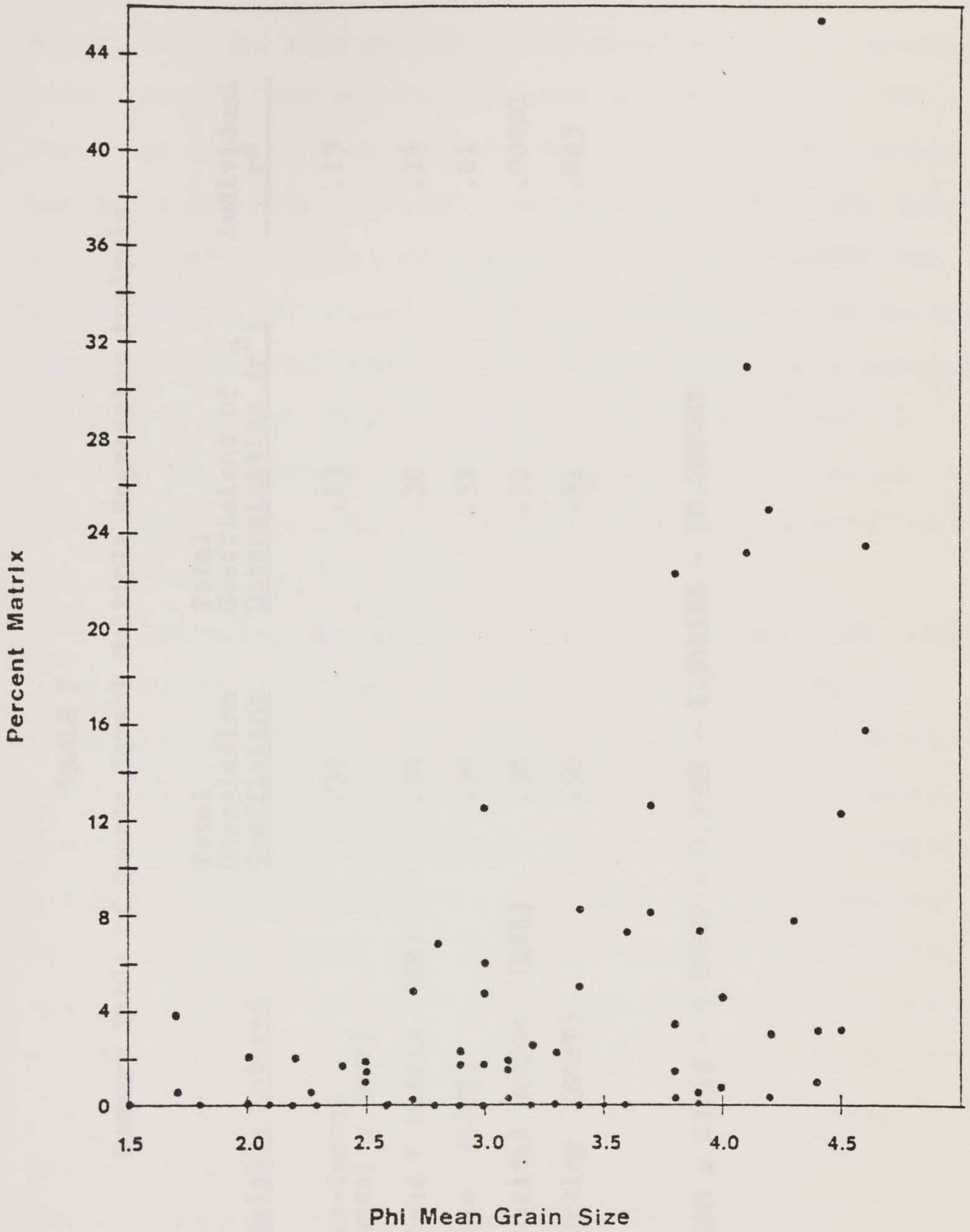

Figure 39. Plot of sample mean grain size versus matrix content.

TABLE 7

Summary Table of Quartz Cement Multiple Regression Analysis

Step	Variable Entered	Total Correlation Coefficient	Total Coefficient of Determination (r^2)	Individual r^2
1	Pre-Cement Porosity (PCP)	.37	.13	.13
2	Shale + Matrix (SH)	.54	.30	.16
3	Size (SIZE)	.56	.31	.01
4	Detrital Quartz (QTZ)	.56	.31	.00001
5	Sorting (SORT)	.56	.31	.003

QCEM = 23.69 - 0.80PCP - 0.39SH - 1.54SIZE - 10.02SORT

is quite reasonable that the more pore space there was to begin with, the more quartz cement would be able to precipitate. This factor was found to account for 13.4% of the variation in secondary quartz. The other important factor was shale and matrix content, explaining 16.3% of the variation. Where detrital or authigenic clays surrounded the quartz grain, the silica in solution had no place to nucleate and could not precipitate. A scatter plot of shale and matrix vs. quartz cement (Fig. 40) reveals that above about 8% matrix, the secondary quartz content is sharply reduced. Below that figure, the matrix seems to have no control over the amount of quartz cement.

Finally, the volume of quartz overgrowths was compared to the depositional environment of the samples (Fig. 41). There was no significant difference at the 95% confidence level between the channel and slope samples or the channel and crest samples in quartz cement. However, the crest samples did have significantly more quartz than the slope samples. It is unlikely though that this was caused by a difference in the chemistry of the solutions in the different environments. Once again, the shale and matrix content appears to be responsible for the amounts of quartz cement precipitated in the two environments. Forty-one percent of the slope samples contain greater than 8% matrix, but only 12% of the crest samples have this much (Fig. 42). It seems likely then that inhibition of quartz precipitation by clays caused the

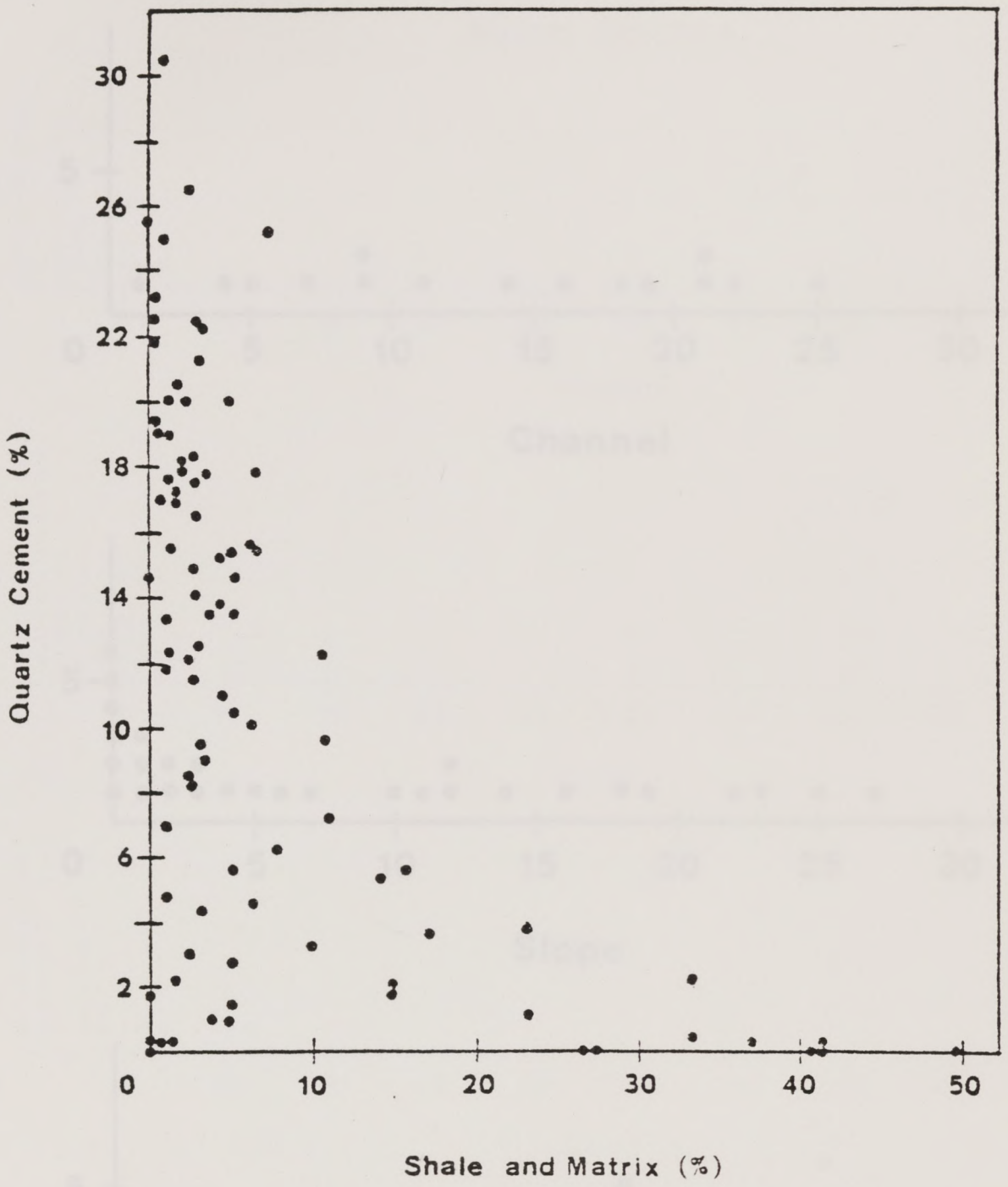

Figure 40. Relationship of quartz cement to shale and matrix content.

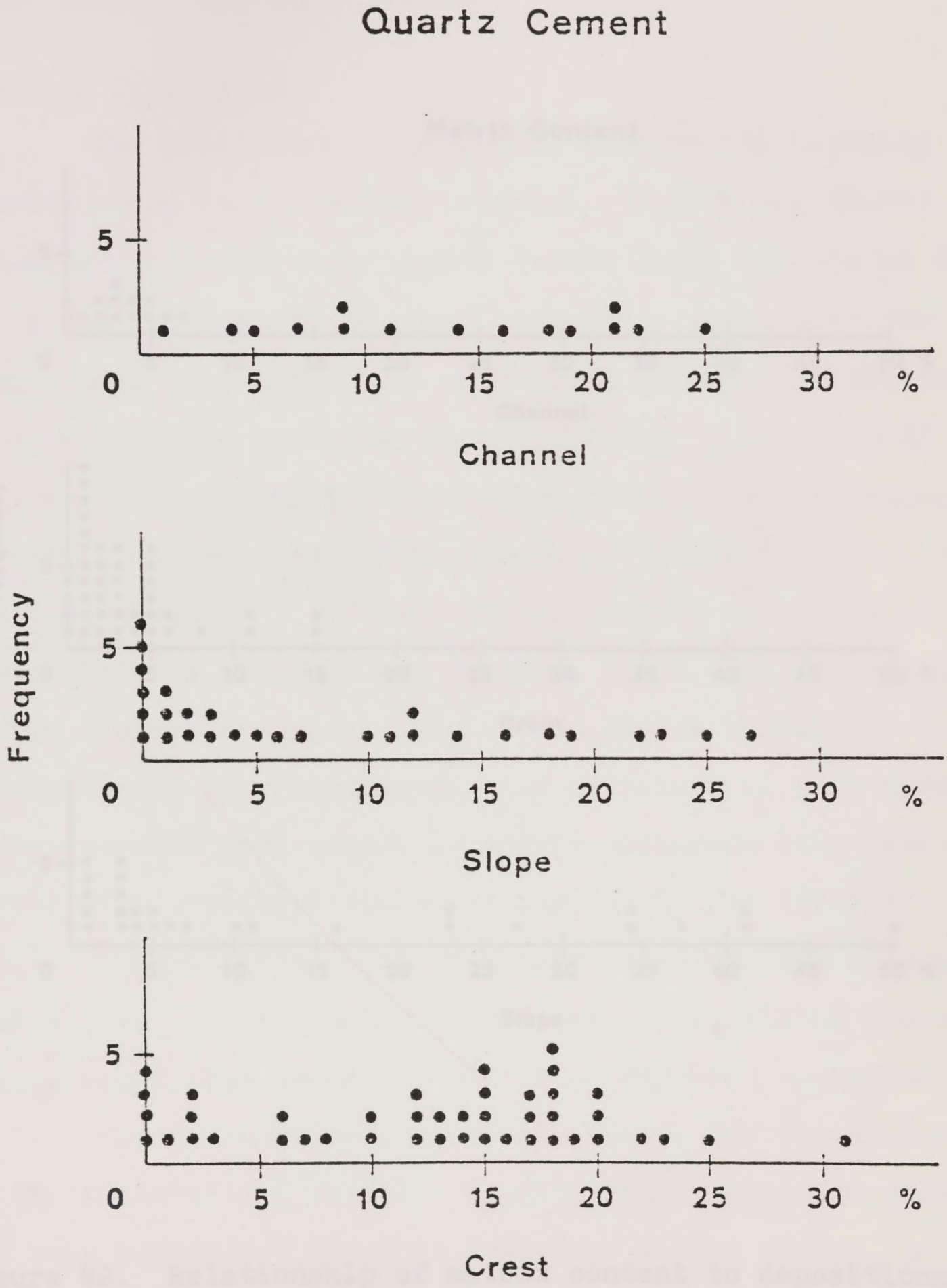

Figure 41. Relationship of quartz cement content to depositional environment.

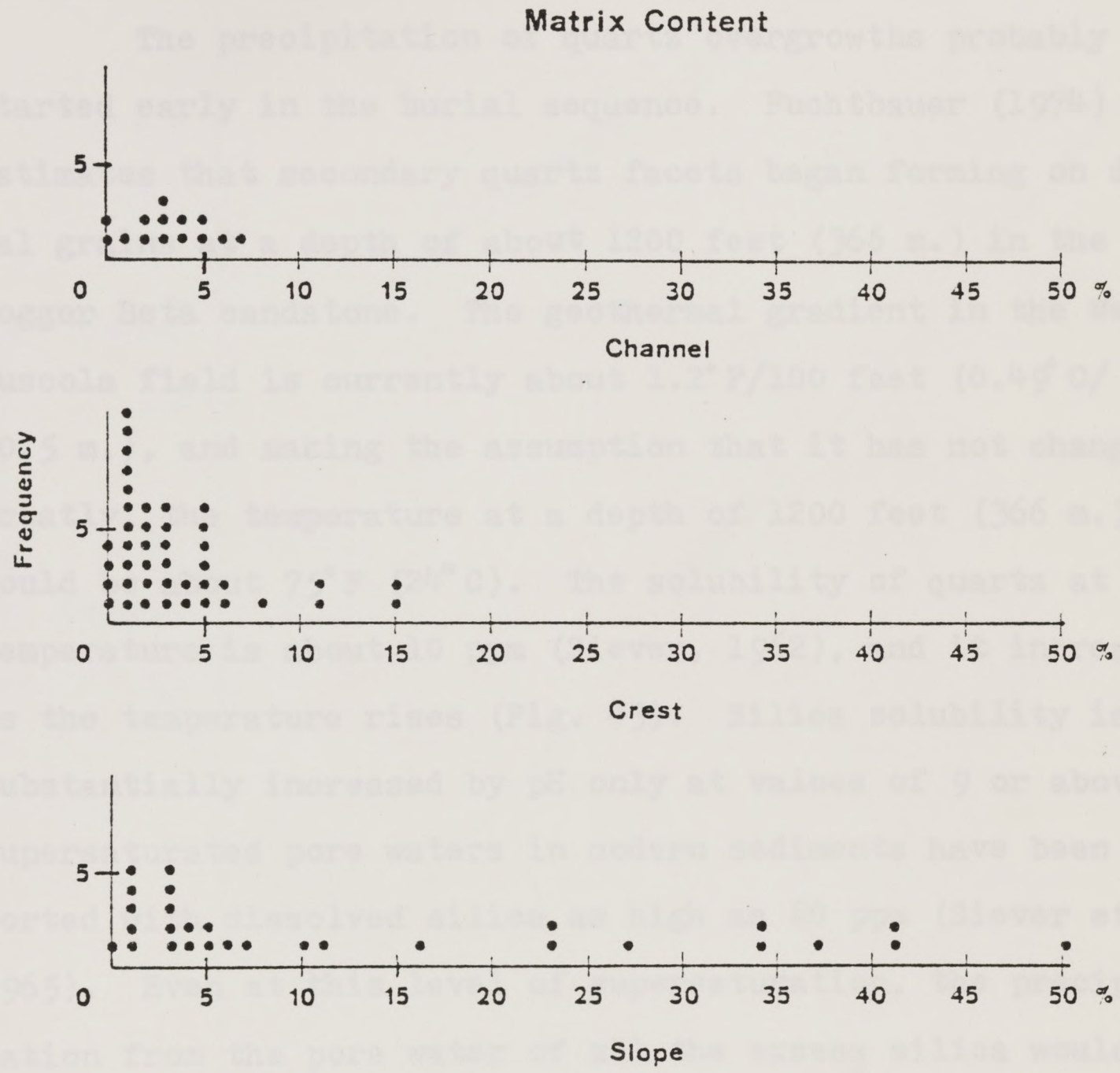

Figure 42. Relationship of matrix content to depositional environment.

difference in cementation, not chemical differences in pore water between the environments.

Chemical Conditions

The precipitation of quartz overgrowths probably started early in the burial sequence. Fuchtbauer (1974) estimates that secondary quartz facets began forming on detrital grains at a depth of about 1200 feet (366 m.) in the Dogger Beta sandstone. The geothermal gradient in the West Tuscola field is currently about 1.2°F/100 feet (0.49°C/30.5 m.), and making the assumption that it has not changed greatly, the temperature at a depth of 1200 feet (366 m.) would be about 75°F (24°C). The solubility of quartz at this temperature is about 10 ppm (Siever, 1962), and it increases as the temperature rises (Fig. 43). Silica solubility is substantially increased by pH only at values of 9 or above. Supersaturated pore waters in modern sediments have been reported with dissolved silica as high as 80 ppm (Siever et al., 1965). Even at this level of supersaturation, the precipitation from the pore water of all the excess silica would make a negligible amount of cement overgrowths on grains.

There are several possible sources for the silica in the interstitial waters. Traditionally, pressure solution has been considered the most important silica source, but it is questionable whether it occurred at all in the "Gray" sandstones, and if it did, it was to such a minor extent that it certainly could not have been an important source. Other

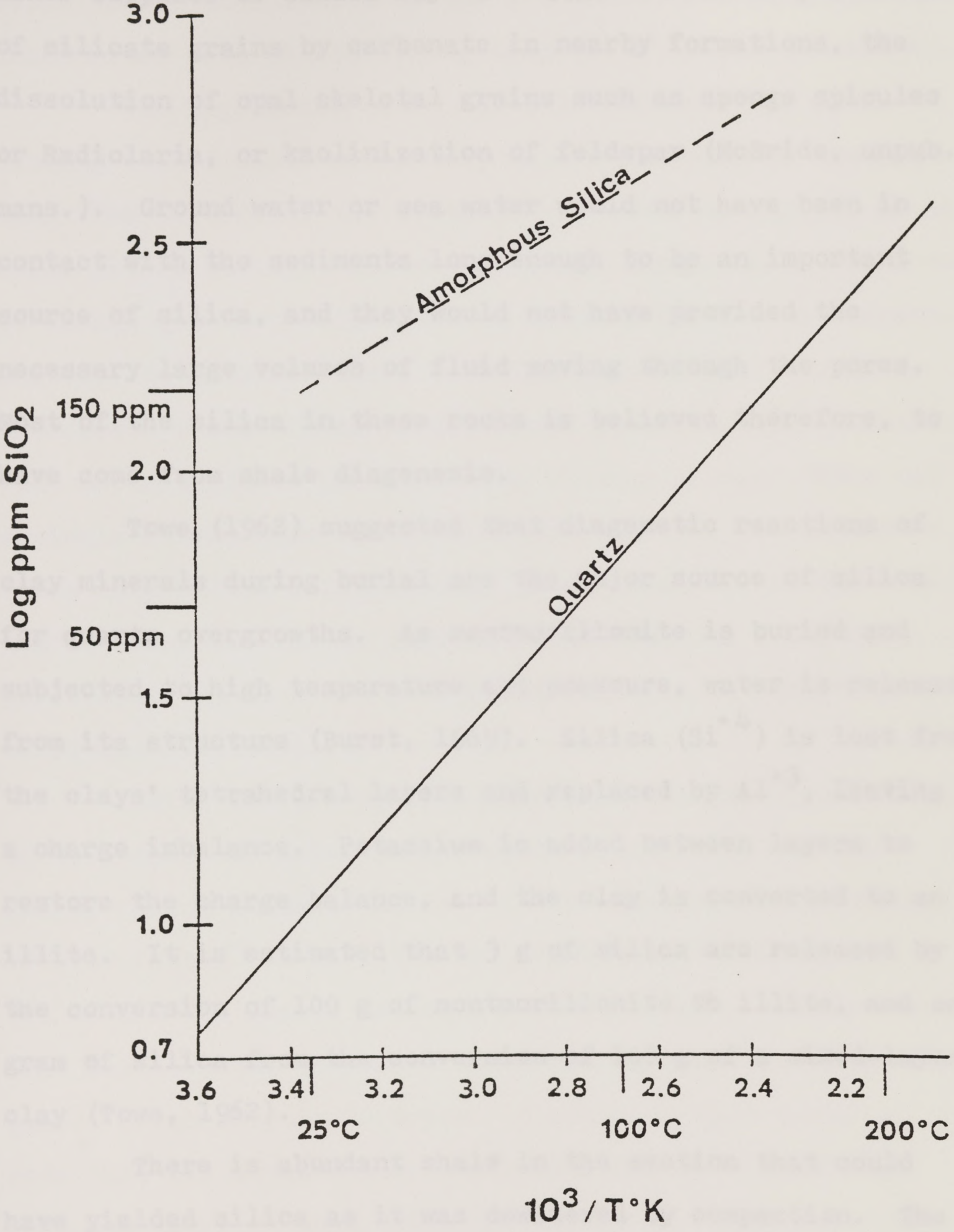

Figure 43. Effect of temperature on quartz and amorphous silica solubility. From Siever (1962).

minor supplies of silica may have come from the replacement of silicate grains by carbonate in nearby formations, the dissolution of opal skeletal grains such as sponge spicules or Radiolaria, or kaolinization of feldspar (McBride, unpub. mans.). Ground water or sea water would not have been in contact with the sediments long enough to be an important source of silica, and they would not have provided the necessary large volumes of fluid moving through the pores. Most of the silica in these rocks is believed therefore, to have come from shale diagenesis.

Towe (1962) suggested that diagenetic reactions of clay minerals during burial are the major source of silica for quartz overgrowths. As montmorillonite is buried and subjected to high temperature and pressure, water is released from its structure (Burst, 1969). Silica (Si^{+4}) is lost from the clays' tetrahedral layers and replaced by Al^{+3}, leaving a charge imbalance. Potassium is added between layers to restore the charge balance, and the clay is converted to an illite. It is estimated that 3 g of silica are released by the conversion of 100 g of montmorillonite to illite, and one gram of silica from the conversion of 100 g of a mixed-layer clay (Towe, 1962).

There is abundant shale in the section that could have yielded silica as it was dewatered by compaction. The present mineral composition of shale beds in the core samples is illite, kaolinite, and chlorite, determined by x-ray analysis. Shale weathering in the source area could have

supplied montmorillonite to the sediments, and then have been transformed into illite during diagenesis to release silica.

Von Engelhardt (1967, p. 511) believes the water flowing out of shale moves very slowly and that it takes a long time to dewater the section. If water moving out of the shale flowed straight across sandstone layers there would not be enough quartz precipitated to account for all the cement. Instead, he believes there is refraction of the flow at boundaries between beds of different permeability, so fluid flow becomes almost parallel with bedding planes. This way a single stream line of solution stays inside the sandstone for a longer time while flowing updip, and more of the silica can be removed. Silica that is in solution at depth will precipitate as it rises because of the drop in temperature, which lowers solubility.

Using the petrographic data, an estimate can be made of the volume of water necessary to precipitate all the quartz cement in these rocks. At the maximum burial depth of 7600 feet (2300 m.), the temperature was about 150°F (66°C) and the quartz solubility was 31.6 ppm. At the current burial depth the temperature averages 114°F (46°C) and quartz solubility is 20.0 ppm. A solution that cooled as it rose this far would become supersaturated with quartz by 11.6 ppm (mg/l). Each cubic centimeter of the fluid would contain 1.16×10^{-2} mg of silica that could precipitate out.

The average pre-cement porosity in these rocks was

22%, and the average amount of quartz cement was 11%, so quartz cement reduced porosity by 11%. At a level of supersaturation of 11.6 ppm quartz, 25,000 cubic centimeters of fluid must pass through one cubic centimeter of sediment in order to precipitate enough quartz to reduce porosity by 11%. Even if the solutions were supersaturated by ten times as much quartz as assumed in these calculations, large volumes of water must have moved through the sediments to cause the observed cementation.

Fisher and other (1969, p. 58) have suggested that quartz cementation starts during deposition and early burial when distributary channel waters with low pH mix with delta front waters of alkaline pH. This is supposed to set up a pH gradient that causes silica to precipitate at the boundary between these zones. There is no evidence in the "Gray" sandstones of such an increase in quartz cement in delta front facies near channels or that cementation started so early. If such an event occurred however, it could only account for a negligible amount of the total quartz cement in the rocks.

They also suggest that a later stage of quartz cementation will occur where the distal delta front sands interfinger with prodelta muds. This starts after only a few hundred feet of burial, as low pH pore waters are squeezed out of mud and into the alkaline delta front sand. Cementation is supposedly completed by burial depths of about

500 feet (150 m). Again, there is no evidence for increased quartz cementation where delta front sand interfingers with prodelta mud. In the "Gray" rocks, considerable compaction took place before cementation started. If quartz cementation had been as early as Fisher and others indicate, the pre-cement porosity should be much higher than it is. It is unlikely, therefore, that the "Gray" sandstones were cemented as early or by the pH gradient mechanism they suggest for deltaic deposits.

Calcite

Calcite cement is restricted to only 13 samples now, but there is evidence that it was once widespread in the "Gray" sandstones. Secondary pores, leached feldspars, corroded quartz (Fig. 44), and canals through grains are common in samples that now do not contain calcite. These features are all believed to form by calcite replacement. Generally, euhedral quartz overgrowths do not appear ragged, as if they had been corroded, so in most samples the calcite probably just grew up against the earlier cement without replacing it.

Thirteen samples have retained at least some of their calcite (Table 3). In samples BH 4657, AMC 4491, and LB-1 4782 the carbonate cement is all calcite, but in the others there is both calcite and Fe-dolomite. The calcite seems to be retained in samples that are relatively cleaner and coarser than the surrounding beds, such as a thin sandstone lense in shale or siltstone. These lenses would be the easiest path

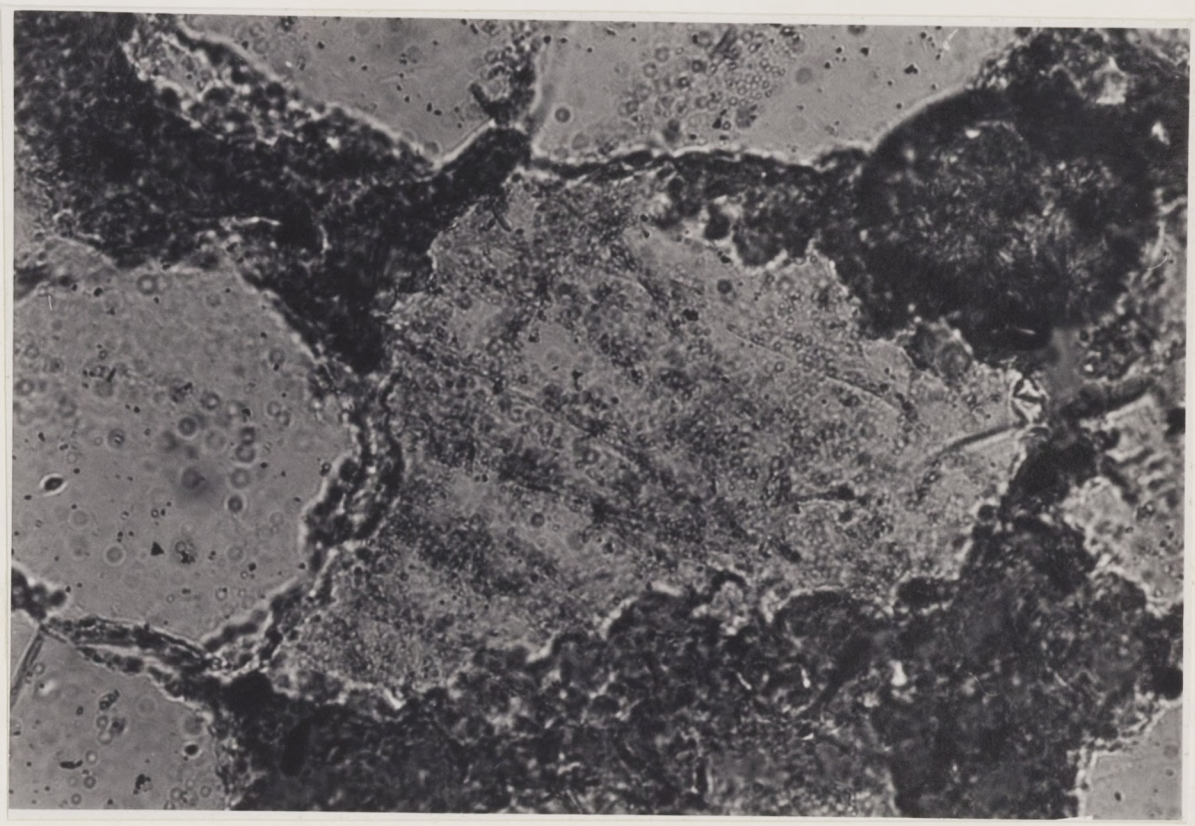

Figure 44. Quartz grain with corroded borders in sample CWS 4600. Bar = 0.05 mm.

for a fluid moving through to follow; their average porosity after quartz cementation (pre-cement porosity - quartz cement) was 25.3%. There was some replacement of quartz by calcite however, so this figure is probably a little too high. The present permeability of these samples is quite low ($\bar{x}$ = 5.6 md), because cement generally completely fills the pores. This low permeability probably protected the calcite in these samples from later fluids that dissolved it from most of the "Gray" rocks.

Chemical Conditions

Calcite is a product of the system

$$CaO - H_2O - CO_2 : Ca^{++}_{(aq)} + CO_3^{=}{}_{(aq)} \rightleftharpoons CaCO_{3(s)}$$

The amount of calcium in seawater is essentially constant at 400 ppm and it is more abundant in subsurface water (Degans and Chilingar, 1967). It can be assumed to be present in the necessary quantity to precipitate calcite, so the abundance of $CO_3^{=}$ becomes the controlling factor (Blatt, 1966). CO_2 is the most likely source of the carbon and it can be generated by the decay of organic material:

$$6O_2 + C_6H_{12}O_5 \rightarrow 5H_2O + 6CO_2$$

The production of CO_2 lowers the pH by generating hydrogen ions, according to the equation:

$$CO_{2(g)} + H_2O_{(l)} \rightleftharpoons H^+ + HCO_3^-{}_{(aq)}$$

and the reduction of pH increases the solubility of calcite (Fig. 45).

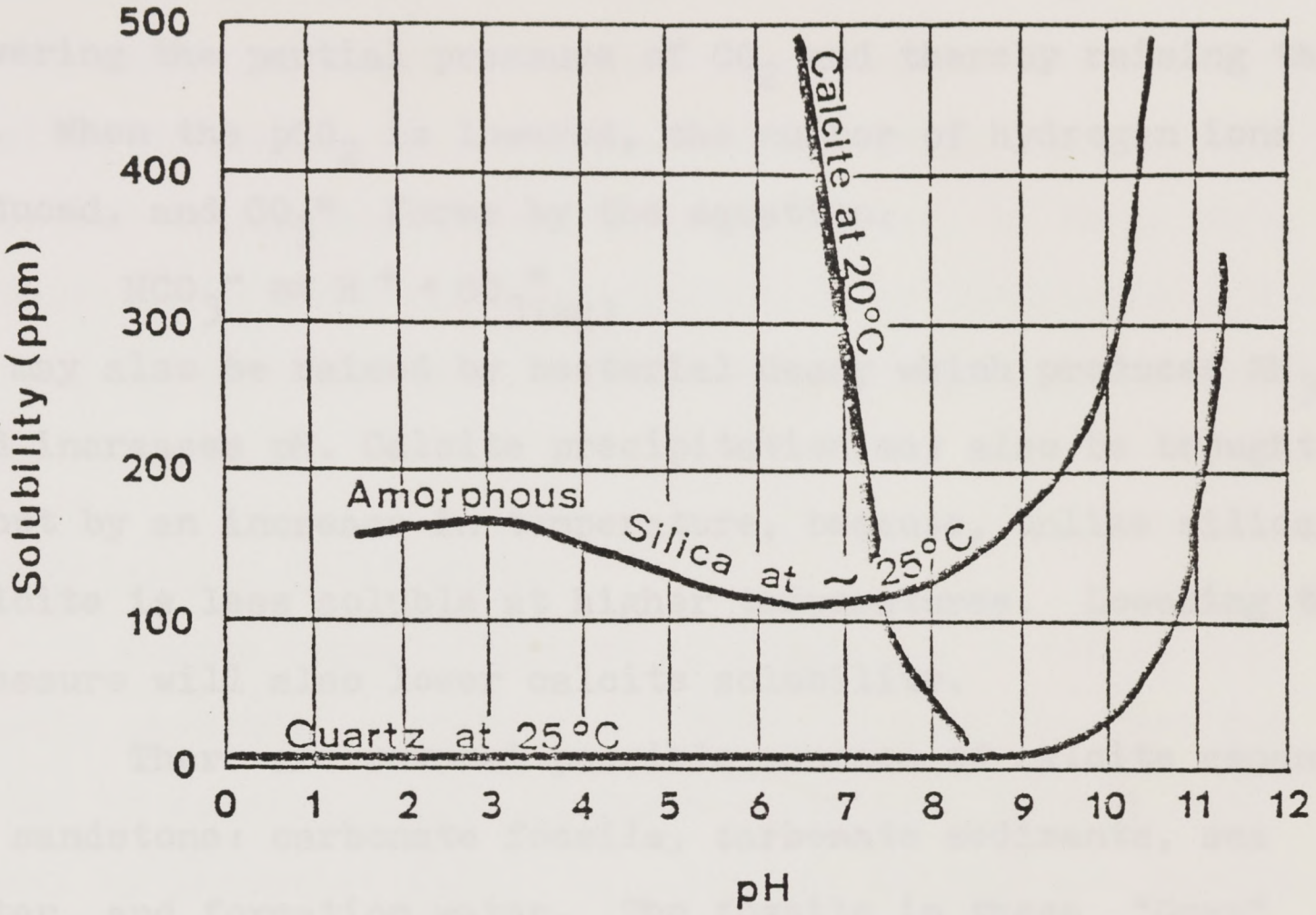

Figure 45. Effect of pH on calcite, quartz, and amorphous silica solubility. From Blatt (1966).

The precipitation of calcite can be brought about by lowering the partial pressure of CO_2 and thereby raising the pH. When the pCO_2 is lowered, the number of hydrogen ions is reduced, and $CO_3^{=}$ forms by the equation:

$$HCO_3^- \rightleftharpoons H^+ + CO_{3(aq)}^{=}$$

pH may also be raised by bacterial decay which produces NH_3 and increases pH. Calcite precipitation may also be brought about by an increase in temperature, because, unlike silica, calcite is less soluble at higher temperatures. Lowering the pressure will also lower calcite solubility.

There are several possible sources of calcite cement in sandstone: carbonate fossils, carbonate sediments, sea water, and formation water. The fossils in these "Gray" cores did not show signs of dissolution, but fossils in underlying beds may have been dissolved and the calcite carried to other sediments where it precipitated as cement. Limestone beds may have undergone compaction and pressure solution that released dissolved Ca^{++} and HCO_3^- to the interstitial waters (Berner, 1971, p. 97). Experiments done on carbonate sediments indicate that fossils may escape fracture despite considerable pressure and compaction (Shinn et al., 1977), so the well preserved fossils in the core samples are not evidence against compaction. Limestone pressure solution seems to be the most likely source of the calcite in the "Gray" sandstones. The other sources probably could not have provided the large volume of calcite cement that once filled

these rocks.

Water squeezed from shale may also provide dissolved calcite. Runnells (1969) believes that mixing two calcite saturated subsurface fluids that differ only in their NaCl content can cause calcite precipitation or dissolution, depending on the concentrations and relative amounts of each fluid present.

Quartz-Calcite Relationship

Quartz cement followed by calcite is a common diagenetic sequence in sandstone. This sequence has been reported by Schmidt (1976) in Lower Cretaceous deltaic sandstone, by Lindquist (1976) in Oligocene deltaic and marginal marine sandstone, and Jacka (1970) in Upper Cretaceous alluvial fan, fluvial and deltaic deposits, to mention a few. Sharma (1965) and Walker (1960) describe the replacement of detrital and authigenic quartz by later calcite cement. It seems likely that this common diagenetic sequence would be caused by an equally common mechanism, rather than something different for each situation. At this time there is no agreement on what this mechanism is or even if one really exists.

Blatt (1966) believes that the change from silica to calcite precipitation is controlled by the pH of the interstitial waters. If a solution is neutral or acidic, calcite solubility is high, but silica can precipitate. Then, if the pH increases, the quartz solubility will increase while

calcite solubility decreases, and calcite will precipitate. Sharma (1965) suggests that shallow sediments which have quartz precipitating in them have a higher partial pressure of CO_2 than sea water and are slightly acidic. When the sediments are buried deeper, the CO_2 is depleted and the pH rises, favoring the precipitation of calcite and the solution of quartz.

The geothermal gradient would add to the effect of any increase in pH with depth. At higher temperatures silica becomes more soluble and calcite less so, which could help trigger the precipitation of calcite (Dapples, 1959). From a study of Pennsylvanian sandstones Siever (1959) suggested that this mechanism was causing a shift from silica to calcite precipitation in deeply buried sediments.

Jacka (1970) offers a different mechanism to account for the diagenesis, that of a diffusion gradient. He believes that silica goes into solution at depth through calcite replacement and diffuses upward until it precipitates under conditions of lower temperature and pH. Large volumes of water flowing through the sediments are not needed because the ions move from higher to lower concentrations, and do not have to be carried by moving fluids. Calcite, on the other hand, goes into solution at shallow depths and diffuses downward until it reaches a zone of higher pH and temperature, where it precipitates. Thus, the change from quartz to calcite cement is caused by sediments moving down through

the zones of stability and precipitation of silica, then calcite.

Pettijohn and others (1972) propose still another explanation for this cementation pattern. With deep burial, pressure solution of limestones occurs, and the dissolved calcite is carried into nearby formations and precipitated. They do not think it is likely that there would be large-scale changes of pH or CO_2 content in the pore fluids of deeply buried sandstones. This explanation seems to be the most reasonable way to explain the change from quartz to calcite precipitation in the "Gray" sandstones.

Dissolution

The next step in the diagenetic sequence of "Gray" sandstone was the dissolution of most of the calcite cement. For this to occur, the sediments must have changed from a zone of calcite stability to one in which calcite dissolved. Schmidt (1976) suggests that calcite dissolution in Alaskan sandstones was caused by the maturation of organic matter. The CO_2 given off by the reaction formed carbonic acid that leached away the carbonate cement.

Another possibility is the mixing of distinct subsurface fluids which when combined are undersaturated with calcite and cause dissolution (Runnells, 1969).

Uplift of the sandstones could also have caused the calcite removal by lowering the temperature and perhaps the pH. Removal of part of the overburden by erosion would have

the effect of raising the beds, and they may have come under the influence of undersaturated fluids of meteoric origin (Pettijohn et al., 1972).

Working alone or in concert, any of these processes may have been responsible for calcite dissolution in the "Gray" sandstone.

Kaolinite

A minor amount of kaolinite cement, up to 5%, is common in the sandstone samples. It occurs in samples from all of the different environments, but not in samples that contain large amounts of detrital clay matrix. The kaolinite forms clusters of "books" (or "worms"), stacks of hexagonal plates, most often inside secondary pores.

Kaolinite forms in an acid environment which is abundant in silica and aluminum but lacking in cations such as potassium or magnesium. It is a common diagenetic product in permeable sediments that have acid waters circulating through (Millot, 1970, p. 327).

The same acid pore fluids that leached the calcite cement could have produced the proper conditions for kaolinite precipitation, and the two processes may have been occurring contemporaneously. Feldspars can also be kaolinized directly, without calcite replacement, again, in a low pH environment where cations are in low concentrations. Some of the kaolinite in the "Gray" sandstone samples may have formed

by this process.

Barite

Barite cement precipitated at approximately the same time as kaolinite, but it is not as common, forming only minor patches (< 1%) in the samples. Von Engelhardt (1967, p.517) believes it usually forms as a late cement, which it is in the "Gray" sandstones. Waters from deeply buried sediments generally lack sulfate anions but contain 1,000 to 3,000 mg/l barium. The formation of barite occurs when deeply buried sandstone, whose pore fluids lack sulfate but are enriched in barium, is uplifted and comes in contact with sulfate-rich waters.

The barium may be picked up from evaporites updip and concentrated in the pore fluids. It may also be coming from the dissolution of feldspars, because $BaAl_2Si0_8$ enters into solid solution with orthoclase (Goldich, 1938, p. 34).

Ferroan Dolomite

Ferroan dolomite was the last major cement to form in the diagenetic sequence of these rocks. It has a mean volume of 6.8% and a standard deviation of 11.4%, and its abundance follows a Poisson distribution (Fig. 46). Most samples have no ferroan dolomite, or only a small amount, but a few contain quite a bit, up to 47%. The Fe-dolomite is found in samples from all different environments, but only

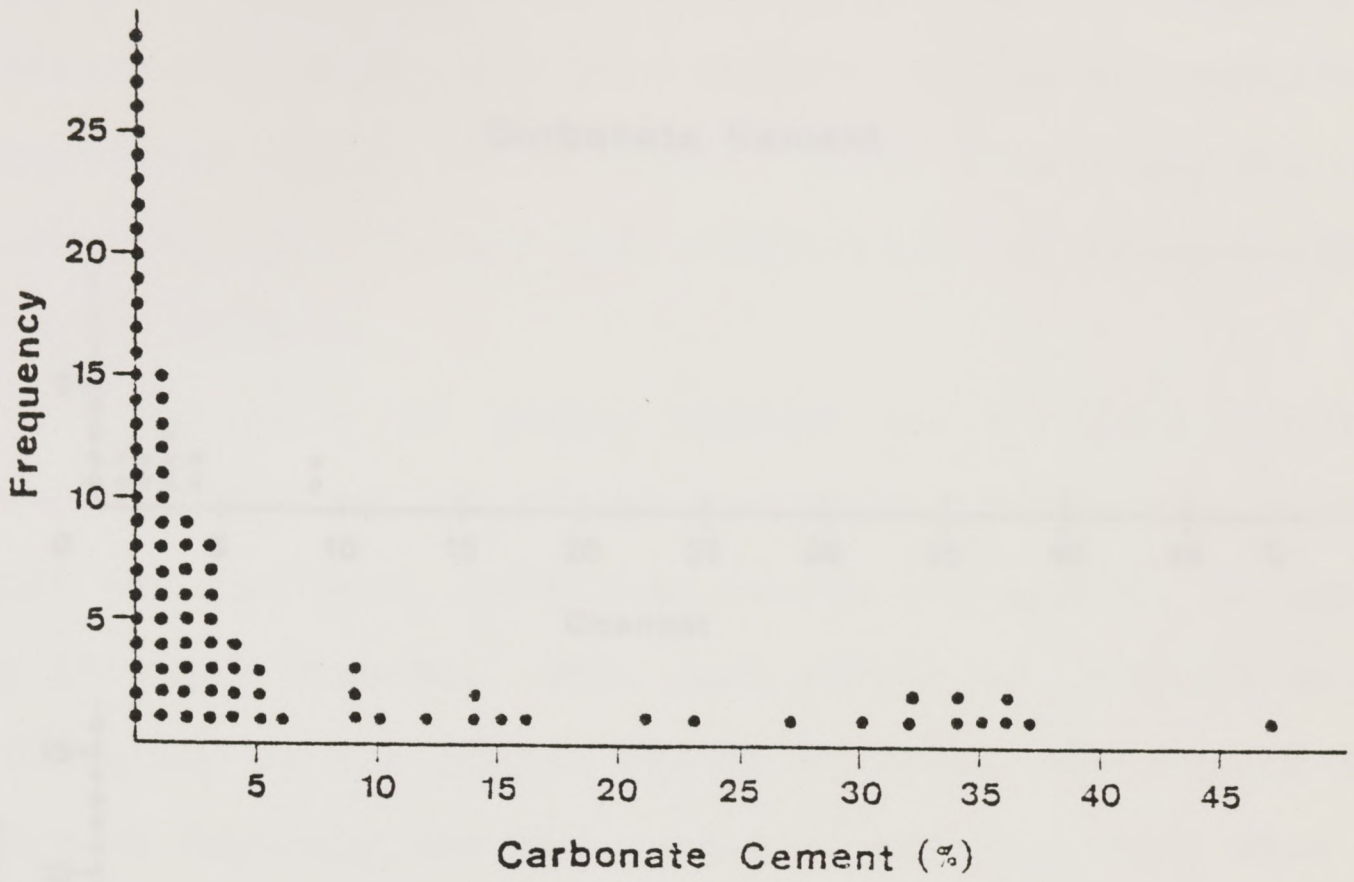

Figure 46. Frequency distribution of carbonate cement.

the crest and slope samples contain large volumes of it; none of the channel samples have more than 10% (Fig. 47).

A multiple regression analysis of the carbonate cement data was done to determine what factors controlled its distribution. Calcite and ferroan dolomite were considered together, but because only three samples are completely calcite cemented, the calcite should not have had a large effect. The results essentially pertain only to the ferroan dolomite, because it was so much more widespread. Distance from shale beds, volume of quartz cement, shale and matrix content, grain size, and sorting were the independent

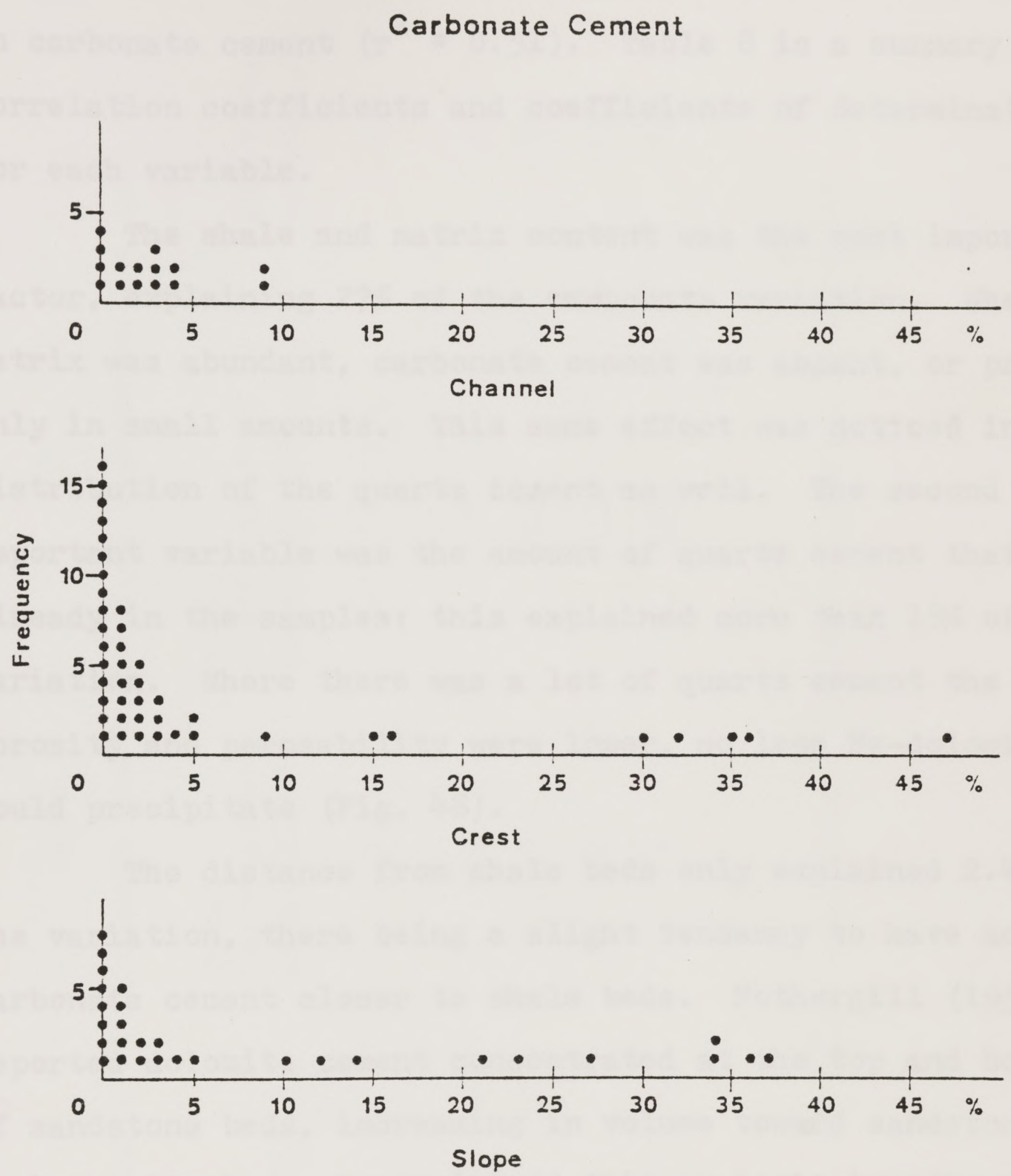

Figure 47. Relationship of carbonate cement to depositional environment.

variables. These five variables had a total correlation coefficient of 0.71, and they explain 51% of the variation in carbonate cement (r^2 = 0.51). Table 8 is a summary of the correlation coefficients and coefficients of determination for each variable.

The shale and matrix content was the most important factor, explaining 27% of the carbonate variation. Where matrix was abundant, carbonate cement was absent, or present only in small amounts. This same effect was noticed in the distribution of the quartz cement as well. The second most important variable was the amount of quartz cement that was already in the samples; this explained more than 18% of the variation. Where there was a lot of quartz cement the porosity and permeability were lower, so less Fe-dolomite could precipitate (Fig. 48).

The distance from shale beds only explained 2.4% of the variation, there being a slight tendency to have more carbonate cement closer to shale beds. Fothergill (1955) reported dolomite cement concentrated at the top and bottom of sandstone beds, increasing in volume toward sandstone-shale boundaries. He explained this by ionic impedance, suggesting that clays act as semi-permeable membranes that impede the passage of certain ions. As permeability is reduced, the ionic concentration in the fluids in sandstones close to shales increases, and a concentration gradient forms. When the ionic concentrations are high enough,

TABLE 8

Summary Table of Carbonate Cement Multiple Regression Analysis

Step	Variable Entered	Total Correlation Coefficient	Total Coefficient of Determination (r^2)	Individual r^2
1	Distance from shale beds (DIST)	.15	.02	.02
2	Quartz cement (QCEM)	.45	.21	.18
3	Shale + Matrix (SH)	.69	.48	.27
4	Size (SIZE)	.71	.50	.02
5	Sorting (SORT)	.71	.51	.01

CARB = 25.09 - 0.19DIST - 1.04QCEM - 0.69SH + 2.46SIZE - 12.35SORT

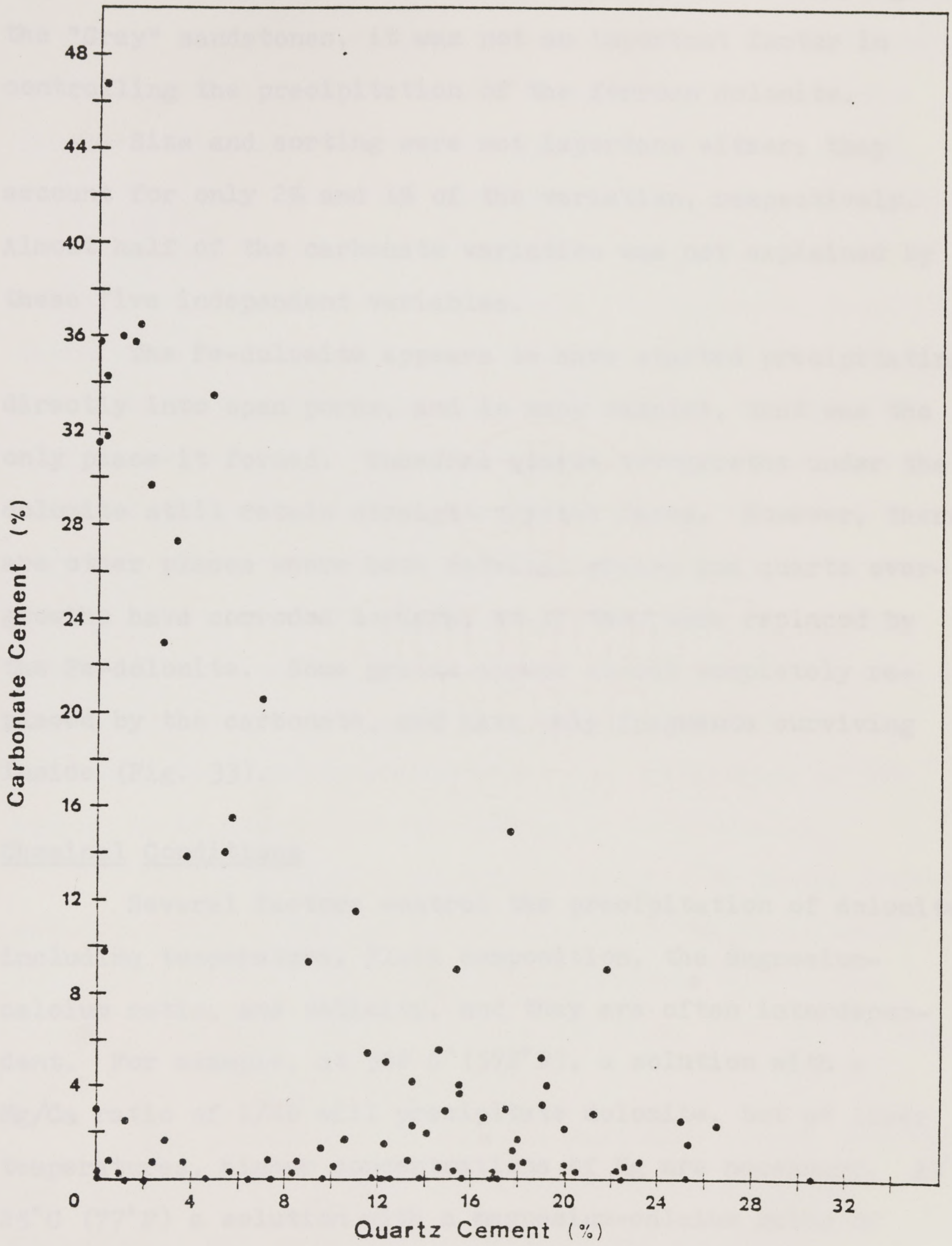

Figure 48. Relationship between quartz and carbonate cement.

carbonate precipitates. If ionic impedance was occurring in the "Gray" sandstones, it was not an important factor in controlling the precipitation of the ferroan dolomite.

Size and sorting were not important either; they account for only 2% and 1% of the variation, respectively. Almost half of the carbonate variation was not explained by these five independent variables.

The Fe-dolomite appears to have started precipitating directly into open pores, and in many samples, that was the only place it formed. Euhedral quartz overgrowths under the dolomite still retain straight crystal faces. However, there are other places where both detrital grains and quartz overgrowths have corroded borders, as if they were replaced by the Fe-dolomite. Some grains appear almost completely replaced by the carbonate, and have only fragments surviving inside (Fig. 33).

Chemical Conditions

Several factors control the precipitation of dolomite, including temperature, fluid composition, the magnesium-calcium ratio, and salinity, and they are often interdependent. For example, at 300 C°(572°F), a solution with a Mg/Ca ratio of 1/20 will precipitate dolomite, but at lower temperatures, higher concentrations of Mg are necessary. At 25°C (77°F) a solution with a magnesium-calcium ratio of about 1/1 can theoretically precipitate dolomite (Hsu, 1963).

Salinity also affects how much magnesium is needed

to form dolomite. In hypersaline environments, Mg/Ca ratios of 5/1 to 10/1 are necessary (Kinsman, 1965), but in dilute, meteoric waters, a ratio of 1/1 is sufficient if crystallization takes place slowly enough (Folk and Land, 1975). Figure 49, taken from Folk and Land (1975), shows the fields of occurrence of calcite and dolomite plotted on a graph of salinity vs. Mg/Ca. Subsurface waters have a wide range of salinities, so the Mg/Ca ratio needed to precipitate dolomite will also vary. The water now in the "Gray" sandstone has a Mg/Ca ratio of 1/6 and a salinity of over 100,000 ppm, which is definitely in the calcite field, so the dolomite must not have precipitated from fluids of this composition. Because ferroan calcite probably precipitated contemporaneously with dolomite, the subsurface fluids must have been at the borderline between calcite and dolomite formation. Generally Fe-dolomite precipitated, but variations in the amount of Mg caused ferroan calcite to form locally.

Mixing of saline subsurface brine with fresh, meteoric water may have triggered the precipitation of Fe-dolomite. This mixing would lower the salinity without appreciably changing the Mg/Ca ratio, putting the fluid into the dolomite field (Folk and Land, 1975).

The subsurface environment must have been a reducing one, because ferrous iron was taken into the dolomite structure. The percentage of iron in the cement is not known, but it can be estimated from the color of the stained

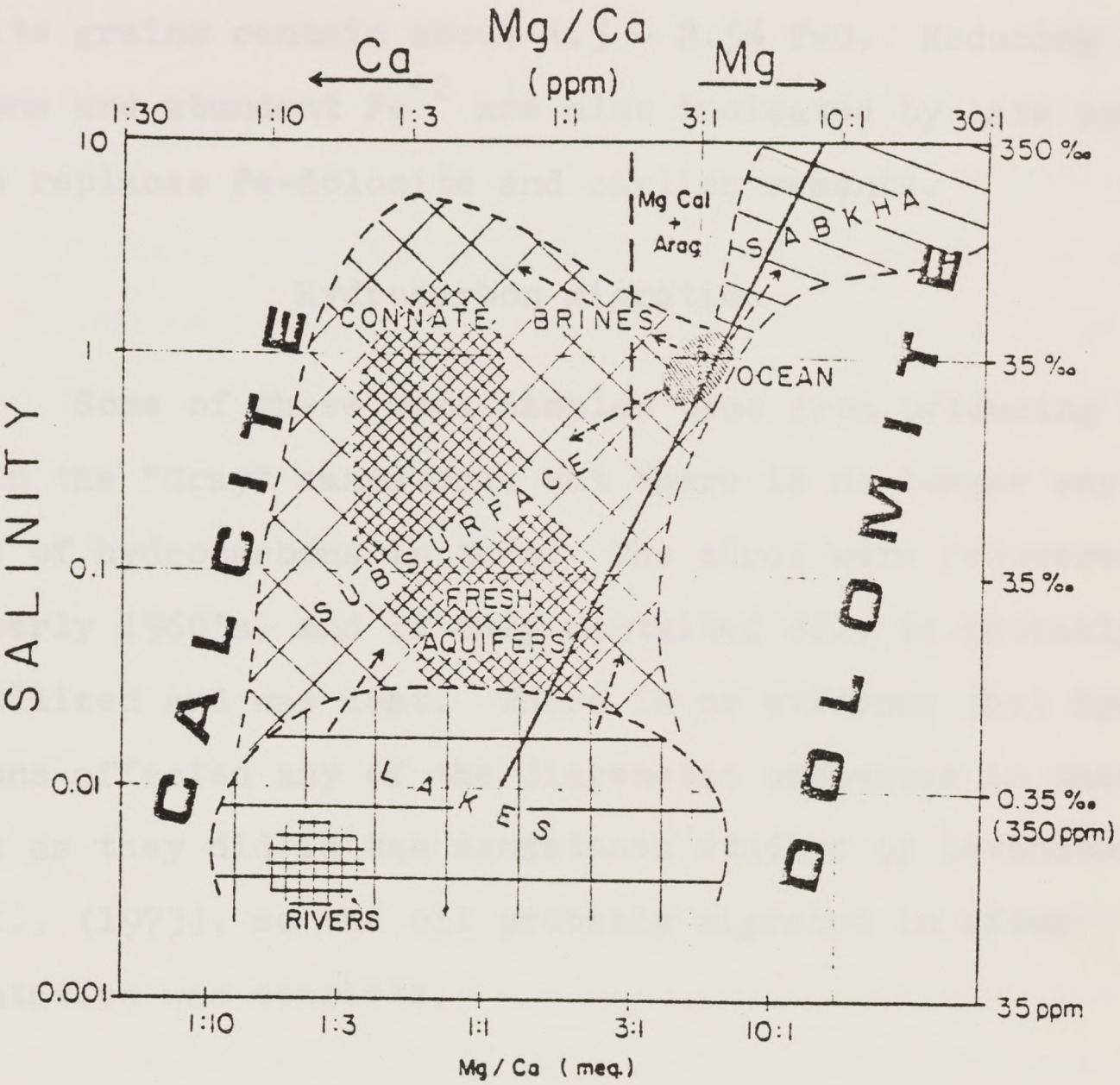

Figure 49. Fields of occurrence of calcite and dolomite plotted on a graph of salinity versus Mg/Ca. From Folk and Land (1975).

ferroan calcite. Lindholm and Finkelman (1972) have published a color chart for semiquantitative determination of ferrous iron in calcite, and based on the chart, these ferroan calcite grains contain about 1.5 - 2.5% FeO. Reducing conditions and abundant Fe^{+2} are also indicated by late pyrite, which replaces Fe-dolomite and earlier cements.

Hydrocarbon Migration

Some of these core samples come from producing zones within the "Gray" sandstone, but there is no longer any evidence of hydrocarbons in them. The cores were recovered in the early 1960's, and if they contained oil, it probably volatilized and was lost. There is no evidence that hydrocarbons affected any of the diagenetic processes in these rocks as they did in the sandstones studied by Levandowski et al., (1973), so the oil probably migrated in after cementation was complete.

POROSITY

The present porosity distribution in sandstones in the West Tuscola field reflects both the original porosity in the sediments and the diagenetic changes that have occurred within them. Figure 50 shows the frequency distribution of present, pre-cement, and secondary porosity in medium and fine sandstone samples. Secondary porosity has a distribution between Poisson and arithmetic normal (Folk, 1977, pers. comm.). Pre-cement porosity has an arithmetic normal distribution ($\bar{x}$ = 23.9%, σ = 7.7%), and the present porosity also has a normal distribution ($\bar{x}$ = 6.8%, σ = 4.1%) except for the cluster of values at zero porosity. Quartz cement, whose volume also has a normal distribution, was mainly responsible for the reduction in porosity to its current values. The cluster of values at zero was caused by Fe-dolomite, whose volume has a Poisson distribution. Most samples have no Fe-dolomite or very little, but a few samples contain over 30%, and these are the samples whose porosity has been completely destroyed.

The distribution of pre-cement porosity in the different deltaic environments is shown in Figure 51. The pre-cement porosities are not significantly different at the 95% confidence level between any of the environments. This suggests that compaction of the sands was nearly the same in all facies. The slope does have more samples with very low

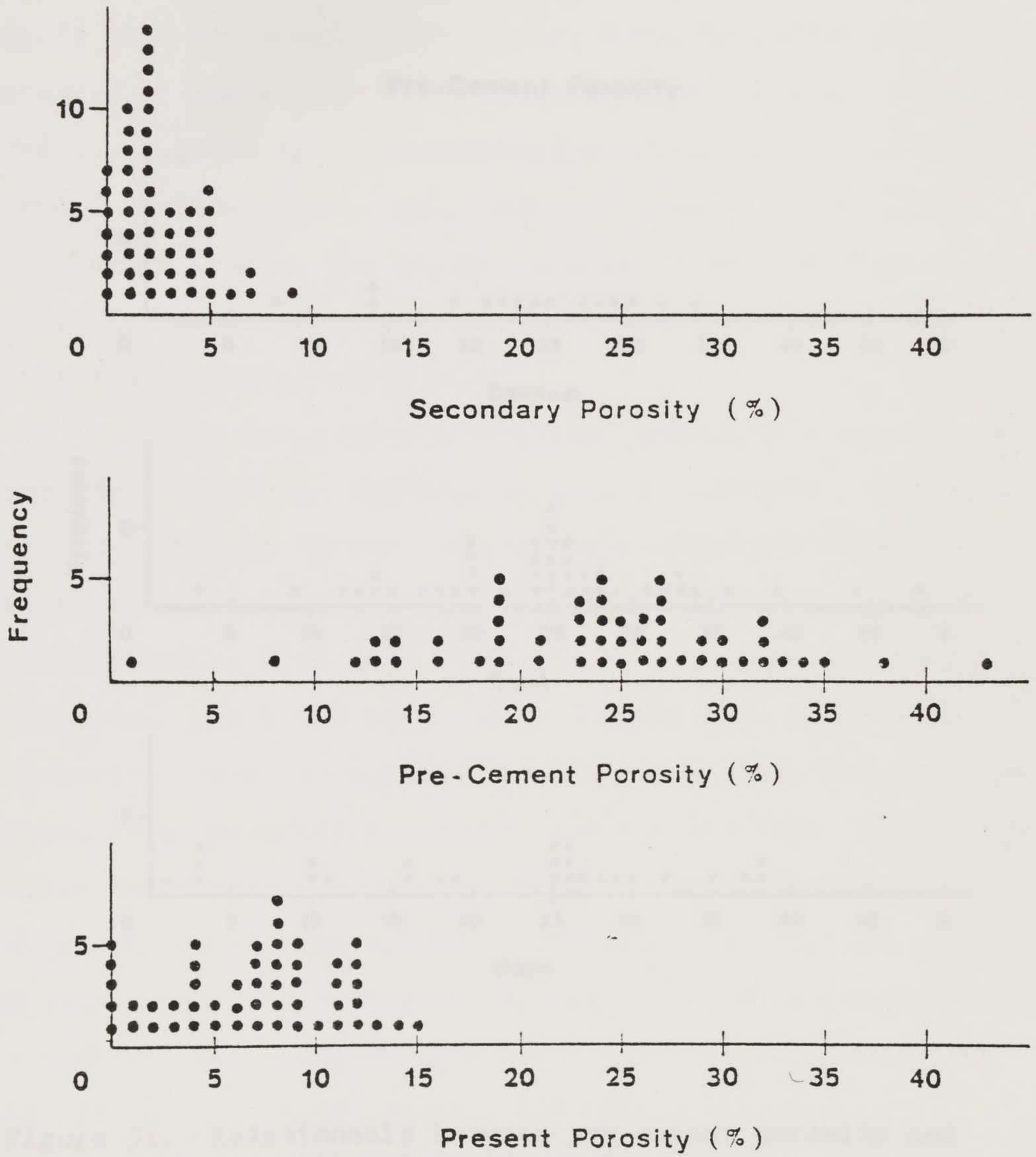

Figure 50. Frequency distribution of present, pre-cement, and secondary porosity in medium and fine sandstone samples.

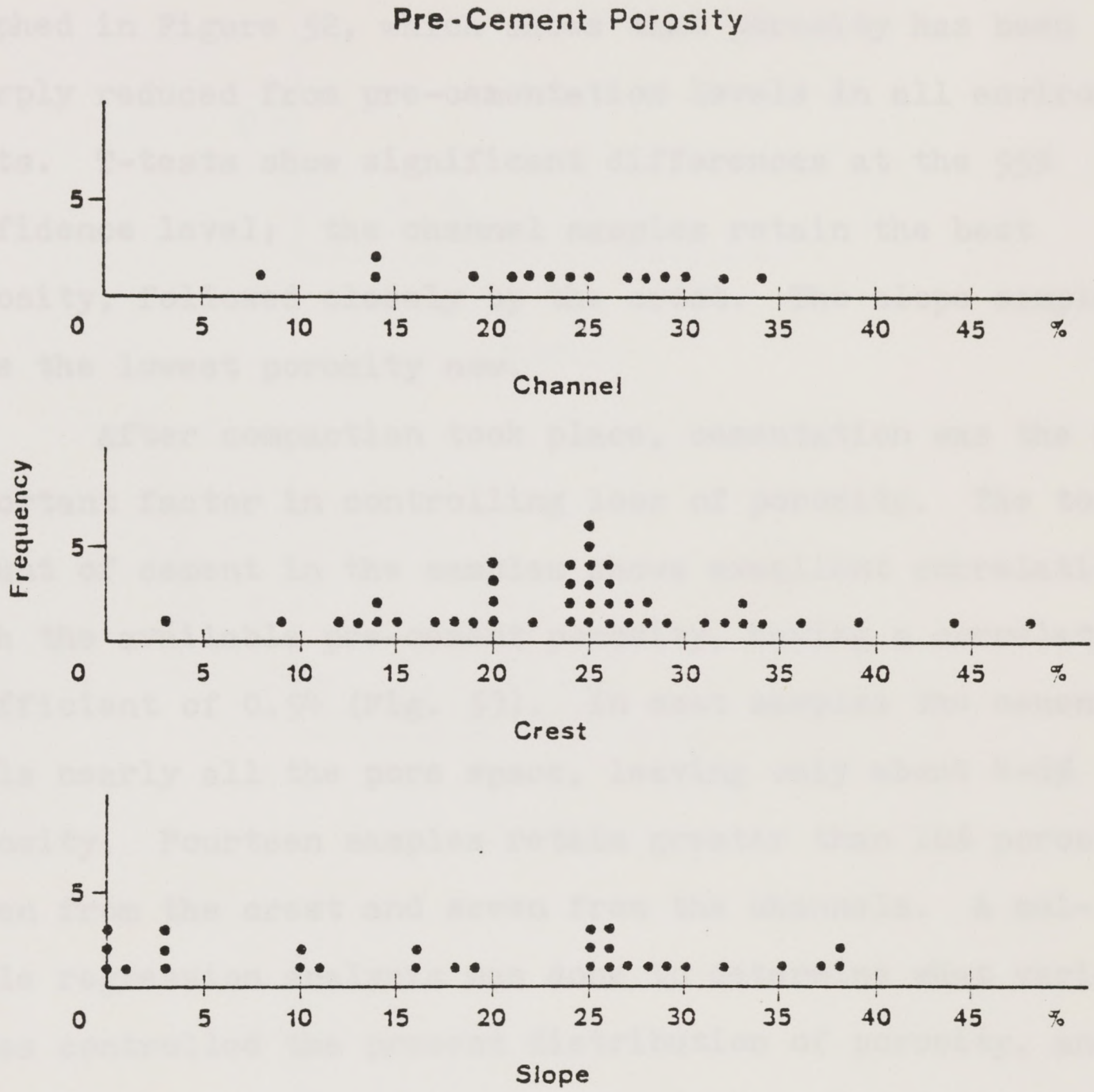

Figure 51. Relationship between pre-cement porosity and depositional environment.

values than either the crest or channels, however, and at the 90% confidence level it does have less pre-cement porosity than the crest. The current porosity distribution is graphed in Figure 52, which shows that porosity has been sharply reduced from pre-cementation levels in all environments. T-tests show significant differences at the 95% confidence level; the channel samples retain the best porosity, followed closely by the crest. The slope samples have the lowest porosity now.

After compaction took place, cementation was the most important factor in controlling loss of porosity. The total amount of cement in the samples shows excellent correlation with the available pre-cement porosity, having a correlation coefficient of 0.94 (Fig. 53). In most samples the cement fills nearly all the pore space, leaving only about 4-6% porosity. Fourteen samples retain greater than 10% porosity, seven from the crest and seven from the channels. A multiple regression analysis was done to determine what variables controlled the present distribution of porosity, and to predict where the best porosity should be. The independent variables were distance from shale beds, sorting, shale and matrix content, total cement, and mean grain size.

These five variables had a total correlation coefficient of 0.78 and explained 61% of the porosity variation. The total amount of cement was by far the most important variable, explaining almost 40% of the variation in porosity

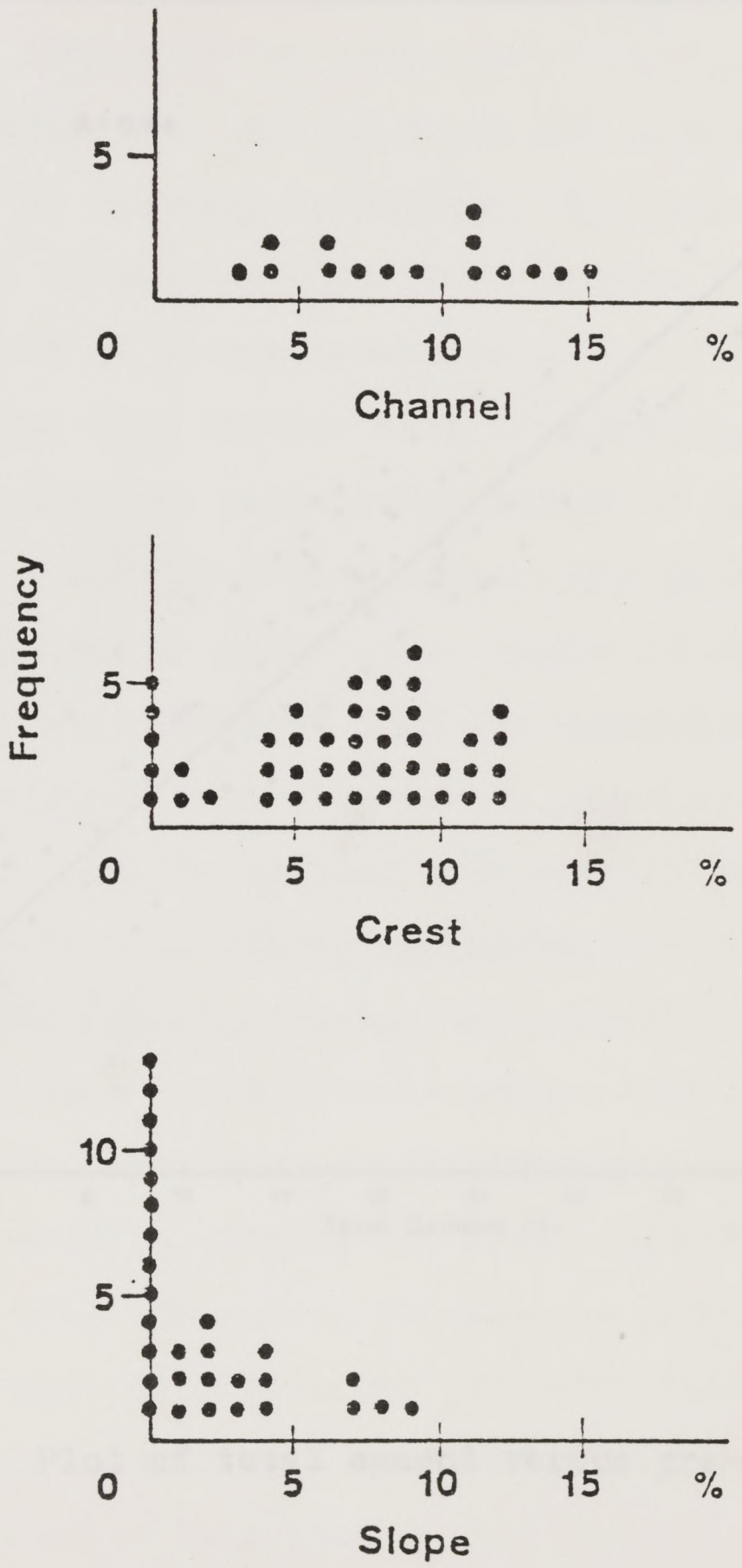

Figure 52. Relationship between present porosity and depositional environment.

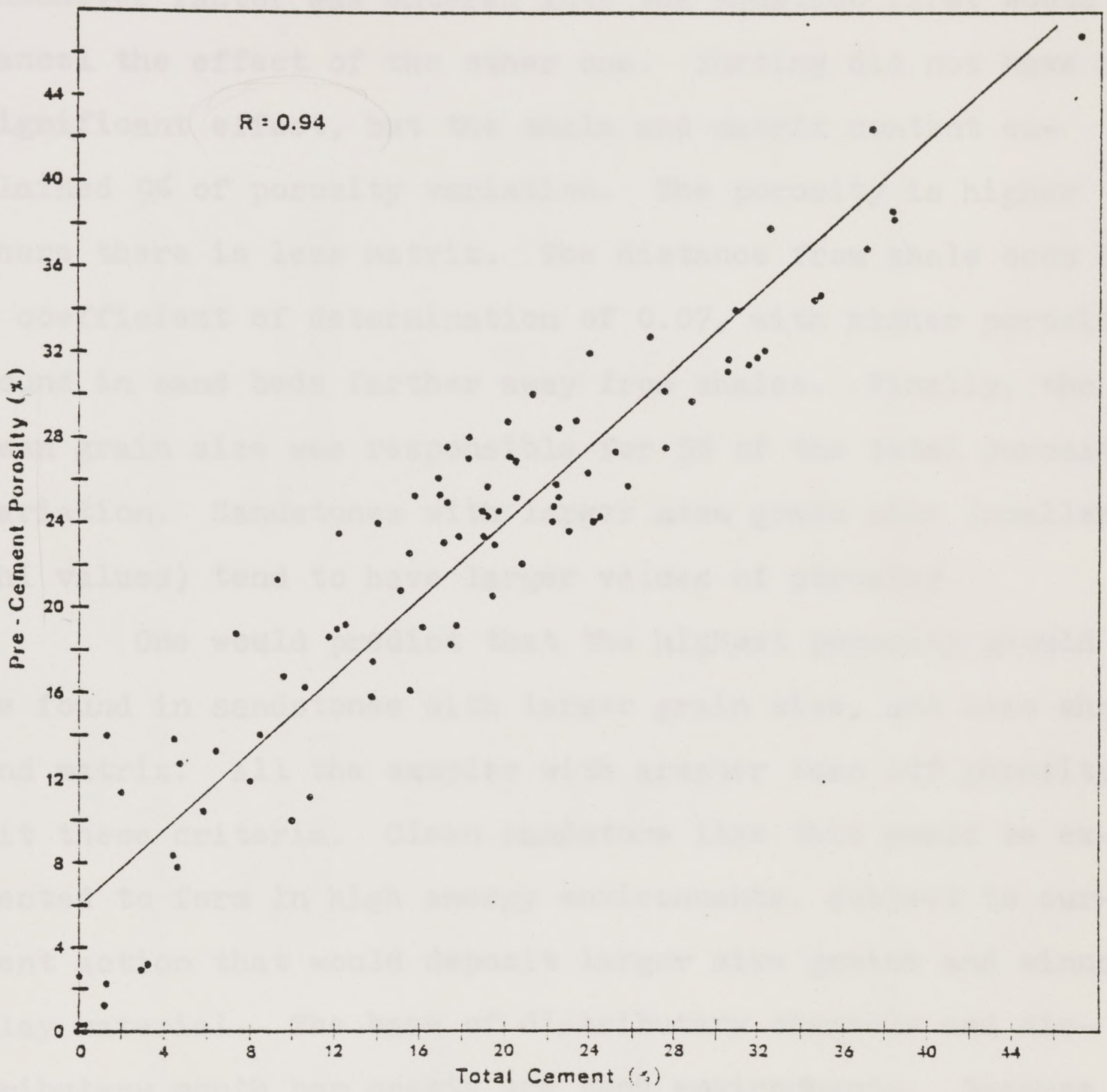

Figure 53. Plot of total cement versus pre-cement porosity.

(Table 9). Pre-cement porosity was not put into the equation because of its close linear relationship to total cement; whichever factor was entered into the equation first would cancel the effect of the other one. Sorting did not have a significant effect, but the shale and matrix content explained 9% of porosity variation. The porosity is higher where there is less matrix. The distance from shale beds had a coefficient of determination of 0.07, with higher porosity found in sand beds farther away from shales. Finally, the mean grain size was responsible for 5% of the total porosity variation. Sandstones with larger mean grain size (smaller phi values) tend to have larger values of porosity.

One would predict that the highest porosity should be found in sandstones with larger grain size, and less shale and matrix. All the samples with greater than 10% porosity fit these criteria. Clean sandstone like this would be expected to form in high energy environments, subject to current action that would deposit larger size grains and winnow clay material. The base of distributary channels and distributary mouth bar crests are such environments. Because mean grain size and matrix content are primary depositional features, their effect on the porosity distribution of a sediment can be predicted by knowing its depositional history.

The other important factor that controls porosity, total cement volume, is strongly correlated with matrix content too. The more matrix present in a sample, the less

TABLE 9

Summary Table of Porosity Multiple Regression Analysis

Step	Variable Entered	Total Correlation Coefficient (r)	Total Coefficient of Determination (r^2)	Individual r^2
1	Distance from shale beds (DIST)	.27	.07	.07
2	Sorting (SORT)	.27	.07	.0002
3	Shale + Matrix (SH)	.39	.16	.09
4	Total Cement (CEM)	.74	.55	.40
5	Size (SIZE)	.78	.61	.05

POR = 18.52 + 0.03DIST - 1.89SORT - 0.24SH - 0.31CEM - 1.63SIZE

cement there will be, but this does not mean that porosity will be higher. The samples with greater than about 8% shale and matrix content start out with lower than average pre-cement porosity. When saturated fluids circulate through them, it does not take very much cement precipitation to fill what porosity is there. Their porosity and permeability can be destroyed by a fairly small amount of cement. On the other hand, sediments that start out with less matrix will have higher pre-cement porosities, and they can hold more cement. It will take a longer time and greater volume of fluid flowing through them to completely cement their pores than it would to cement a less porous sediment. If something interrupts cementation, such as an end of the compaction that provides silica-rich solutions from shale beds, these cleaner sands will still retain some of their porosity. So, assuming cementation does not go to completion, in which case there would not be porosity remaining anywhere, sands with high primary porosity, deposited in current-worked, high energy environments should retain the best porosity after diagenesis.

There are two types of secondary pores in these rocks. Most of the secondary porosity was originally primary porosity that was lost by calcite cementation and then recovered when the calcite dissolved. This process does not add any more porosity to what was present at the time of deposition, but merely recovers it. The other type of secondary porosity is formed by the dissolution of framework grains or grains replaced by calcite such as clay clasts and feldspar, and this

does add to the original porosity. As much as 8.5% in some samples was counted as secondary porosity, and even assuming half of that volume is taken up by framework wreckage (probably a generous estimate), that means over 4% porosity has been gained. This 4% could be the difference between a producing and a non-producing sandstone.

Sandstones that contain large amounts of feldspar, clay clasts, and other unstable grains would be expected to have the most secondary porosity. Feldspar grains should be fairly evenly distributed, but clay clasts would be more common in environments that undergo current scouring. Distributary channels and channel mouth bars are often scoured by flood waters which could rip up previously deposited, semi-consolidated sediments. Secondary porosity might be expected to be high in these environments if the clasts are deposited quickly, before they are destroyed. Adjacent low energy environments, such as the delta front slope, might have more of them intact.

CONCLUSIONS

The "Gray" interval of the Pennsylvanian Strawn series in Taylor County, Texas, was deposited in a high-constructive (river-dominated) delta on a stable cratonic platform. The uplift of the Ouachita Fold Belt to the east was the source of the clastic debris carried across the Fort Worth Basin by river; the detritus was deposited in deltas on the Concho Platform. The deltaic facies that could be differentiated in these cores include prodelta, delta front slope, channel mouth bar crest, distributary channel, inter-distributary bay, and marsh. Facies were identified by their vertical stratigraphic sequence, texture, sedimentary structures, and fossil content. The "Gray" interval is currently about 4500 feet (1372 m.) deep in the West Tuscola field, but it was probably buried to a depth of 7500 feet (2286 m.) previously.

Representative sandstone and coarse siltstone samples were taken from the different facies. Their porosities range from 0 to 15.2%, with a mean of 5.3% and standard deviation of 4.2%. The permeability ranges between 0 and 387 md. The samples are mainly fine to very fine, submature to mature, shale-bearing sublitharenite.

Primary porosity was best in sediments with large mean grain size, little detrital clay matrix, and located farther away vertically from shale beds. Sediments like this

are deposited in high energy environments such as distributary channels and channel mouth bars. Porosity in clean sandstone at the time of deposition may be as high as 45%, but it quickly is lost by burial compaction, reduced to about 35% within the first tens of feet of burial. The average pre-cement porosity in these samples was 22%, so more porosity was lost during deeper burial, probably by grain rotation and deformation of ductile grains.

Cementation started by the precipitation of authigenic chlorite as rims around some quartz grains. Where the rims are thick, they were able to inhibit the precipitation of quartz overgrowths. Some chlorite is found over the quartz cement, so some chlorite precipitation must have continued after quartz cementation started.

Quartz is the most abundant cement in these sandstones, with a mean volume of 11.0% (σ = 8.2%). Quartz cementation was most extensive in sediments with larger mean grain size, greater pre-cement porosity, and less detrital shale and matrix. In samples with greater than 8% matrix, the amount of quartz cement is sharply reduced. Slope samples, which tend to be finer-grained and contain more matrix, have significantly less quartz cement than channel or crest samples. The normally distributed pre-cement porosity was reduced by quartz cement to the present porosity values, which are also normally distributed.

The source of the quartz in overgrowths may have been

from diagenetic clay mineral reactions during burial that released silica. Compaction of shale may have squeezed out the silica-rich pore fluids and forced them into the sandstone beds updip, where the quartz precipitated.

Calcite precipitated next, and it probably filled most of the remaining pore space, as well as replaced some feldspar grains and clay clasts. Pressure solution of limestone is a possible source of calcite. The calcite cement was removed later, perhaps by uplift of the rocks into a zone where they came in contact with acidic waters of meteoric origin. Compaction had ended by this time because delicate framework wreckage and large secondary pores that were opened up by the calcite dissolution were not destroyed.

Late cements formed after the removal of the calcite. Kaolinite and barite are rare but occur in widespread patches. They often occupy secondary pores that contain wreckage of original framework grains.

Ferroan dolomite was the last cement to precipitate, and its abundance in the samples has a Poisson distribution. Where it is absent or present in only small patches, the porosity remains fairly high, but in the samples where it is very abundant, the porosity is almost completely destroyed. Very abundant Fe-dolomite has only been found in some crest and slope samples, and not in any channel samples. Ferroan dolomite is most likely to occur in samples that do not contain much matrix and have not been extensively cemented by

quartz overgrowths.

The diagenetic changes that took place in these rocks have strongly reduced or destroyed their original porosity. Secondary porosity has added a few percent to what remains, and it could make an important difference between a producing and non-producing sandstone. Rocks that started out with the highest porosity at deposition have the best chance of retaining some of it through diagenesis. The particular environment a sediment was deposited in had less control over the type and amount of cement that precipitated than the texture; where matrix is abundant, cements do not precipitate. Chemical differences among environments at the time of deposition were evened out during burial and are not important by the time cementation started. The fluids that moved through the sediments have had essentially uniform compositions over the area considered in this study, so the same cements should be found throughout the samples. Minor local variations in fluid composition, perhaps related to the surrounding framework composition, could be responsible for particular locations of the rarer cement types, like barite. The location of the abundant cements, like quartz, is more likely to be controlled by textural variations.

APPENDIX I

Core Descriptions

Depth in core in feet	Thickness in feet	Description
#1 Alton Roberts 4614-4664 feet		
4614-4617	3	Sandstone, light gray (N7), low angle cross-bedded, very fine-grained. Some disturbed bedding. Erosional base.
4618-4619	2	Shale, dark gray (N4/0 2.5Y), fissile, with plant debris.
4620-4624	5	Sandstone, light gray (7/1 5Y), fine-grained. Horizontal laminations and low angle cross-bedding. Erosional base.
4625-4627	3	Shale-siltstone, dark gray (N4/0 2.5Y), abundant plant debris.
4628-4633	6	Sandstone, light gray (7/1 5Y), low angle cross-bedded, medium-grained. Cross-beds outlined by organic matter. Erosional base.
4634-4636	3	Shale-siltstone, dark gray (N4/0 2.5Y), coarsening upward.
4637-4639	3	Sandstone, white (8/0 7.5YR), horizontally laminated, fine-grained. Vertical and horizontal burrows present. Abundant clay clasts.
4640-4645	6	Sandstone, white (8/1 5Y), cross-bedded, medium-grained.
4646-4650	5	Sandstone, light gray (7/1 5Y), cross-bedded, medium-grained. Parting laminae of clay clasts

		and shells. Abundant forams, brachiopods, mollusks.
4651-4657	7	Sandstone, white (8/1 5Y), cross-bedded, medium-grained.
4658-4664	6	Sandstone, light gray (7/1 5Y), structureless, fine-grained. Clay chips, plant fragments concentrated in black, organic-rich horizontal laminae.
	Total = 50	

Ledbetter B-1 4781-4818 feet

4781-4783	3	Siltstone, light gray (7/0 2.5Y), horizontally laminated, coarse-grained, interbedded with organic-rich parting laminae 1/32" thick. Also some thin shale beds, horizontal and vertical burrows present.
4784-4792	9	Shale-siltstone, dark gray (N4/0 2.5Y), fissile, interbedded with sandstone laminae 1/32 to 3/4" thick. Vertical and horizontal burrows present in sandstones. Shales contain fragments of brachiopods, crinoids, and bryozoans.
4793-4797	5	Siltstone, light gray (7/0 2.5Y), horizontally laminated, coarse-grained, with thin organic partings and thicker shale layers. Abundant vertical and horizontal burrowing gives a marbled appearance.
4798-4806	9	This section of core missing.
4807-4812	6	Sandstone, light gray (7/0 2.5Y), very fine-grained, with shale layers. Horizontal laminations distorted by burrowing. Some laminae made of clay clasts or organic material.
4813-4818	6	Light gray (7/0 2.5Y) interbedded coarse siltstone and shale marbled together by abundant burrows. Fossil fragments concentrated in shale layers.
	Total = 37	

F.A. Boyd #1 4811-4881 feet

4811-4817	7	Shale, dark gray (N4/0 2.5Y), with abundant plant fragments and patches of shiny black organic material.
4818-4822	5	Interbedded gray (N6/0 2.5Y) coarse siltstone and shale. Sandstones horizontally laminated or rippled, and burrowed. Load structures of sand into shale. Shales contain gastropods, plant fragments.
4823-4828	6	Sandstone, light gray (7/1 5Y), cross-bedded and horizontally laminated, fine-grained. Erosional base.
4829-4834	6	Sandstone, white (8/0 2.5Y), horizontally laminated, very fine-grained, and interbedded with shale. Horizontal burrows. Plant fragments in shales.
4835-4856	22	Sandstone, light gray (7/1 5Y), horizontally laminated, fine to very fine-grained, fining upwards. Occasional shale layers, horizontal burrows.
4857-4878	12	Light gray (7/1 5Y) interbedded fine sandstone and shale, marbled by burrowing. Sand packages up to 10" thick.
4879-4881	3	Shale, structureless, dark gray (N4/0 2.5 Y). No fossils or plant debris.
	Total = 70	

#2 Graham 4861-4939 feet

4861-4868	8	Sandstone, light gray (7/1 5Y), horizontally laminated, very fine-grained. Clay clast-rich laminae with shiny black organic patches. Local ripples in sandstones. Fines upward, gradational basal contact.
4869-4883	15	Sandstone, gray (6/1 5Y), cross-bedded, medium-grained. Erosional base, fines upward.

4884	1	Sandstone, light gray (7/1 5Y), very fine-grained, interbedded with silty shale.
4885-4895	11	Sandstone, light gray (7/1 5Y), very fine-grained, with thin organic-rich partings. Clay clast-rich laminations broken up by burrowing.
4896-4898	3	Shale, dark gray (N4/0 2.5Y), fissile, with black organic patches and streaks.
4899-4919	21	Sandstone, light gray (7/1 5Y), laminated, fine-grained, with organic laminae and shale layers. Some cross-bedded sandstone. Gradational basal contact.
4920-4936	17	Sandstone, light gray (7/1 5Y); interbedded with gray shale (5/0 2.5Y). Horizontal burrows, load structures of sand into shale. Fewer shale layers toward both the top and bottom. Shale x-rayed.
4937-4939	3	Sandstone, light gray (7/1 5Y), structureless, fine-grained, with a few shale layers at the top.

Total = 78

W.A. Graham B-1 4868-4930 feet

4868-4872	5	Silty-shale, gray (N5/0 2.5Y), with black organic patches. Gastropods, brachiopods, plant fragments.
4873-4876	4	Shale, dark gray (N4/0 2.5Y), fissile, with plant fragments.
4877-4882	6	Interbedded coarse siltstone, light gray (7/0 2.5Y) and shale. Mostly horizontally laminated, some ripple cross-laminae in the coarser layers. Horizontal burrows.
4883-4888	6	Sandstone, light gray (7/0 2.5Y), cross-bedded, fine-grained. Some disturbed bedding.
4889-4894	6	Interbedded fine sandstone, light gray (7/1 5Y), and shale. Some thicker sand packages are cross-bedded. Horizontal burrows.

4895-4897	3	Sandstone, light gray (7/1 5Y), horizontally laminated, fine-grained. Abundant clay clasts.
4898-4904	7	This section of core missing.
4905-4917	13	Sandstone, light gray (N7) to white (8/1 5Y), horizontally laminated, medium to fine-grained, with a few cross-bedded layers. More massive, less distinct laminations toward the base. Gradational basal contact.
4918-4923	6	Interbedded coarse siltstone, light gray (7/1 5Y) and shale. Burrows give marbling effect.
4924-4930	6	Silty shale, gray (N5/0 2.5Y),no fossils, not fissile.

Total = 62

#1 Denton 4815-4865, 5017-5037 feet

4815-4829	15	Packstone to wackestone,light gray (N7/0 2.5Y). (Sparse biomicrite). Vertical and horizontal burrows, occasional horizontal shale laminations, geopetal fillings in fossils. Mollusks, green algae, bryozoans, crinoids, forams, red algae, brachiopods, ostracods.
4830-4833	4	Wackstone to packstone, gray (N6/0 2.5Y), (sparse to packed biomicrite.) Abundant shale laminations. Bryozoans, gastropods, forams, red algae, ostracods, crinoids.
4834-4838	5	Sandstone, light gray (N7/0 2.5Y), massive, very fine-grained. Occasional vague horizontal laminae, cross-bedding. Rare horizontal burrows.
4839-4850	12	Interbedded white (N8/0 2.5Y) coarse siltstone and gray (N5/0 2.5Y) shale with very abundant horizontal and vertical burrows. Marbled appearance.
4851-4856	6	Sandstone, white (N8/0 2.5Y), very fine-grained, interbedded with shale.

4857-4864	8	Interbedded light gray (N7/0 2.5Y) coarse siltstone and shale, highly burrowed. Marbled appearance. Shale sample x-rayed.
4865	1	Sandstone, light gray (N7/0 2.5Y), massive, very fine-grained. Discontinuous wisps of organic material. Fossil fragments.
Total =	50	

5017-5022	6	Sandstone, white (N8/0 7.5YR), cross-bedded, fine-grained. Cross-bedding defined by darker laminae with abundant clay clasts.
5023-5024	2	Interbedded light gray (N7/1 5Y) coarse siltstone and shale with abundant burrows giving marbled appearance.
5025-5027	3	Siltstone, gray (N6/0 2.5Y), horizontally laminated, fine-grained, interbedded with shale. Rare burrows.
5028-5037	9	Sandstone, light gray (N7/0 2.5Y), horizontally laminated, fine-grained, interbedded with shale. Rare horizontal burrows. Sand packages up to 8" thick.
Total =	20	

Brown #2 4585-4632 feet

4585-4588	4	Sandstone, light gray (7/1 5Y), horizontally laminated, very fine-grained. Shale layers 1/32" separate sand packages $\frac{1}{4}$" to $\frac{1}{2}$" thick. Rare horizontal burrows. Abundant clay clasts.
4589-4590	2	Sandstone, light gray (7/0 2.5Y), structureless, fine-grained. Local wispy horizontal streaks. Abundant clay clasts.
4591-4598	8	Sandstone, horizontally laminated, light gray (7/0 2.5Y), fine-grained, packages separated by thin shale laminae. Clay clasts surrounded by iron stains. Occasional horizontal burrows.

4599-4612	14	Sandstone, gray (6/1 5Y), structureless, fine-grained. Some horizontal laminations and wisps of organic material.
4613-4627	15	Sandstone, light gray (7/1 5Y), horizontally laminated, fine-grained, with occasioal shale layers. Abundant clay clasts. Orange iron-stained spots.
4628-4632	4	Sandstone, light gray (7/1 5Y), structureless, fine-grained, with faint horizontal wisps.

Total = 47

#2 Oscar Little 4527-4564 feet

4527-4531	5	Silty shale, gray (N5/0 2.5Y), with occasioal very fine sandstone layers. Sandstone layers are burrowed and have horizontal laminations. Slump structures of sand into shale. Patches of black organic matter. Framboidal nodules of hematite.
4532-4538	7	Sandstone, light gray (7/1 5Y), massive, fine-grained. Local horizontal laminations, most destroyed by burrowing. Occasional shale layers 1/32" to ½" thick.
4539-4544	6	Sandstone, light gray (7/1 5Y), horizontally laminated, fine-grained, interbedded with shale. Some horizontal burrows and slumps of sand into shale.
4545-4553	9	Sandstone, light gray (7/1 5Y), massive and horizontally laminated, fine to very fine-grained. Slump structures into rare shale layers.
4554-4564	10	Sandstone, light gray (7/0 2.5Y), horizontally laminated, fine-grained, interbedded with shale. Local burrows and slump structures. Rare glauconite grains. Organic wisps in sand layers.

Total = 37

#3 McCullum 4515-4558

4515-4520	6	Silty shale, dark gray (N5/0 2.5Y), with layers of very fine sandstone ½" to 6" thick. Burrows, slump structures, shiny black organic patches. Plant fragments, brachiopods.
4521-4526	6	Sandstone, light gray (N7/0 7.5YR) and gray (5/1 10YR), fine-grained, with dark organic-rich layers in cross-beds or horizontal laminations. Vertical and horizontal burrows. Plant material, forams, brachiopods, gastropods common.
4527-4536	10	Sandstone, light gray (7/1 5Y), horizontally laminated, fine-grained, with local cross-bedding.
4537-4554	18	Sandstone, light gray (7/1 5Y), massive, fine-grained. Rare shale layers, ¼-½" thick, sometimes burrowed into the sandstones. Plant fragments.
4555-4557	3	Light gray (7/1 5Y) interbedded very fine sandstone and shale. Burrows, slump structures, some surviving horizontal laminations.

Total = 43

#1 Roberts 4438-4534 feet

4438-4446	9	Shale, very dark gray (N3/0 2.5Y), organic rich, with occasional lenses of very fine sandstone. Abundant plant fragments at the top.
4447-4451	5	Sandstone, light gray (N7), horizontally laminated, fine-grained. Vertical and horizontal burrows that disturb the laminations. Forams concentrated in layers.
4452-4455	4	Sandstone, light gray (7/0 2.5Y), horizontally laminated, very fine-grained, interbedded with shale. Some horizontal and vertical burrows.

4456-4458	3	Sandstone, white (8/0 2.5Y), cross-bedded, very fine-grained. Plant fragments and clay clasts concentrated in certain layers.
4459-4464	6	Shale, dark gray (N4/0 2.5Y), unfossiliferous.
4465-4476	12	Sandstone, gray (N6), massive, fine-grained, with abundant forams and brachiopods. Local horizontal laminations.
4477-4486	10	Silty sandstone, light gray (7/0 2.5Y), massive, very fine-grained. More horizontal laminations toward the base. Forams concentrated in layers.
4487-4490	4	Sandstone, light gray (7/0 2.5Y), fine-grained, interbedded with shale. Horizontal burrows.
4491-4497	7	Sandstone, light gray (N7), horizontally laminated, fine-grained, rare cross-beds.
4498-4501	4	Sandstone, light gray (N7/0 2.5Y), very fine-grained, interbedded with shale. Layers disturbed and marbled by slumping.
4502-4534	33	Shale, gray (N5/0 2.5Y), unfossiliferous.
Total =	96	

Atwood #1 4422-4473 feet

4422-4427	6	Sandstone, light gray (7/1 5Y), horizontally laminated, fine-grained. Rare low-angle cross-beds, occasional shale layers decreasing toward the top.
4428-4433	6	Sandstone, light gray (N7/0 2.5Y), very fine-grained, interbedded with shale (siltstone toward the top). Burrows, load structures.
4434-4451	18	Shale, fissile, gray (N5/0 2.5Y), with occasional rippled sand laminae $\frac{1}{4}$" thick. Some burrowing at the top, and layers with concentrations of forams. Coarsens upward.

4452-4455	4	Interbedded gray (N6/0 2.5Y) coarse siltstone and shale. Burrows, horizontal laminations, microfaulting.
4456-4458	3	Sandstone, light gray (7/1 5Y), cross-bedded, fine-grained, with local horizontal laminations.
4459	1	Shale, gray (6/1 5Y), with lenses of very fine sandstone. Shale sample x-rayed.
4460-4462	3	Sandstone, light gray (7/1 5Y), massive, very fine-grained, with local faint horizontal laminations. Abundant clay clasts.
4463	1	Interbedded light gray (N7/0 2.5Y) very fine sandstone and black shale. Burrows.
4464-4469	6	Siltstone, light gray (7/1 5Y), horizontally laminated, coarse-grained, with thin, faint shale layers.
4470-4473	3	Sandstone, light gray (7/1 5Y), horizontally laminated, very fine-grained, with dark, organic shale laminae 1/32" to $\frac{1}{4}$" thick. Burrows, organic wisps.
	Total = 51	

F.F. Hodge #1 4564-4621 feet

4564-4567	4	Shale, unfossiliferous, gray (N5/0 2.5Y).
4568-4569	2	Siltstone, light gray (N7), horizontally laminated, coarse-grained, with occasional cross-beds.
4570-4579	10	Shale, gray (N5/0 2.5Y), with lenses of cross-bedded or horizontally laminated very fine sandstone. Horizontal burrows.
4580-4585	6	Interbedded shaly sandstone, gray (6/1 5Y), and shale. Vertical and horizontal burrows. Increasing sand toward the base. Forams.
4586-4606	21	Light gray (7/1 5Y) horizontally laminated coarse siltstone to very fine sandstone.

		Grain size fines upward. Local cross-bedding, rare shale layers. Abundant clay clasts.
4607-4621	14	Siltstone, light gray (7/0 2.5Y), laminated, coarse-grained, interbedded with shale. Sand in layers up to 6" thick. Burrows and marbled appearance in shalier parts.
	Total = 57	

F.F. Hodge #3 4582-4659 feet

4582-4590	9	Sandstone, light gray (7/1 5Y), horizontally laminated, fine and very fine-grained, with thin layers of shale and clay clasts.
4591-4599	9	Sandstone, light gray (7/1 5Y), very fine-grained, interbedded with shale. Sandstone in packages up to 8" thick. Horizontal burrows, marbled appearance.
4600-4605	6	Sandstone, light gray (7/0 5Y), massive, fine-grained, with evenly disseminated clay clasts.
4606-4643	38	Sandstone, light gray (7/0 2.5Y), horizontally laminated, very fine-grained, interbedded with shale. Horizontal burrows, marbled appearance. Clay clasts in thicker sand layers.
4644-4646	3	Sandstone, white (8/0 2.5Y), massive, very fine-grained, with evenly disseminated clay clasts.
4647-4659	13	Shale, interbedded with light gray (7/1 5Y), horizontally laminated coarse siltstone. Horizontal burrows, marbled appearance.
	Total= 77	

Buchanan 4550-4658 feet

4550-4555	6	Siltstone, light gray (7/1 5Y), massive, coarse-grained, with some horizontal laminations and clay clasts.
4556-4567	12	Siltstone, light gray (7/1 5Y), cross-bedded, coarse-grained, with abundant clay clasts. Dark wisps of organic material.
4568-4569	2	This section of core missing.
4570-4574	5	Sandstone, light gray, horizontally laminated, very fine-grained, interbedded with shale. Horizontal burrows.
4575-4580	6	Sandstone, light gray (7/0 2.5Y), cross-bedded, very fine-grained, with laminae well outlined by plant debris and clay clasts. Also local concentrations of forams.
4581-4616	36	Siltstone, light gray (7/1 5Y), coarse-grained, interbedded with shale. Some small ripple cross-beds. Horizontal burrows give a swirled, marbled appearance. Load structures of sand into shale. Grain size fines upward.
4617-4620	4	Sandstone, light gray (7/1 5Y), massive, fine-grained, with local faint horizontal laminations.
4621-4625	5	Interbedded shale and light gray (7/0 2.5Y) coarse siltstone. Horizontally laminated, horizontal burrows.
4626-4640	15	Sandstone, light gray (7/1 5Y), massive, fine-grained, with an occasional burrowed layer of shale. Local faint horizontal laminae.
4641-4654	14	Interbedded shale and light gray (7/0 2.5Y) horizontally laminated, coarse-grained siltstone. Horizontal burrows.
4655-4658	3	Sandstone, light gray (7/0 2.5Y), massive, fine-grained, with abundant clay clasts.
	Total = 108	

#2 C.W. Stockton 4642-4680 feet

4642-4647	6	Interbedded shale and light gray (N7/0 2.5Y), coarse-grained siltstone. Siltstone layers up to 6" thick, shale ¼-6". Vertical and horizontal burrows, load structures. Shale sample x-rayed.
4648-4650	3	Silty shale, gray (N6/0 2.5Y), with thin, rippled lenses of coarse siltstone.
4651-4653	3	Sandstone, light gray, massive, fine-grained, with black wisps of plant debris.
4654-4657	4	Shale, dark gray (N4/0 7.5YR), interbedded with very fine-grained sandstone. Vertical and horizontal burrows and slump structures give a marbled appearance. Some plant debris.
4658-4679	22	Sandstone, light gray, massive, fine-grained, with occasional cross-beds. Black wisps of plant debris.

Total = 38

#1 L.A. Boden 4519-4526, 4573-4616 feet

4519-4521	3	Shale, dark gray (N4/0 2.5Y).
4522-4525	3	Interbedded shale and light gray (N7/0 2.5 Y), coarse-grained siltstone. Silt in layers up to 4" thick. A few horizontal burrows and convolute bedding.
4573-4590	18	Dark gray (5/0 7.5 YR) shale to fine siltstone. Small lenses of coarse siltstone. Convolute folding, horizontal burrows in coarser layers. Concentrations of crinoids, forams, and gastropods.
4591-4593	3	Interbedded shale and light gray, very fine-grained sandstone. Horizontal burrows, convolute bedding.
4594-4595	2	Sandstone, light gray (7/0 7.5YR), massive fine-grained, with faint horizontal bedding. Orange spots of iron stain.

4596-4597	2	Shale, unfossiliferous, gray (N5/0 7.5YR).
4598-4603	6	Sandstone, light gray (7/0 7.5YR), massive, fine-grained, with local low-angle cross-beds.
4604-4612	9	Interbedded shale and light gray (N7/0 2.5Y), coarse-grained siltstone. Some horizontal burrows, convolute bedding. Less shale and larger grain size toward the top.
4613-4616	3	Shale, gray (N5/0 2.5Y), with layers of coarse siltstone. Vertical and horizontal burrows, and convolute bedding associated with siltstone layers. Shale x-rayed.
Total =	50	

#1 Alice McCarver 4476-4526 feet

4476-4484	11	Shale, dark gray (4/0 2.5YR), with coarse siltstone layers. Burrows in siltstone. Forams, green algae, mollusks, plant debris.
4485	1	Sandstone, gray (5/0 2.5YR), massive, very fine-grained, with abundant forams and green algae. Black organic wisps.
4486-4522	37	Shale, dark gray (N4/0 2.5Y), unfossiliferous, with some fossiliferous coarse siltstone layers. Forams, worm tubes, green algae, burrows in siltstones. One siltstone layer cross-bedded, with clay drapes.
4523-4526	4	Interbedded shale and gray (6/0 7.5YR), coarse-grained siltstone. Siltstone layers ¼-7" thick, some cross-bedded. Wisps of organic material, vertical and horizontal burrows in siltstones.
Total =	50	

APPENDIX 2

Table 3 contains the thin section data obtained by point counting. The following abbreviations are used in this table:

QTZ	=	Monocrystalline detrital quartz grains
POLY	=	Polycrystalline detrital quartz grains
OR	=	Orthoclase feldspar
PLAG	=	Plagioclase feldspar
SCP	=	Leached feldspar grains ("Swiss cheese")
SIL	=	Very fine-grained siliceous rock fragments
SRF	=	Sedimentary rock fragments
MRF	=	Metamorphic rock fragments
QCEM	=	Quartz cement
CARB	=	Carbonate cement
KAO	=	Kaolinite cement
MTX	=	Detrital clays
POR	=	Intergranular porosity
SEC	=	Secondary porosity
Other	=	Grains not included in any of the above categories, such as plant material, fossils, and heavy minerals.
CEM	=	Sum of quartz and carbonate cement
TPOR	=	POR + ($\frac{1}{2}$ SEC) = Total porosity
PCP	=	Pre-cement porosity
ϕ	=	Porosimeter porosity in %
PERM	=	Permeability in millidarcies
ENV	=	Depositional environment
DIST	=	Vertical distance to nearest shale
Q:F:R	=	Ratio of framework grains, quartz:feldspar:rock fragments. Chert included with rock fragments
$\overline{x}$	=	Mean phi grain size of framework grains

σ = Phi standard deviation of grain size

CAL = + denotes presence of calcite in that slide

BIBLIOGRAPHY

Adams, W.L., 1964, Diagenetic aspects of lower Morrowan, Pennsylvanian sandstones, northwestern Oklahoma, Am. Assoc. Petroleum Geologists Bull., v. 48, p. 1568-1580.

Almon, W.R., Fullerton, C.B., and Davies, D.K., 1976, Pore space reduction in Cretaceous sandstones through chemical precipitation of clay minerals, Jour. Sed. Petrol., v. 46, p. 89-96.

Berner, R.A., 1971, Principles of chemical sedimentology, New York, McGraw-Hill Book Company, 240 p.

Blatt, H., 1966, Diagenesis of sandstones: Processes and problems, Wyoming Geol. Assoc., Permo-Penn. Symposium (Casper, Wyo.), Twentieth Annual Conference, p. 63-65.

Brown, L.F. and Goodson, J.L., 1972, Geologic atlas of Texas, Abilene sheet, Univ. Texas (Austin) Bur. Econ. Geology.

Brown, L.F., Cleaves, A.W., and Erxleben, A.W., 1973, Pennsylvanian depositional systems in North-central Texas, Univ. Texas (Austin) Bur. Econ. Geology, Guidebook No. 14, 122 p.

Burst, J.F., 1969, Diagenesis of Gulf Coast clayey sediments and its possible relation to petroleum migration, Am. Assoc. Petroleum Geologists Bull., v. 53, p. 73-93.

Carrigy, M.A. and Mellon, G.B., 1964, Authigenic clay mineral cements in Cretaceous and Tertiary sandstones of Alberta, Jour. Sed. Petrol., v. 34, p. 461-472.

Cleaves, A.W., 1975, Upper Desmoinesian-Lower Missourian depositional systems (Pennsylvanian), North-central Texas, Unpub. Ph.D. dissert., Univ. Texas at Austin, 256 p.

Dapples, E.C., 1959, The behavior of silica in diagenesis, in Ireland, H.A. ed., Silica in sediments, Soc. Econ. Paleontologists and Mineralogists Spec. Pub. 7, p. 36-54.

Davis, J.C., 1973, Statistics and data analysis in geology, New York, John Wiley & Sons, Inc., 550 p.

Degens, E.T. and Chilingar, G.V., 1967, Diagenesis in subsurface waters, in Larsen, G. and Chilinger, G.V., eds., Diagenesis in sediments, Developments in Sedimentology 8, New York, Elsevier, 551 p.

Dickson, J.A.D., 1966, Carbonate identification and genesis as revealed by staining, Jour. Sed. Petrol., v. 36, p. 491-505.

Ethridge, F.G., Gopinath, T.R., and Davies, D.K., 1975, Recognition of deltaic environments from small samples, in Broussard, M.L. ed., Deltas, models for exploration, Houston Geol. Soc., p. 151-164.

Fisher, W.L., Brown, L.F., Scott, A.J., and McGowen, J.H., 1969, Delta systems in the exploration for oil and gas - a research colloquium, Univ. Texas (Austin) Bur. Econ. Geology, 212 p.

Flawn, P.T., Goldstein, A., King, P.B., and Weaver, C.E., 1961, The Ouachita System, Univ. Texas (Austin) Bur. Econ. Geology, Pub. # 6120, 401 p.

Folk, R.L., 1974, Petrology of sedimentary rocks, Austin, Texas, Hemphill's Book Store, 182 p.

Folk, R.L. and Land, L.S., 1975, Mg/Ca ratio and salinity: two controls over crystallization of dolomite, Am. Assoc. Petroleum Geologists Bull., v. 59, p. 60-68.

Fothergill, C.A., 1955, The cementation of oil reservoir sands and its origin, 4th World Petroeum Cong., Rome, Proc., Sec. 1, p. 301-314.

Fox, J.E., et al., 1975, Porosity variation in the Tensleep and its equivalent the Weber sandstone, western Wyoming: a log and petrographic analysis, Rocky Mt. Assoc. of Geol., 1975 Symposium.

Fuchtbauer, H., 1974, Sediments and sedimentary rock, 1: Part II, New York, Halsted Press, 464 p.

Galloway, W.E., 1974, Deposition and diagenetic alteration of sandstone in northeast Pacific Arch - related basins: implications for graywacke genesis, Geol. Soc. America Bull., v. 85, p. 379-390.

Goldich, S.S., 1938, A study in rock weathering, Jour. Geology, v. 46, p. 17-58.

Heald, M.T., 1956, Cementation of Simpson and St. Peter sandstones in parts of Oklahoma, Arkansas, and Missouri, Jour. Geology, v. 64, p. 16-30.

Heald, M.T. and Anderegg, R.C., 1960, Differential cementation in the Tuscarora sandstone, Jour. Sed. Petrol., v. 30, p. 568-577.

Heald, M.T. and Larese, R.E., 1974, Influence of coatings on quartz cementation, Jour. Sed. Petrol., v. 44, p. 1269-1274.

Hsu, K.J., 1963, Solubility of dolomite and composition of Florida ground waters, Jour. Hydrology, v.1, p. 288-310.

Huang, W.H. and Keller, W.D., 1970, Dissolution of rock-forming silicate minerals in organic acids: simulated first-stage weathering of fresh mineral surfaces, Am. Mineralogist, v. 55, p. 2076-2094.

Jacka, A.D., 1970, Principles of cementation and porosity occlusion in Upper Cretaceous sandstones, Rocky Mountain region, in Wyoming Geol. Assoc. Guidebook, 22nd, p. 265-285.

Jonas, E. and McBride, E.F., 1977, Diagenesis of sandstone and shale: application to exploration for hydrocarbons, Dept. of Geol. Sciences, Univ. Texas at Austin Continuing Education Pub. #1.

Kinsman, D.J.J., 1965, Gypsum and anhydrite of Recent age, Trucial Coast, Persian Gulf, in Rau, J.L., ed., Second Symposium on Salt, v. 1: Cleveland, Ohio, Northern Ohio Geol. Soc., p. 302-326.

Krumbein, W.C. and Pettijohn, F.J., 1938, Manual of sedimentary petrography, New York, Appleton-Century-Crofts, Inc., 549 p.

Levandowski, D.W. et al., 1973, Cementation in Lyons sandstone and its role in oil accumulation, Denver Basin, Colorado, Am. Assoc. Petroleum Geologist Bull., v. 57, p. 2217-2244.

Lindholm, R.C. and Finkelman, R.B., 1972, Calcite staining: semiquantitative determination of ferrous iron, Jour. Sed. Petrol., v. 42, p. 239-242.

Lindquist, S.J., 1976, Sandstone diagenesis and reservoir quality, Frio Formation (Oligocene), South Texas, Unpub. Master's thesis, Univ. Texas at Austin, 147 p.

Millot, G., 1970, Geology of clays, New York, Springer-Verlag, 429 p.

Netto, A.S.T., 1974, Petroleum and reservoir potentialities of the Agua Grande member (Cretaceous), Reconcavo Basin, Brazil, Unpub. Master's thesis, Univ. Texas at Austin, 143 p.

Nie, N.H. et al., 1975, SPSS Statistical package for the social sciences, New York, McGraw-Hill, 661 p.

Pettijohn, F.J., Potter, P.E., and Siever, R., 1972, Sand and sandstone, New York, Springer-Verlag, 618 p.

Pettijohn, F.J., 1975, Sedimentary Rocks, New York, Harper and Row, 628 p.

Rosenfeld, M.A., 1949, Some aspects of porosity and cementation, Producers Monthly, v. 13, p. 39-42.

Runnells, D.D., 1969, Diagenesis, chemical sediments, and the mixing of natural waters, Jour. Sed. Petrol., v. 39, p. 1188-1201.

Schmidt, V., 1976, Secondary porosity in the Parsons Lake sandstone, 1976 Ann. Mtgs., 21st Mineralogical Assoc. Canada, 29th Geol. Assoc. Canada, Edmonton, p. 50.

Schoeppel, D.J., and Gilarranz, S., 1966, Use of well log temperatures to evaluate regional geothermal gradients, Jour. Petroleum Tech., v. 237, p. 667-673.

Shannon, J.P. Jr. and Dahl, A.R., 1971, Deltaic stratigraphic traps in West Tuscola field, Taylor County, Texas, Am. Assoc. Petroleum Geologists Bull., v. 55, p. 1194-1205.

Sharma, G.D., 1965, Formation of silica cement and its replacement by carbonates, Jour. Sed. Petrol., v. 35, p. 733-745.

Shinn, E.A., et al., 1977, Limestone compaction: an enigma, Geology, v. 5, p. 21-24.

Siever, R., 1959, Petrology and geochemistry of silica cementation in some Pennsylvanian sandstones, in Ireland, H.A. ed., Silica in sediments, Soc. Econ. Paleontologists and Mineralogists Spec. Pub. 7, p. 55-79.

Siever, R., 1962, Silica solubility, 0 -200 C, and the diagenesis of siliceous sediments, Jour. Geology, v. 70, p. 127-150.

Siever, R., Beck, K.C., and Berner, R.A., 1965, Composition of interstitial waters of modern sediments, Jour. Geology, v. 73, p. 39-73.

Sippel, R.F., 1968, Sandstone petrology, evidence from luminescence petrography, Jour. Sed. Petrol., v. 38, p. 530-554.

Stalder, P.J., 1973, Influence of crystallographic habit and aggregate structure of authigenic clay minerals on sandstone permeability, Geol. en Mijnbouw, v. 52, p. 217-220.

Stanton, G.D., 1977, Factors influencing porosity and permeability of Lower Wilcox (Eocene) sandstone, Karnes County, Texas, Unpub. Master's thesis, Univ. Texas at Austin, 158 p.

Stanton, G.D. and McBride, E.F., 1976, Factors influencing porosity and permeability of Lower Wilcox (Eocene) sandstone, Karnes County, Texas, Am. Assoc. Petroleum Geologists Bull., v. 60, p. 725-726.

Towe, K.M., 1962, Clay mineral diagenesis as a possible source of silica cement in sedimentary rocks, Jour. Sed. Petrol., v. 32, p. 26-28.

Von Engelhardt, W., 1967, Interstitial solutions and diagenesis in sediments, in Larsen, G. and Chilingar, G.V., eds., Diagenesis in sediments, Developments in Sedimentology: 8, New York, Elsevier, 551 p.

Walker, T.R., 1960, Carbonate replacement of detrital crystalline silicate minerals as a source of authigenic silica in sedimentary rocks, Geol. Soc. America Bull., v. 71, p. 145-151.

The vita has been removed from the digitized version of this document.